

**AN INVESTIGATION OF THE DYNAMIC RESPONSE OF AIRWAY
SMOOTH MUSCLE IN SENSITIZED ANIMAL MODELS.**

Miguel Jo-Avila

**A thesis submitted to Auckland University of Technology
in fulfilment of the degree of
Doctor of Philosophy (Phd)**



2014

School of Engineering

Primary Supervisor: Professor Ahmed Al-Jumaily

Acknowledgments

There are many people without whom this work would have not been possible. First and foremost, I would like to express my gratitude to my primary supervisor Prof. Ahmed Al-Jumaily for giving me the opportunity to work in this project, provide his guidance and expertise all the way through and support me in all the decisions that I made. I would also like to thank my second supervisor Dr Luis Sobrevia for his involvement in the project even at the distance and my third supervisor Dr Jun Lu for his insight into physiological aspects of the work and all his help related with the development of the animal models and the ethical regulations.

I would also like to thanks to Dr Gijs Ijpma, Dr Prisca Mbikou, Dr Prashika Reddy and Mg. Meha Mathur, for their invaluable guidance through the beginning of the project, Dr Mohammad Al-Rawi for his helpful hand during the experiments conducted at Auckland University, Yasmitha Manilal, Prachi Redey, Codey Bell and Kevin Roos for keep me sane during the most complicated stages of my studies. My sincere thanks go to the entire IBTec team for have been there when I needed them the most, the chemistry technicians, KODE Biotech staff and Auckland AEC and VJU staff.

Further, I would like to thank to IBTec for supporting this research through the IBTec scholarship and the School of Engineering for supporting my fees scholarship.

Finally I would like to thanks and dedicate this thesis to my mother, father, brother, and nephews who supported me at the distance through this journey.

Abstract

Asthma is a chronic respiratory disease, characterized by inflammation, airway hyperresponsiveness (AHR) and obstruction of the airways. During an asthma attack, the contraction of airway smooth muscle (ASM) in combination with increased mucus production reduces the bronchial diameter, increasing the resistance to airflow into the lungs. New Zealand has one of the highest prevalence rates for asthma in the world, with a total estimated cost around NZ\$ 825 million per year.

The intrinsic causes of asthma are currently not well understood. Several treatments have been developed, but none of them present a cure for this chronic disease. Most of these treatments pharmacological with side effects sometimes fatal and affecting many patients. Some patients show no response to existing treatments.

ASM contraction is believed to be the main driving mechanism in asthma attacks. The response of ASM in healthy and asthmatic airways seems to be influenced by breathing patterns such as tidal breathing and deep inspiration, with strong differences between healthy and asthmatic airways. Therefore understanding airway mechanics and the dynamic response of ASM *in vivo* seems to be an essential component in the search for a new alternative in the treatment of asthma.

The proposed research investigates the response of ASM in sensitized models in the presence of imposed oscillations *in vivo* and *in vitro*. The results from this study in combination with the previous work done in this area will help to increase the understanding of how length oscillations affect the response of ASM in healthy and asthmatic subjects.

Table of Contents

| | |
|--|-----------|
| Chapter 1 | 13 |
| Background..... | 13 |
| 1.1. Introduction..... | 13 |
| 1.2. Respiratory physiology..... | 14 |
| 1.3. Airway smooth muscle..... | 15 |
| 1.4. Structure of the contractile apparatus..... | 16 |
| 1.5. Thesis structure | 22 |
| 1.6. Closure | 23 |
| Chapter 2 | 24 |
| Asthma, ASM and mechanical response..... | 24 |
| 2.1. Introduction..... | 24 |
| 2.2. Asthma | 24 |
| 2.3. Asthma Treatments | 25 |
| 2.4. Airway remodeling in asthma..... | 28 |
| 2.5. ASM and asthma..... | 29 |
| 2.6. Mechanical oscillations..... | 29 |
| 2.7. Summary and objectives | 32 |
| 2.8. Closure | 34 |
| Chapter 3 | 35 |
| Animal model and sensitization | 35 |
| 3.1. Introduction..... | 35 |
| 3.2. Animal models | 35 |
| 3.3. Selection criteria | 36 |
| 3.4. Asthmatic models..... | 37 |
| 3.5. Asthma assessment techniques | 40 |
| 3.6. Pilot group..... | 46 |
| 3.7. Selected Techniques to evaluate the model | 49 |
| 3.8. Animal assessment..... | 54 |
| 3.9. Closure | 60 |
| Chapter 4 | 61 |
| In vitro experimental investigation | 61 |
| 4.1. Introduction..... | 61 |
| 4.2. Tissue acquisition..... | 62 |
| 4.3. In vitro set-up | 62 |
| 4.4. Programs..... | 65 |
| 4.5. Reference diameter (Do) | 66 |
| 4.6. Pilot study experiments (healthy airways)..... | 67 |
| 4.7. Data reduction..... | 70 |
| 4.8. Relaxation..... | 70 |
| 4.9. Breathing, ISO and SILO | 72 |
| 4.10. Healthy and asthmatic airways | 72 |
| 4.11. Tissue acquisition..... | 73 |

| | | |
|---|---|------------|
| 4.12. | <i>Experiments</i> | 74 |
| 4.13. | <i>Relaxation</i> | 75 |
| 4.14. | <i>Closure</i> | 80 |
| Chapter 5 | | 81 |
| <i>In vivo</i> experimental setup | | 81 |
| 5.1. | <i>Introduction</i> | 81 |
| 5.2. | <i>Experimental layout</i> | 82 |
| 5.3. | <i>Animal containment</i> | 83 |
| 5.4. | <i>Measurement components</i> | 86 |
| 5.5. | <i>Drugs and allergen delivery system</i> | 97 |
| 5.6. | <i>Pressure oscillation setup</i> | 98 |
| 5.7. | <i>Calibration of devices and oscillation setup</i> | 100 |
| 5.8. | <i>Testing in vivo</i> | 105 |
| 5.9. | <i>Closure</i> | 107 |
| Chapter 6 | | 108 |
| <i>In vivo</i> experimental investigation | | 108 |
| 6.1. | <i>Introduction</i> | 108 |
| 6.2. | <i>In vivo Testing</i> | 108 |
| 6.3. | <i>Experimental data</i> | 109 |
| 6.4. | <i>Statistical analysis of results</i> | 118 |
| 6.5. | <i>Closure</i> | 130 |
| Chapter 7 | | 132 |
| Discussion and conclusions | | 132 |
| 7.1. | <i>Introduction</i> | 132 |
| 7.2. | <i>Length oscillations</i> | 132 |
| 7.3. | <i>SILO in vitro</i> | 133 |
| 7.4. | <i>SILO in vivo</i> | 135 |
| 7.5. | <i>SILO vs ISO</i> | 136 |
| 7.6. | <i>Summary</i> | 136 |
| 7.7. | <i>Conclusions</i> | 137 |
| 7.8. | <i>Future work</i> | 138 |
| References | | 140 |
| Appendix | | 154 |
| Appendix A: Ethical approval..... | | 154 |
| Appendix B: Labview programs used for in vitro test | | 157 |
| Appendix C: Matlab analysis code..... | | 163 |
| Appendix D: <i>in vivo</i> no processed data | | 165 |

Table of figures

| | |
|--|----|
| Figure 1.1: Respiratory system[14]..... | 15 |
| Figure 1.2: Components of cytoskeleton and myofilaments on SM | 16 |
| Figure 1.3: Components contractile apparatus [24]..... | 17 |
| Figure 1.4: Myosin structure (Adapted from reference [25])..... | 17 |
| Figure 1.5: Smooth muscle contraction process [15]..... | 21 |
| Figure 1.6: Four state model of Hai and Murphy (1988) [42]..... | 22 |
| Figure 2.1: Bronchodilation and bronchoconstriction in response to deep inspiration [26]..... | 31 |
| Figure 3.1: Mice upper airways anatomy [134]..... | 38 |
| Figure 3.2: Mice lower airways [134]. | 40 |
| Figure 3.3: Invasive plethysmograph [136]..... | 41 |
| Figure 3.4: Non-invasive methods: Whole-body plethysmography [135]..... | 42 |
| Figure 3.5: Scheme for venturi. | 43 |
| Figure 3.6: Lung volumes occurring during breathing. | 44 |
| Figure 3.7: Control protocol, the weight and the behavior of the mice was checked on day 0, 7 and 14 and later on 24, 28 and 32 before the experimental protocols..... | 47 |
| Figure 3.8: Sensitization protocol: The sensitization protocol was divided in two stages: first stage; induction of immunoresponse (injection of allergen) from day 0-14 and a Second stage; induction of AHR (nebulization of allergen) from day 24-32..... | 49 |
| Figure 3.9: Sketch plethysmograph diagram (image modify from [136])..... | 50 |
| Figure 3.10: Overview plethysmograph and data acquisition system: a) testing chamber; b) pressure transducer; c) Data acquisition system; d) software..... | 51 |
| Figure 3.11: Scheme of connection of nebulizer and subject for drug delivery. a) Nebulizer and solution chamber for nebulization of drugs (Ach, ISO, saline); b) pneumotachograph; c) mice; d) pressure transducer. | 52 |
| Figure 3.12: R_L for Ach dose-response asthmatic subjects: axis y corresponds to the value of R_L observed with the different experimental conditions presents in axis x ($n = 6$). | 54 |
| Figure 3.13: R_L for ISO dose-response asthmatic subjects: axis y corresponds to the value of R_L observed with the different experimental conditions presents in axis x ($n = 6$). | 55 |
| Figure 3.14: Comparison of R_L between asthmatic and healthy subjects. Axis y corresponds to the value of R_L observed with the different experimental conditions presents in axis x ($n = 6$). | 56 |
| Figure 3.15: Comparison of R_L between asthmatic and healthy subjects. Axis y corresponds to the value of R_L observed with the different experimental conditions presents in axis x ($n = 6$) and its statistical significance (* or # = p value < 0.05). | 56 |
| Figure 3.16: BAL images a) sensitized animals, b) control (healthy) animals: Epithelial cells, WC (white cells) and RC (red cells)..... | 57 |
| Figure 3.17: ELISA OVA IgE Standar concentration curve: axis y corresponds to the optical density for each concentration, and axis x corresponds to the concentration of each standard. a) 7.8, b) 15.6, c) 31.2, d) 62.5, e) 125, f) 250, g) 500 ng/mL..... | 58 |
| Figure 3.18: BAL concentration a) sensitized animals, b) control (healthy) animals (p value < 0.05 ; $n = 11$). | 59 |
| Figure 4.1: System diagram of tissue testing set-up. | 62 |
| Figure 4.2: Caption of in vitro testing set-up: 1) Dual-mode lever system (Aurora scientific inc); 2) Tissue bath (5ml water jacket reservoir); 3) muscle lever (the tissue is fix to this lever arm that generate oscillations and register changes in tension); 4) Bottom glass hook (tissue is fixed at this point); 5) 1L water jacketed reservoir for physiological solution; 6) Heater, pump, and water reservoir (to maintain all the system under physiological temperature 37°C). | 63 |
| Figure 4.3: Tissue bath, with all the accessories, inlets and outlets..... | 64 |
| Figure 4.4: Example of determination for optimal diameter. In the caption the last contraction obtained which corresponds to number 5 was not bigger than the previous number 4, so optimal diameter was considered reached. | 67 |
| Figure 4.5: Experiments type. a) Relaxation induced using just ISO (10-6M); b) relaxation induced by ISO in combination with tidal oscillations (4%:2.7Hz); c) relaxation induced by tidal oscillations in combination with superimposed oscillations (1 and 1.5%: 5, 10, 15 and 20Hz)..... | 69 |
| Figure 4.6: Effect of Isoproterenol and the combined effect of ISO and mechanical oscillations equivalent to breathing on contractile force, represented as % relaxation on Y axis ($n=6$). | 71 |
| Figure 4.7: Effect of mechanical oscillations equivalent to breathing with and without superimposed length oscillations on contractile force ($n=6$). | 71 |
| Figure 4.8: a) Anesthiated mice is placed in plastic square; b) Pre tracheal muscles are dissected in order to expose the trachea; c) The trachea is removed from mice and cleaned from surroundings tissue ; | |

| | |
|--|-----|
| d) Dissected trachea is cut into smaller pieces (2-3mm) and mounted onto wire hooks leaving the ASM untouched..... | 74 |
| Figure 4.9: Compared effect of Isoproterenol and the combined effect of ISO and mechanical oscillations equivalent to breathing on contractile force on healthy and asthmatic airways. @, * and # indicates statistical significance between the means of the effect of breathing, ISO and Breathing + ISO on healthy airways and effect of the same experimental condition asthmatic airways respectively (n=6, p value < 0.05). | 76 |
| Figure 4.10: Effect of mechanical oscillations equivalent to breathing with and without superimposed length oscillations (1% amplitude) on contractile force. * indicates statistical significance for the mean of SILO at 10 Hz when compared to the mean to breathing alone (n=7). | 77 |
| Figure 4.11: Effect of mechanical oscillations equivalent to breathing with and without superimposed length oscillations (1.5% of amplitude) on contractile force. * indicates statistical significance for the means of the effect of SILO when combined with breathing and compared with the effect of breathing alone using Wilcoxon; # indicates statistical significance between the means of the effect of SILO when combined with breathing and compared with the effect of breathing alone using t test on asthmatic airways (n=7). | 78 |
| Figure 4.12: Effect of ISO compared with mechanical oscillations equivalent to breathing + superimposed length oscillations (1% of amplitude) on contractile force. * indicates statistical significance for the mean of SILO at 5 Hz when compared to the mean to the effect of ISO alone (n=7). | 79 |
| Figure 4.13: Effect of ISO compared with mechanical oscillations equivalent to breathing + superimposed length oscillations (1.5% of amplitude) on contractile force. * indicates statistical significance for the means of the effect of SILO when combined with breathing and compared with the effect of ISO alone using Wilcoxon; # indicates statistical significance between the means of the effect of SILO when combined with breathing and compared with the effect of ISO alone using t test on asthmatic airways (n=7). | 79 |
| Figure 5.1: 1) Thermostated plexiglas chamber; 2) Pneumotachometer; 3) Tracheal cannula; 4) Oesophageal catheter; 5) Tube supplying the nebulised solution; 6) Nebulizer; 7) Connection pipes; 8) Differential pressure transducer; 9) Tam-A Transducer amplifier (c) and Plugsys amplifier module (d); 10) Connection pipe; 11) Honeywell pressure transducer; 12) 16 channels data acquisition board Labchart; 13) Computer with data acquisition Labchart. | 83 |
| Figure 5.2: Front of testing chamber: a) front inlet for Pneumotachograph, b) front inlet for eosophageal cannula, c) Inner basin for warm water, d) Side inlet for warmed water, e) side outlet for water, e) insulation..... | 84 |
| Figure 5.3: back of testing chamber: a) inlet for temperature probe. | 84 |
| Figure 5.4: Insulation scheme: a) acrylic wall, b) water basin, c) acrylic wall, external insulation chamber and d) acrylic wall..... | 85 |
| Figure 5.5: Thermo regulated bath: a) heat pump, b) outlet for warm water, c) return inlet for water from the chamber, d) Plastic container. | 86 |
| Figure 5.6: Respiratory parameters: a) Flow; b) Tp pressure (tracheal); c) Ptp pressure (transpulmonar); d) R _L (lung resistance); C _{dyn} (dynamic compliance) [138]..... | 87 |
| Figure 5.7: HSE-Pneumotachometer PTM Type 378/0.9 For Mice: a) Tracheal cannula, b) outlet to measure pressure at level of the mouth (before resistance), c) outlet to measure atmospheric pressure (after resistance), e) outlet for air and f) reduction of diameter of the tube (resistance). | 88 |
| Figure 5.8: DLP 2.5 Differential pressure transducer: a) inlet for pressure signal from the mouth, b) inlet for pressure signal from environment, c) differential pressure transducer..... | 88 |
| Figure 5.9: TAM-A transducer amplifier module and PLUGSYS Minicase type 609 | 89 |
| Figure 5.10: Eosophageal catheter (obtained from data sheet)..... | 91 |
| Figure 5.11: Sensor technics model 26PC0050D6A: a) Inlet for pressure signal from mid thorax, b) inlet for pressure signal from the environment. | 91 |
| Figure 5.12: Scheme of location for eosophageal catheter and tracheal cannula. a) Pressure transducer; b) Differential pressure transducer; c) Pneumotachograph (venturi); d) eosophageal catheter (located at mid thorax through the oesophagus); e) Tracheal cannula. | 92 |
| Figure 5.13: Location of tracheal cannula and oesophageal catheter: a) Pneumotachograph (venturi); b) Tracheal cannula; c) eosophageal catheter; d) Tracheal pressure and e) atmospheric pressure..... | 93 |
| Figure 5.14: Powerlab 16/30 and cds for Chart scope and Chart Pro | 94 |
| Figure 5.15: Labchart program: a) Tracheal pressure (Tp, mmH ₂ O); b) Flow L/s; c) Volume (L); d) minute ventilation (ml/min); e) Tidal volume (Tv, L); f) Transpulmonar pressure (Ptp mmH ₂ O); g) Lung Resistance (R _L , mmH ₂ O/L/s) and h) Dynamic compliance (C _{dyn} , L/mmH ₂ O). | 96 |
| Figure 5.16: Particle size chart (from datasheet provided for jet nebulizer). | 97 |
| Figure 5.17: Nebulization setup: a) Jet nebulizer from Harvard apparatus; b) AMPRO air brush compressor. | 98 |
| Figure 5.18: a) waveform generator; b) Power amplifier; c) shaker; d) chamber; e) piston. | 99 |
| Figure 5.19: Pressure oscillation setup: a) Shaker, b) Chamber, c) Piston and base..... | 100 |

| | |
|---|-----|
| Figure 5.20: Water manometer used for calibration curve for pressure transducer for Tp. | 101 |
| Figure 5.21: Calibration curve for pressure transducer for Tp | 102 |
| Figure 5.22: Calibration curve for pressure transducer for Ptp. | 103 |
| Figure 5.23: Pressure observed with device..... | 105 |
| Figure 6.1: Comparison of the R_L response to ACh $10^{-2}M$ observed from healthy (control) and asthmatic (sensitized) subjects, axis y corresponds to R_L obtained for each experimental condition presented in axis x (\square = healthy; \bullet = asthmatic; n=10). | 110 |
| Figure 6.2: Comparison of the C_{dyn} response to ACh $10^{-2}M$ observed from healthy (control) and asthmatic (sensitized) subjects, axis y corresponds to C_{dyn} obtained for each experimental condition presented in axis x (\square = healthy; \bullet = asthmatic; n=10). | 111 |
| Figure 6.3: Changes of R_L observed as result of the application of SILO with 5Hz frequency and amplitudes in the range of 100 – 400 mV are presented in axis y for each experimental condition presented in axis x (\square = healthy; \bullet = asthmatic; n=10). | 112 |
| Figure 6.4: Changes of C_{dyn} observed as result of the application of SILO with 5Hz frequency and amplitudes in the range of 100 – 400 mV are presented in axis y for each experimental condition presented in axis x (\square = healthy; \bullet = asthmatic; n=10). | 113 |
| Figure 6.5: Changes of R_L observed as result of the application of SILO with 10Hz frequency and amplitudes in the range of 100 – 400 mV are presented in axis y for each experimental condition presented in axis x (\square = healthy; \bullet = asthmatic; n=10). | 114 |
| Figure 6.6: Changes of C_{dyn} observed as result of the application of SILO with 10Hz frequency and amplitudes in the range of 100 – 400 mV are presented in axis y for each experimental condition presented in axis x (\square = healthy; \bullet = asthmatic; n=10). | 114 |
| Figure 6.7: Changes of R_L observed as result of the application of SILO with 15Hz frequency and amplitudes in the range of 100 – 400 mV are presented in axis y for each experimental condition presented in axis x (\square = healthy; \bullet = asthmatic; n=10). | 115 |
| Figure 6.8: Changes of C_{dyn} observed as result of the application of SILO with 15Hz frequency and amplitudes in the range of 100 – 400 mV are presented in axis y for each experimental condition presented in axis x (\square = healthy; \bullet = asthmatic; n=10). | 116 |
| Figure 6.9: Changes of R_L observed as result of the application of SILO with 20Hz frequency and amplitudes in the range of 100 – 400 mV are presented in axis y for each experimental condition presented in axis x (\square = healthy; \bullet = asthmatic; n=10). | 117 |
| Figure 6.10: Changes of C_{dyn} observed as result of the application of SILO with 20Hz frequency and amplitudes in the range of 100 – 400 mV are presented in axis y for each experimental condition presented in axis x (\square = healthy; \bullet = asthmatic; n=10). | 117 |
| Figure 6.11: GraphPad Prism 5.0 TM screenshot. | 120 |
| Figure 6.12: Comparison of the R_L response to ACh $10^{-2}M$ observed from healthy (control) and asthmatic (sensitized) subjects, axis y corresponds to R_L obtained for each experimental condition presented in axis (n=10). | 121 |
| Figure 6.13: Comparison of the C_{dyn} response to ACh $10^{-2}M$ observed from healthy (control) and asthmatic (sensitized) subjects, axis y corresponds to C_{dyn} obtained for each experimental condition presented in axis (n=10). | 122 |
| Figure 6.14: Data for changes of R_L obtained as result of the application of SILO with 5Hz frequency and amplitudes in the range of 100 – 400 mV are presented in axis y for each experimental condition presented in axis x (* p value <0.05, n=10). | 123 |
| Figure 6.15: Data for changes of C_{dyn} obtained as result of the application of SILO with 5Hz frequency and amplitudes in the range of 100 – 400 mV are presented in axis y for each experimental condition presented in axis x (n=10). | 124 |
| Figure 6.16: Data for changes of R_L obtained as result of the application of SILO with 10Hz frequency and amplitudes in the range of 100 – 400 mV are presented in axis y for each experimental condition presented in axis x (* p value <0.05, n=10). | 125 |
| Figure 6.17: Data for Changes of C_{dyn} obtained as result of the application of SILO with 10Hz frequency and amplitudes in the range of 100 – 400 mV are presented in axis y for each experimental condition presented in axis x (n=10). | 126 |
| Figure 6.18: Data for changes of R_L obtained as result of the application of SILO with 15Hz frequency and amplitudes in the range of 100 – 400 mV (* p value <0.05, n=10). | 127 |
| Figure 6.19: Data for changes of C_{dyn} obtained as result of the application of SILO with 15Hz frequency and amplitudes in the range of 100 – 400 mV (n=10). | 128 |
| Figure 6.20: Data for changes of R_L obtained as result of the application of SILO with 20Hz frequency and amplitudes in the range of 100 – 400 are presented in axis y for each experimental condition presented in axis x mV (n=10). | 129 |
| Figure 6.21: Data for changes of C_{dyn} obtained as result of the application of SILO with 20Hz frequency and amplitudes in the range of 100 – 400 mV are presented in axis y for each experimental condition presented in axis x (n=10). | 130 |

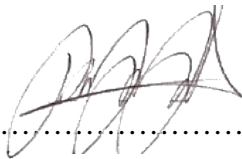
| | |
|---|-----|
| Figure A.1: back panel Converter.vi | 157 |
| Figure A.2: Front panel ASM_Length.vi front panel | 158 |
| Figure A.3: Back panel ASM_Length.vi back panel..... | 159 |
| Figure A.4: Front panel Low_res_signal.vi front panel..... | 160 |
| Figure A.5: Back panel Low_res_signal.vi back panel..... | 161 |
| Figure A.6: SubVI_button_timer.vi back panel..... | 162 |
| Figure A.7: Changes of flow observed as result of the application of SILO: a) 5Hz; b) 10Hz; c) 15Hz; and d) 20Hz frequency and amplitudes in the range of 100 – 400 mV are presented in axis y for each experimental condition presented in axis x (□ = healthy; ● = asthmatic; n=10)..... | 165 |
| Figure A.8: Changes of Tp observed as result of the application of SILO: a) 5Hz; b) 10Hz; c) 15Hz; and d) 20Hz frequency and amplitudes in the range of 100 – 400 mV are presented in axis y for each experimental condition presented in axis x (□ = healthy; ● = asthmatic; n=10)..... | 166 |
| Figure A.9: Changes of Ptp observed as result of the application of SILO: a) 5Hz; b) 10Hz; c) 15Hz; and d) 20Hz frequency and amplitudes in the range of 100 – 400 mV are presented in axis y for each experimental condition presented in axis x (□ = healthy; ● = asthmatic; n=10)..... | 167 |
| Figure A.10: Changes of Tv observed as result of the application of SILO: a) 5Hz; b) 10Hz; c) 15Hz; and d) 20Hz frequency and amplitudes in the range of 100 – 400 mV are presented in axis y for each experimental condition presented in axis x (□ = healthy; ● = asthmatic; n=10)..... | 168 |

List of tables

| | |
|--|-----|
| Table 3.1: Details of sensitization protocol for control group..... | 47 |
| Table 3.2: Details of sensitization protocol for asthmatic group..... | 48 |
| Table 3.3: OD for each concentration of the commercial standards..... | 58 |
| Table 3.4: Details of DO for each group tested (healthy and asthmatics) and IgE concentration for samples..... | 59 |
| Table 4.1: Column stats for response of airways from healthy and asthmatic airways to breathing, ISO and ISO + breathing. | 76 |
| Table 4.2: Statistical significance table for the effect of mechanical oscillations equivalent to breathing with and without superimposed length oscillations (amplitude 1%) on contractile force. Yellow box indicate statistical significance. | 77 |
| Table 4.3: Statistical significance table for the effect of mechanical oscillations equivalent to breathing with and without superimposed length oscillations (amplitude 1.5%) on contractile force. Yellow boxes indicate statistical significance. | 78 |
| Table 5.1: Pneumotachograph specifications..... | 88 |
| Table 5.2: DLP 2.5 Differential pressure transducer specifications | 89 |
| Table 5.3: TAM-A amplifier specifications..... | 90 |
| Table 5.4: Sensor technics pressure transducer specifications [19] | 92 |
| Table 5.5: Channels and unit used for the readings. | 95 |
| Table 5.6: Pressure data obtained with differential pressure transducer for Tp..... | 101 |
| Table 5.7: Pressure data obtained with differential pressure transducer for Ptp..... | 102 |
| Table 5.8: Pressure observed with device..... | 104 |
| Table 6.1: experimental data for RL and Cdyn for 5Hz data set (pre analysis) | 112 |
| Table 6.2: experimental data for RL and Cdyn for 10Hz data set (pre analysis) | 113 |
| Table 6.3: experimental data for RL and Cdyn for 15Hz data set (pre analysis) | 115 |
| Table 6.4: experimental data for RL and Cdyn for 20Hz data set (pre analysis) | 116 |
| Table 6.5: Data for RL and Cdyn for 5Hz | 123 |
| Table 6.6: Statistical significance table for the effect of SILO at 20Hz and all amplitudes. Yellow box indicate statistical significance. | 124 |
| Table 6.7: Data for RL and Cdyn for 10Hz..... | 125 |
| Table 6.8: Statistical significance table for the effect of SILO at 10Hz and all amplitudes. Yellow box indicate statistical significance. | 126 |
| Table 6.9: Data for RL and Cdyn for 15Hz..... | 127 |
| Table 6.10: Statistical significance table for the effect of SILO at 15Hz and all amplitudes. Yellow box indicate statistical significance. | 128 |
| Table 6.11: Data for RL and Cdyn for 20Hz..... | 129 |
| Table 6.12: Statistical significance table for the effect of SILO at 20Hz and all amplitudes. Yellow box indicate statistical significance. | 130 |
| Table A.1: Summary table for flow, Tp, Ptp and Tv for 5Hz and all amplitudes tested..... | 169 |
| Table A.2: Summary table for flow, Tp, Ptp and Tv for 10Hz and all amplitudes tested..... | 169 |
| Table A.3: Summary table for flow, Tp, Ptp and Tv for 15Hz and all amplitudes tested..... | 170 |
| Table A.4: Summary table for flow, Tp, Ptp and Tv for 20Hz and all amplitudes tested..... | 170 |

Attestation of Authorship

“I hereby declare that this submission is my own work and that to the best of my knowledge and belief, it contains no material previously published or written by another person (except where explicitly defined in the acknowledgments), no material which to a substantial extent has been submitted for the award of any other degree or diploma of a university or other institution or higher learning.”

 (Signed)

29/10/2013
..... (Date)

List of Terms and abbreviations

| | |
|------------------------|--|
| ASM | Airway Smooth Muscle |
| ACh | Acetylcholine |
| AHR | Airway hyperresponsiveness |
| ATP | Adenosine triphosphate |
| C_{dyn} | Dynamic compliance |
| DI | Deep inspiration |
| Do | Optimal diameter |
| EFS | Electrical Field Stimulation |
| IP | Intraperitoneal |
| ISO | Isoproterenol |
| LFOT | Low-frequency forced oscillation technique |
| PSS | Physiological solution |
| Ptp | Transpulmonar pressure |
| R_L | Pulmonary resistance |
| SILO | Super imposed length oscillations |
| SM | Smooth muscle |
| Tp | Tracheal pressure |
| TO | Tidal oscillations |
| Tv | Tidal volume |
| WBP | Whole body plethysmograph |

Chapter 1

Background

1.1. Introduction

Asthma is a chronic respiratory disease, characterized by inflammation, airways hyperresponsiveness and obstruction of the airways. During an asthma attack, the contraction of ASM in combination with an increased mucus production reduces the bronchial diameter, and increases the resistance to airflow into the lungs. Some of the most recurrent symptoms of asthma are wheezing, shortness of breath, chest tightness and coughing.

It is estimated that around 300 million people of different ages, and all ethnic backgrounds, suffer from asthma [1, 2], and this number is expected to rise at 100 million by 2025 [2]. New Zealand has one of the highest prevalence rates for asthma. The burden of this disease to governments, health care systems, families, and patients is increasing worldwide too. In New Zealand the total cost of asthma is estimated around NZ\$ 825 million per year [3]

The intrinsic causes of asthma are currently not well understood, however several treatments have been developed, but none of them present a cure for this disease. Most of these treatments are pharmaceutical [4] with some side effects which sometimes are fatal [5]. Others hardly show any effect to patient's condition [6].

Airway smooth muscle (ASM) contraction is believed to be the main driving mechanism in asthma attacks. The response of ASM in healthy and asthmatic airways seems to be influenced by breathing patterns such as tidal breathing and deep inspiration, with strong differences between healthy and asthmatic airways [7, 8]. Therefore understanding airway mechanics and the dynamic response of ASM *in vivo* seems to be an essential component in the search for a new alternative in the treatment of asthma.

The Institute of Biomedical Technologies (IBTec) has been working in this area for over 15 years, studying the response of ASM and different length oscillations condition applied to isolated strips of trachealis smooth muscle. The proposed research will investigate the response of ASM in sensitized models in the presence of imposed

oscillations *in vivo*. It is believed that mechanical oscillations act directly in perturbing the binding between actin and myosin [9-11]. If this statement is correct we hypothesize “that imposing breathing oscillations at different frequencies and amplitudes can contribute to relaxing ASM in sensitized animal models”. The results from this study in combination with previous work done in this area will help to increase understanding of how length oscillations affect the response of ASM in healthy and asthmatic subjects. Furthermore the combination of data *in vivo* and *in vitro* from healthy and asthmatic airways may allow us to develop a method to help in relieving contracted airways in asthmatic subjects.

This chapter summarize the respiratory system, physiology and the ASM role in the contraction process.

1.2. Respiratory physiology

The role of the respiratory system is to provide oxygen and remove carbon dioxide in the body tissues [12]. In order to reach this objective without exposing the body to any risk, this system is continuously acting as a first line of defence through the nose, filtering air particles and heating the air to near core body temperature [13]. Any remaining particles are caught by mucus lining the airways walls, which is propelled towards the throat by cilia extending from the epithelial cells lining the airways. After passing the larynx the filtered air enters into the trachea which consists of a series of “C” shaped cartilage discs with a layer of smooth muscle and epithelium. At the end of the trachea the airways split into two primary bronchi, each leading to a single lung which are composed of lobes (3 lobes in the right lung and 2 lobes in the left lung). The primary bronchi further divide into smaller and smaller branches (secondary, tertiary, etc), finally becoming even smaller structures called bronchioles, which have terminal branches called terminal bronchioles which end in alveolar sacks, where the gas exchange takes place (Fig 1.1) [4].

Figure 1.1: Respiratory system[14]

1.3. Airway smooth muscle

Smooth muscle is a key component of all hollow organs such as airways, vasculature, bladder and gastrointestinal tract. Smooth muscle can contract to change the shape or size of the organ. The key difference with skeletal muscle is its capability to sustain contractions at reduced energy cost [15, 16]. In airways the smooth muscle is surrounded by many other airway wall components such as elastin and collagen. However, smooth muscle is the only active component and consequently held responsibility for acute asthma attacks. During a normal breath cycle, the muscle displays passive and active forces. The passive forces correspond to the force observed during the resting state. These forces maintain the tone of the muscle, while the active forces shorten the muscle during a contraction [16].

Muscle contraction has been interpreted in terms of a model called "sliding filament model" firstly proposed by Huxley and Niedergerke [17] and for Huxley and Hanson [18].

The fundamental molecular mechanism of force development in smooth and striated muscles is similar. In both cases, the production of force occurs as a result of the cyclical interaction of contractile filaments, composed of actin and myosin, this interaction is known as cross-bridge cycling. In the following sections a detailed explanation of this process is presented.

1.4. Structure of the contractile apparatus

The contractile apparatus in smooth muscle is composed of actin which forms the thin filaments, myosin which forms the thick filaments and dense bodies and plaques which serve as attachment points for the thin filaments[15]. Intermediate filaments link the dense bodies into a cytoskeletal network which maintains the rigidity of the cell in the absence of contraction [19, 20] (Fig 1.2.).

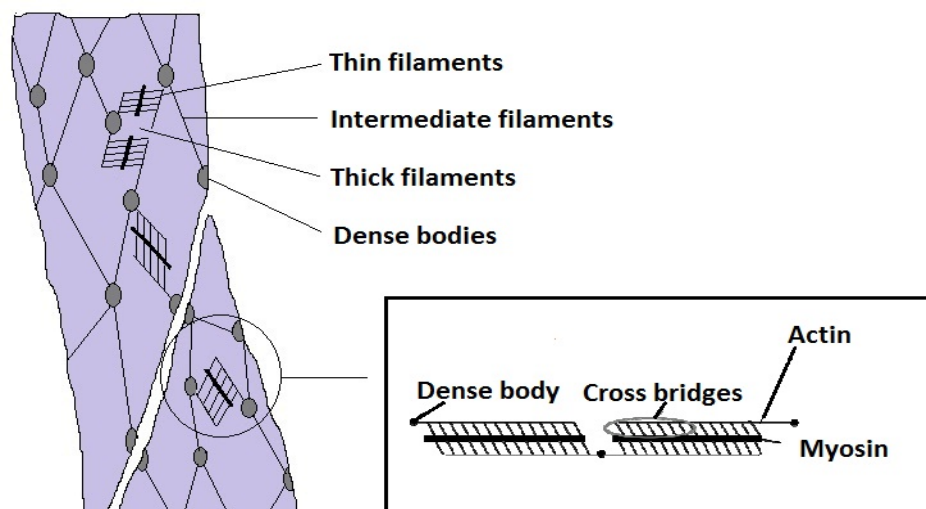


Figure 1.2: Components of cytoskeleton and myofilaments on SM

a. Thin filaments

Actin is the principal protein constituent of the thin filaments [7]. This protein can be found as monomeric G-actin or as filamentous F-actin, which forms a double-stranded helical array (Fig 1.3) [21]. Other proteins can be associated with actin such as: tropomyosin, caldesmon, and calponin. Caldesmon seems to participate in the activation or inhibition of the actin-tropomyosin complex in the presence or absence of Ca^{2+} [22],

but not all about this regulatory process of caldesmon over the thin filaments is totally understood [21, 23] . Electron microscopy studies of single thin filaments have shown that when caldesmon is phosphorylated, it displaces tropomyosin to reveal the myosin binding sites on actin [23].

Figure 1.3: Components contractile apparatus [24]

b. Thick Filaments

Monomeric myosin molecules polymerized to form myosin filaments or thick filaments. This large and asymmetric protein consists of six polypeptide chains: two heavy chains (~205 kDa each) that form a dimer , and two pairs of light chains: “regulatory chain” (20kDa) and “essential chain” (17kDa) [21]. The heavy chain dimer consists of a main body and two terminal globular heads (fig 1.5). The light chains (one essential and one regulatory) are located in the neck region of each myosin head (Fig 1.4).

Figure 1.4: Myosin structure (Adapted from reference [25])

c. Intermediate filaments

The intermediate filaments have a diameter of 7-15 nm [15, 21]. These filaments link the dense bodies into a cytoskeletal network which maintains the rigidity of the cell [19, 20], and they are grouped into bundles that run along the length of the cell and show

ramifications to the cell membrane. There are six types of intermediate filaments: type I, II, III, IV, V and VI, based on their composition. Type III intermediate filaments are mostly found in the ASM. This type contains four different proteins, where desmin and vimentin are the predominant ones in ASM [21, 26]. Other protein that can be found related to the intermediate filaments in ASM is plectin, which forms crosslinks between actin, microtubules, intermediate filaments, and thick filaments. Vimentin and plectin have been attributed to the observed changes in length adaptability of ASM during maturation [26].

d. Membrane-associated dense plaques

In electron micrographs, bundles of actin filaments and intermediate filaments can be seen penetrating the inner surface of electron dense areas of the membrane termed "dense bands" or "dense plaques" [21]. The primary components of these sites are transmembrane integrins, which attach to extracellular matrix proteins at one end and to cytoskeletal proteins at the other end.

In smooth muscle, other proteins such as vinculin, talin, α -actinin, and paxillin have been localized at the membrane-associated dense plaque sites. There is biochemical evidence that vinculin, talin, and α -actinin function to link actin filaments to transmembrane integrins; however the nature of the molecular interactions of this linkage is still not clear [27-29].

e. Cytosolic dense bodies

Dense areas have also been observed in electron micrographs of the smooth muscle cell cytoplasm, and are referred to as "dense bodies". Dense bodies in ASM act as striated muscle Z-disks equivalents, and they are considered anchorage sites in a network of thin and intermediate filaments [20]. These structures are distributed relatively uniformly throughout the cell cytoplasm and virtually all cytoplasmic dense bodies appear in association with the actin filaments [15, 19-21].

Laterally aligned dense bodies move rapidly toward one another during contraction, indicating attachment to contractile filaments. Analysis of the movement of dense bodies in contracting isolated smooth muscle cells suggests that they provide mechanical coupling between the contractile apparatus, the cytoskeleton, and the cell surface [30].

f. Dynamic relation of structural components

The filaments of smooth muscle have the ability to change in length during the relaxation or contraction of the muscle. The change in length of these filaments is due to (de)polymerization [21]. Smooth muscle contains large amounts of gelsolin and profilin, both acting as potent regulators of actin filament polymerization. Studies in smooth muscle from canine trachea also have shown that the amount of G-actin in airway smooth muscle is ~40% of the total actin content, but after the contractile stimulation the G-actin content decreases by ~30%. This finding suggest that the stimulation of the smooth muscle activates the polymerization of the G-actin into F-actin [31, 32].

After length changes ASM goes through an adaptation process, in order to optimally respond to a new stimulus. This partial recovery of its ability to generate maximal force at different lengths is named length adaptation [33, 34]. Many research groups have attributed the length adaptation of ASM to actin mobility [8, 21, 31, 35, 36]. This concept is supported by the finding that inhibition of the actin polymerization process results in an important reduction in ASM force generation [31]. Other studies have observed that myosin polymerization could be more important than actin polymerization in relation to length adaptation in ASM [19, 37, 38]. It has been demonstrated in porcine trachea that the thin / thick filaments ratio decreases when the muscle is contracted [38]. In pig tracheal smooth muscle the thick filament content may increase upon contraction, but there is no agreement on the extent of this [39]. In the following paragraph we will discuss the contractile process.

The contractile apparatus in smooth muscle is capable of a) generating maximal force over a large length range and b) maintaining force at low ATP turnover rate. ATP is a molecule that provides chemical energy in many biological processes. It has been observed *in vitro* by single-molecule techniques that the concentration of ATP can modulate force controlled length change in smooth muscle [40]. The most commonly accepted sequence of events in smooth muscle contraction is as follows:

In the resting state myosin is detached from actin, and the myosin binding site on actin is not available. After stimulation of smooth muscle the myosin binding site in the actin become available. The resting myosin is activated first through phosphorylation of its regulatory light chain, and an ATP molecule attaches at its ATP binding site located in

its head. This leads to the reorientation of myosin, leading to its interaction with the myosin binding site in actin.

The sequence of the contractile process could be summarized as follows:

1. Phosphorylation of the regulatory light chain on the myosin (fig 1.5. a): The myosin light chain kinase (MLCK) is activated through the Ca^{2+} -calmodulin complex. Once the MLCK is activated it phosphorylates the regulatory light chain of the myosin. This step is crucial for the interaction of SM myosin with actin.
2. ATP hydrolysis (fig 1.5. b): The myosin head has an ATP binding site, where the hydrolysis of ATP occurs. This hydrolysis reorients the myosin head.
3. Attachment of myosin to actin (Cross-bridge) (fig 1.5. c): the reoriented myosin head attaches to the myosin binding site on the actin and releases the previously hydrolyzed phosphate and ADP.
4. Power stroke (fig 1.5. d): the cross-bridge generates force that displaces the thin actin filament along the thick filament; this displacement generates shortening of the muscle which corresponds to contraction.
5. Detachment of myosin from actin (fig 1.5. e): after the power stroke, the stability of the cross bridge is disrupted by the binding of another molecule of ATP, and as a result the myosin head becomes detached from actin.

Figure 1.5: Smooth muscle contraction process [15]

The cross-bridge cycle corresponds to the physical interaction of myosin and actin, which generates displacement of thick filaments over thin filaments. This cycle in smooth muscle is strongly dependent on the activation of the MLCK which phosphorylates the regulatory light chain of the myosin. In addition to this phosphorylation step, the binding of a molecule of ATP is also needed to energize the myosin cross-bridge for the development of force. It has been proposed that myosin of smooth muscle can exist in two different states: phosphorylated and dephosphorylated [41-43]. Hai and Murphy suggested that in smooth muscle exists a second and slower cross-bridge cycle. This second state appears when myosin heads attach to actin and subsequently dephosphorylate, resulting in a more stable attachment. According to the four-state model of Hai and Murphy actin and myosin could be found during the contraction as follows: **A** actin (thin filament); **M** myosin (detached, unphosphorylated); **Mp** (detached, phosphorylated); **AMp** (attached, phosphorylated); **AM** (attached,

unphosphorylated). The cross-bridge is believed to move constantly between these states and its representation accounts to two different cycle speeds and a dependence of cycling speed on phosphorylation (Fig 1.6), due to the rate of detachment being lower from **AM** to **A+M** than **AMP** to **A+Mp**. The activation of the muscle initially drives the majority of cross-bridges to the fast configuration, but when the length is stabilized, the slow cycling configuration becomes prevalent [13, 41-43].

Figure 1.6: Four state model of Hai and Murphy (1988) [42]

Smooth muscle dysfunction is associated with a number of diseases, such as erectile dysfunction, vascular and respiratory disorders etc. [7, 44-47]. ASM plays an important role in a number of respiratory diseases, such as asthma [7] and chronic obstructive pulmonary diseases [44]. Many of these are chronic diseases with no known cures.

1.5. Thesis structure

This thesis intends to cover in the following chapters: Current knowledge on asthma and its therapies (chapter 2); Animal models and sensitization protocols, in order to generate asthmatic subjects for the study (chapter 3); Testing of superimposed oscillations (SILO) on intact airways (*in vitro*) from healthy and asthmatic subjects, to determine effect of these types of oscillations in these two types of airways (chapter 4); Techniques to evaluate bronchoconstriction *in vivo* and construction of setup to evaluate respiratory function in animal models (chapter 5); Testing of SILO *in vivo* on intact airways from healthy and asthmatic subjects, in order to compare response of ASM from healthy and asthmatic subjects in the presence of SILO *in vitro* and *in vivo* (chapter 6); and finally a chapter for the discussion and conclusions of the results (chapter 7).

1.6. Closure

This chapter presented the basis of the system that will be studied as well as some muscle components and their function. To understand how these components interact and change during asthma, it will be necessary to have more details on how asthma alters the basic structure of the airways. The next chapter will discuss these topics and present some information related with physiological oscillations and its impact on the airways.

Chapter 2

Asthma, ASM and mechanical response

2.1. Introduction

This chapter discusses asthma, its available treatments, airway remodelling and the effects of different breathing patterns. Relevant literature are cited and discussed and the main objectives of the research are spelled at the end of this chapter.

2.2. Asthma

Asthma is the most common respiratory disease and it is estimated that approximately one in six New Zealand adults has the condition of asthma. Some studies show that the prevalence of this disease has increased in the last 20 years [48], especially in children [49]. It is a chronic disease which is characterized by recurrent attacks of breathlessness, wheezing, chest tightness, shortness of breath, and coughing, but the frequency and severity of these symptoms vary from person to person. Symptoms may occur several times in a day or week in affected individuals, and for some people become worse during physical activity or at night. During an asthma attack, the lining of the bronchial tubes swell, causing the airways to narrow and reduce the flow of air into and out of the lungs. Recurrent asthma symptoms frequently cause sleeplessness and daytime fatigue [50]. The airway narrowing that occurs in asthma is caused by three major factors: inflammation, bronchospasm, and hyperreactivity. The inflamed tissues produce an excess amount of mucus, which blocks the smaller airways and contributes to a reduction in the lumen of airways. The constriction of the smooth muscle around the bronchial passages causes the reduction of the lumen of the airways.

In healthy subjects, an allergen challenge does not fully collapse the airways. In contrast, allergen challenge results in exaggerated airway narrowing at relatively low allergen concentrations in asthmatic patients. The increased response of the asthmatic airways is known as hyperreactivity, while the high sensitivity to low concentrations of allergens is termed as hypersensitivity of the airways, both collectively known as airway hyper responsiveness (AHR) [51].

An asthma attack can be caused by a number of factors such as exercise or allergen exposure. Asthmatic airways are characterized by many features, such as reversible airway obstruction, chronic inflammation, AHR, and airway remodelling. Airway remodelling corresponds to structural changes observed in the airway walls of asthmatic patients. The most common among these changes are epithelial proliferation [52], reticular basement membrane thickening, sub epithelial fibrosis, increase in vascularity, goblet cell hyperplasia and hypertrophy, and an increase in airway smooth muscle (ASM) mass.

2.3. Asthma Treatments

Traditionally the asthma symptoms have been treated using pharmaceutical bronchodilators and inflammation suppressors. Currently other alternatives have been developed, in order to reduce the drugs intake. In the following the existing treatments for asthma are discussed. The first section discussed medicinal treatments, while the second focuses on alternative, non-medicinal treatments.

2.3.1. Medicinal Treatments

Currently, there is no definitive cure for asthma, although medications can relieve the symptoms. Generally there are two types of medication: 1) bronchodilators that induce relaxation of ASM, e.g. Beta-2 adrenergic receptors agonists [4]; 2) agents that aim to prevent attacks by reducing inflammation of the airways, e.g. corticosteroids [49, 53]. Some of these drugs have shown notable side effects [5] some of which may be attributed to overuse of medication and some to difficulties with distribution of medicine in the lungs.

a. Beta-2 adrenergic receptor agonists

β_2 -adrenoreceptor agonists are a type of drug used to combat symptoms of asthma and other pulmonary diseases [54]. These types of drugs induce dilation of the airways through the activation of the β_2 -adrenoreceptors. The activation of β_2 -adrenoreceptors increases the formation of cAMP and activates different pathways that lead to bronchorelaxation [55]. According to its period of action these drugs could be divided into short and long acting β_2 -adrenoreceptors agonists.

The short acting β_2 -adrenoreceptors agonists include drugs such as salbutamol, terbutaline, and isoproterenol. These medications are useful in treating mild to moderate symptoms of asthma [56], and they are normally used for acute asthma attacks [57]. On the other hand the longer acting β_2 -adrenoreceptors agonists, such as salmeterol and formoterol, can be used regularly. They normally take longer to work but their effects last longer. These are particularly useful when the asthma symptoms appear during sleep [49, 58]. Some of these types of drugs are non-specific for adrenoreceptors subtypes, acting in different ways and on different receptors at the same time. An example is Isopreterenol which acts on β_2 and β_1 adrenoreceptors.

b. Corticosteroids

Corticosteroids are a type of steroid hormones that are commonly produced in the adrenal cortex. They are involved in a wide range of physiological systems. These drugs can be sub classified into two types of corticosteroids: the minerocorticosteroids and glucocorticosteroids, which are used in asthma. Corticosteroids drugs are widely used to treat different diseases such as asthma, especially in the treatment of children [49, 53, 58] . These drugs work by inhibiting phospholipase A2, which is an important pathway in the production of precursors for inflammatory response, inhibiting the action of the products of this pathway, such as leukotrienes and prostaglandins. These two molecules are released into an area during the inflammation, inducing dilatation and increasing permeability of the blood vessels, which can result in narrowing of the airways, increasing of mucus in the respiratory tract and increase of inflammatory cells. Corticosteroid drugs which inhibit this pathway can stop prostaglandins and leukotrienes from being formed [57].

2.3.2. Alternative treatments

Drug-free approaches include breathing techniques such as Buteyko [59] and continuous positive airways pressure (CPAP), which at best result in reduce dependency on medication. Also an invasive treatment, bronchial thermoplasty eliminates airway constriction, but requires expensive invasive techniques.

a. Buteyko breathing technique

The Buteyko method is a program that teaches patients to change their breathing pattern, in order to control the breathing and reduce the symptoms during an asthma attack. Dr. Buteyko noticed that subjects with airway disease breathe more heavily than others. He proposed a series of exercises based on healthy breathing, including breathing with low frequency and more controlled in comparison with asthmatic breathing patterns. This program has shown to decrease the intake of drugs, but it did not improve lung function. This may explain the lack of interest by physicians for this technique [59, 60].

b. Continuous positive airways pressure (CPAP)

This technique, widely used to treat sleep apnea, imposes a continuing flux of pressured air into the airways, in order to avoid the reduction of the lumen and the collapse of airways, consequently increasing the average lung volume. For overweight asthmatics, who also suffer from sleep apnea as a complication, this technique has shown improvement in quality of life, and has been correlated with a reduction of serum levels of inflammatory cytokines, chemokines, and vascular endothelial growth factor after the application of this technique [61-63].

c. Bronchial thermoplasty

This technique is similar to the bronchoscope clinical exam where a flexible tube is introduced into the airways. In this procedure the flexible tube emits radio frequency energy to specific sections of the airway wall to reduce ASM content. As a result the airways are less prone to contraction, which results in improved lung function and decrease in medicine intake. The cost, invasiveness and non-responders of this procedure limit the application to severe cases [64-66].

It seems that with our current knowledge, a definitive physical treatment of asthma is still distant, and still remains a necessity, especially because the current therapies mostly focus in the chemical pathways relieving the acute response during an asthma attack but does not consider the mechanical elements involved.

2.4. *Airway remodeling in asthma*

Remodeling is a dynamic process in which the extracellular matrix is deposited and degraded in response to a trauma, resulting in reconstruction of damaged tissue. Remodeling is characteristic to chronic asthmatics, due to the constant damage of the airways during the inflammatory process of the disease. The inflammation by itself is responsible for some features of asthma, including reversible bronchospasm, tissue injury and subsequent structural changes called remodeling [67], which alter the normal response of airways. These alterations are not currently treated by the traditional anti-inflammatory therapies [68]. Traditionally these changes had been observed in pathological analyses, and these changes have been confirmed *in vivo* using high-resolution computed tomography[69].

The structural changes include: increase in smooth muscle mass, change in the composition of the extracellular matrix leading to subepithelial fibrosis and increased vascularity. The increase in ASM mass includes hypertrophy (the increase in size) and hyperplasia (increase in number) of the ASM cells [7, 70]. The increased thickness of the reticular membrane has been described as a common and early feature in the pathology of asthma [71]. The epithelial basement membrane in the airways is composed of two layers, the basal lamina and reticular lamina, but only the reticular basal membrane is thickened in asthma. This membrane consists of type I, III and V collagen and fibronectin [72]. The thickness of the reticular membrane results from an increase in the deposition of immunoglobulins, collagen I and III, tenascin and fibronectin. The proteins are produced by activated myofibroblasts, which lead to subepithelial fibrosis. An increase in vascularity has been observed in humans and sheep [73]. Abnormal vessels characterized by oedematous walls and thickening of the sub endothelial basement membrane, have been found in airways during inflammatory disorders [74]. It has also been observed that the increase in the number of blood vessels is strongly related to the severity of asthma [73]. In some cases of airway remodeling goblet cell hyperplasia and hypertrophy and subsequent increase in mucus production has been found [67].

The remodeling process is induced by different mediators, which according to their specific pathways could lead to the features mentioned. The complex interplay of factors that contribute to remodelling includes different inflammatory factors, which are

produced by immune cells recruited to the inflamed airways. Among these inflammatory factors can be found; cytokines such as interleukins 5, 11 and 13 [72, 75], transforming growth factor β 1 [72], epidermal growth factor, fibroblast growth factor, the endothelial growth factor, elastase, endothelin, matrix metalloproteinases 2 and 9, and the tissue inhibitor of metalloproteinase 1 [67], and tryptase [76] etc. These factors can stimulate epithelial cells, fibroblasts, and smooth muscle [77].

2.5. *ASM and asthma*

As described previously in this chapter there are three main factors responsible for the narrowing of the airways during an asthmatic attack, these are: AHR, inflammation and intermittent airways constriction (bronchospasm). Even though these three factors have been the focus of many studies in the past, airway smooth muscle is considered the main effector of the narrowing of the airways. Narrowing has been observed to occur either in the presence or absence of inflammation showing how important ASM is during an asthma attack [7]. ASM has shown an exceptional capacity to shorten its initial length by 80-90% when stimulated *in vitro*. Reduction of length at this level could easily result in complete closure of the airways *in vivo* [78], but complete airways closure does not appear to occur normally in healthy subjects.

Experimental data obtained by Martin et al and other groups [78, 79] suggested that alterations in the mass of ASM or changes in its contractile force may explain the excessive narrowing in asthma. Even though ASM is the main effector of airways narrowing, the interaction with other structures such constituents of the airway wall and lung parenchyma could also be important. In special, it needs to be considered that cyclical stress applied to ASM by physiological phenomena such as tidal breathing or deep inspiration help to maintain the airways dilated. Biochemical changes and alterations in the dynamic properties of ASM occurring during the development of the disease seem to increase the ASM resistance to the dilating influence of breathing and deep inspiration.

2.6. *Mechanical oscillations*

Different oscillations are constantly present affecting our body, some of them coming from external sources and others produced by different physiological phenomena. Among the oscillations resulting from physiological phenomena, include the

oscillations generated by the breathing process which affect the thoracic box. Volume changes associated with breathing have been shown to result in changing airway diameters [80]; and thus generate length changes in the ASM [7, 21]. Length oscillations for the purpose of this project will be defined as the application of external sinusoidal length change on ASM. Several studies have shown that a control over this length change can induce “bronchoprotective response” and “bronchodilation response” in contracted airways from healthy subjects [21, 26, 36, 81].

2.6.1. Oscillations and ASM

During breathing the lungs contract and expand, which results in changes of the airway wall diameter. Consequently the ASM in the airway is exposed to continuous length changes. Assuming that airway compliance is similar to total lung compliance, then ASM length oscillation can be derived from the cube root of the lung volume changes ($\sqrt[3]{\Delta V}$) as suggested by Hughes et al and Fredberg et al [80, 82]. Values have been calculated to be about 4% for normal breathing and about 25-30% for deep inspiration [36]. It has been hypothesized that these oscillations have the ability to disrupt the crossbridge cycle [10]. Alternatively temporal rearrangement of the contractile apparatus may occur, which may also result in force reduction during the contraction (relaxation).

For purpose of this research the length changes observed during the normal breathing will be called as tidal oscillations (TO), and that observed during the deep inspiration as deep inspiration (DI) oscillations.

a. Tidal oscillations

Several studies have shown that the application of TO (4% amplitude) either mechanically [13, 82, 83], or as volume oscillations in different portions of airways [84, 85] result in some form of relaxation in healthy subjects. TO is capable of reducing constriction when applied before stimulation i.e. a bronchoprotective response, and also relaxing muscle when applied during contraction i.e. a bronchodilation response. Also tidal oscillations have been shown to induce similar levels of relaxation in pre-contracted ASM compared to medicinal bronchodilators such as Isoproterenol [10, 84].

b. Deep Inspiration

Length oscillations that mimic DI have the ability to dilate airways [8] previously constricted by chemical stimulation [86-90]. The application of DI oscillations applied before a contraction reduces the subsequent response (contraction) of the ASM with allergen challenge [88, 91] (Fig 2.1). These mechanisms seem to be related with cytoskeletal reorganization [26]. However, in asthmatic subjects the beneficial effect of deep inspiration is absent [7, 85, 92]. When DI oscillations are applied in asthmatic patients, the response of their airways varies according to the severity of the asthma, resulting in an increase in constriction in severe cases of asthma and only a mild dilation in less severe cases [7, 36].

Figure 2.1: Bronchodilation and bronchoconstriction in response to deep inspiration [26]

Even if DI and TO have shown utility treating pre-contracted smooth muscle *in vitro* from healthy subjects, the response of the asthmatic airways under these dynamic condition seems to be altered and ineffective [7]. However other frequencies or wave types may give better results in asthma [93, 94].

c. Other oscillations patterns

It has been established that imposition of periodic load fluctuations on smooth muscle inhibits development of active force and stiffness [95], and that length oscillations cause long term (>30 min) reductions in isometric force when ASM is allergen challenged after the cessation of oscillations [96]. The Institute of Biomedical Technologies

(IBTec) has conducted several *in vitro* tests on porcine tracheal smooth muscle, subjecting them to frequencies of 0.2-80 Hz and amplitude of 2-8 % of reference length [16]. This specific length corresponds to the length in which the smooth muscle generates the higher contraction in the presence of bronchoconstrictors, after several stretches and induced contractions [13, 16, 97]. In this proposal, the amplitudes of oscillations are expressed as percentage of the reference length. Muscle contractile force reduction has been observed up to 40% at frequencies above 20 Hz and amplitudes of 6 % [16]. It has also been shown that the force reduction observed in ASM has a strong dependence on oscillation amplitude and a weak dependence on oscillation frequency [13].

d. Superimposed oscillations

Several groups have studied the response of ASM in the presence of oscillations that mimics breathing and deep inspiration [7, 8, 10, 16, 36, 81, 82, 84, 92, 93, 98], but little is known yet about the effects of superimposition of length oscillations on breathing patterns. Superimposed oscillations on isolated pre-contracted healthy porcine airways with frequencies in the range of 10-30 Hz and an amplitude of 1%, have been tested previously by our group [83], showing improvement of the relaxation observed.

2.7. Summary and objectives

Several groups focussing on airway smooth muscle and asthma have studied the effect of different types of bronchorelaxant drugs in the treatment of this disease. In the last couple of decades other groups have also started to focus not only on the chemical pathways but also on the mechanical properties of the airway smooth muscle and the effect of breathing oscillations on ASM [8, 10, 13, 16, 18, 21, 26, 36, 85, 97]. Studies have shown that the application of oscillations mimicking physiological processes such as breathing and deep inspiration can induce relaxation in contracted airway smooth muscle [8, 10, 13, 18, 36, 85, 97]. These findings suggest that these oscillations could be acting directly on the dynamic process of the contraction and more specifically on the cross-bridge cycle [7, 10, 11, 36, 97]. However, more evidence is needed. Some issues with the existing studies regarding the effect of oscillations on ASM are:

- (1) It is assumed that the relaxation of contracted airways is due to the direct effect on the crossbridge cycle, when it could be more related to an adaptive response of the tissue [26]
- (2) Most of the studies have been carried out in isolated smooth muscle, which ignores other structures which may play a role during asthma attacks such as cartilage, parenchyma, etc.
- (3) Most of the experiments have been done in tissues obtained from healthy animals, even though it has been proven that these oscillation patterns act differently in asthmatic smooth muscle [7, 8, 36]
- (4) Most studies have focussed only on physiological oscillation patterns of deep inspiration and breathing [36, 84, 85, 97, 99]
- (5) Not many studies have been conducted in the presence of bronchodilator medication.

With regards to the aforementioned points, this study is the first of its kind to take into consideration the effect of non-physiological mechanical oscillations on sensitized airways. The novelty of this research is that it combines traditional oscillations on these types of airways in combination with super imposed length oscillations (SILO), which gives a more realistic scenario of how these oscillations affect ASM to reduce assumptions in asthmatic models.

This project aims to investigate the effect of different types of mechanical oscillations in contracted airway smooth muscle such as: physiological oscillations, imposed oscillations, different wave types etc., in order to demonstrate their relaxant effect. This goal is expected to be fulfilled through the following steps:

1. Testing of superimposed length oscillations (SILO) on intact tissue from healthy airways.
2. Generation of asthmatic model in order to observe and compare the effect of SILO on healthy and asthmatic (sensitized) airways.
3. Testing the effect of SILO on intact airways from healthy and asthmatic subjects in static conditions (*in vitro*).
4. Testing the effect of SILO on intact airways from healthy and asthmatic subjects in dynamic conditions (*in vivo*).

The understanding of how mechanical oscillations affect the airways *in vitro* and *in vivo* on sensitized subjects is important to fully understand the dynamic response of airway smooth muscle, in order to develop new therapies for asthma.

2.8. *Closure*

The need arises here during a severe asthmatic attack, an inhaler may be ineffective, putting the patient in severe risk of hypoxia, which if untreated could lead to brain death due to lack of oxygen [100]. A possible solution is to use oscillations at a specific frequency and amplitude, induced into the affected area of the airways which has proven to be able to relax pre contracted smooth muscle from healthy subjects [10, 81-84, 98, 99, 101], but studies carried on asthmatics subjects using physiological oscillations have not been as effective inducing the same relaxation observed on healthy airways [7, 102]. To our best knowledge, only physiological oscillations similar to those occurring during breathing have been tested on asthmatics airways [7, 36]. This study hypothesize that oscillations are capable to disrupt the interaction between myosin and actin during the contraction even on asthmatic airways, but most likely the parameters to be used need to be different to those occurring during breathing, because of all the changes occurring on the airways during the remodelling and adaptation of the airways during the development of this disease [24, 33, 35, 51, 52, 67, 68, 70, 71, 79, 89, 102-104]. Superposed oscillations seem to be an interesting alternative because they do not completely change the breathing patterns but they modulate the breathing waves, so different superposed oscillations should be tested. Since this is a novel study and cannot be carried out on humans, the testing needs to be carried out first *in vitro* using ASM from healthy mice and sensitized models mimicking the disease (Chapter 4) and after this stage it would be needed to be tested *in vivo* (Chapter 5), but in order to proceed with these two experiments an asthmatic animal model needs to be developed (Chapter 3).

Chapter 3

Animal model and sensitization

3.1. Introduction

Studies in animal models form the basis for much of our current understanding of the pathophysiology of asthma [103, 105-118]. Animal models are an invaluable tool that allows studies to be conducted in the setting of an intact immune and respiratory system. These models have highlighted the importance of Th-2 type driven allergic responses in the progression of asthma, and have been useful in the identification of potential drug targets for interventions involving allergic pathways.

Animal models are a great tool in the study of different diseases, helping us to characterize and understand in a better way their physiopathology, but a model must fulfil some requirements to be considered a good model of the pathology in study. This chapter covers: animal models available for respiratory studies; the animal selected for this study, the characteristics which determined the choice of model; functional evaluation of respiratory system; results and discussion.

3.2. Animal models

The range of animal models available is vast. The most popular models are rodents such as inbred mice, rats and guinea-pigs. Rodents have the benefit of being easy to handle and being relatively cost effective compared to other animals [105, 106, 118]. Mice present advantages for physiological studies of asthma: because of their size, short cycles of breeding and the existing data and expertise in working with them. The recent advances in transgenic technology and the development of species-specific probes, particularly mice, have allowed detailed mechanistic studies to be conducted [119]. Also some larger animal models such as sheep and dogs have been developed, but they are very costly, with few probes available for characterizing allergic responses in the airways in these species [118, 120]. Despite these advances in technology, there are a number of issues with current animal models for asthma that must be considered. Some of these are the differences in immunology and anatomy between mice and humans, the requirement of adjuvant during sensitization in most models which could be induced by

its own immunological response, and the acute nature of the allergic response. No animal model completely captures all features of human asthma; however research has focused more in the immunological response, rather than emulating all features of the human asthma, by sensitizing and challenging animals with a variety of foreign proteins. These types of methodologies have led to an increased understanding of the immunological factors that mediate the inflammatory response [72, 107, 121] and its physiological expression in the form of airways hyper responsiveness (AHR) [51, 89].

3.3. Selection criteria

To study asthma in animal models, the criteria which define a good animal model of asthma needs to be considered, such as:

- Sensitivity mediated by IgE to the antigen that results in bronchoconstriction
- Increased airway resistance
- Chronic inflammation of the airways characterized by increase of eosinophiles and cytokines
- Non-specific hyper responsiveness
- Excessive production of mucus associated with goblet-cell metaplasia and hypertrophy of the submucosal glands
- Tissue remodelling including thickening of the collagen layer beneath the basement membrane and smooth muscle hyperplasia [106]

Unfortunately there is not a single model that unites all these criteria; however different models have been proposed to study different features of asthma.

The design of a sensitization protocol to develop an animal model has to take into account technical details such as the type of allergen, use of adjuvants and the method of administration of the allergen. Common types of allergens used are Ovalbumin (OVA) and House Dust Mite (HDM) as well as custom made allergen mixes. OVA is the most popular antigen as it is readily available and the animal can be easily prevented from any prior exposure through the environment [118, 122]. Adjuvant such as Alum, heat killed *bordetella pertussis* and ricin are used to improve the immunological response against the allergen. Among the adjuvants alum is most commonly used as it promotes and improves the response against the allergen, but has the inconvenience of inducing an immunologic response by itself [118]. The allergen can be administered by different methods, among them are intraperitoneal (IP) injection; subcutaneous (SC)

injection and aerosolization. The choice of protocol of sensitization will depend on the features of asthma that need to be present in the model.

3.4. Asthmatic models

There are two types of asthmatic models, acute and chronic model. The terms “acute” and “chronic” are referring basically to the duration of the exposure of the animal model (mice) to the allergen.

3.4.1. Acute model

The acute asthma model is a short term protocol, where the duration of sensitization is between 3 and 6 weeks [108, 123-130].

The symptoms of asthma obtained from this protocol are:

- Airways Hyper Response (AHR) [108, 124-130]
- Inflammatory response involving an increase of IgE; IL-4; IL-5; LTh2; IFN γ , eosinophiles and mastocytes [108, 123-130],
- Hyperplasia and hypertrophy of calciformes cells [129, 130].

However, there are also some disadvantages to this model: The distribution of pulmonary inflammation in the animal model is different than in human asthma; also because of the short-term nature of the acute models, many of the lesions observed in chronic human asthma, such as chronic inflammation of the airways, and airway remodelling are absent. Furthermore many of the key features appear to be short-lived and, in some models, airway inflammation and AHR have been shown to recover after a couple of days following the final allergen challenge.

3.4.2. Chronic model

The chronic asthma model is a long term protocol where the duration of the sensitization is more than 2 months [103, 108, 117, 127, 129, 131, 132].

The features of asthma obtained from this protocol are:

- Allergic inflammation characterised by eosinophilic influx into the airway mucosa [103, 127, 129, 132]
- AHR [103, 108, 122, 129].

In addition, some chronic asthmatic models present:

- Airway remodelling with goblet cell hyperplasia, epithelial hypertrophy, and either subepithelial or peribronchiolar fibrosis [122, 127, 129, 131, 132].

It is different from the acute model such that some of the key features of the chronic allergen exposure models persist after the final challenge [127, 129], and the persistence of AHR and lung inflammation vary depending on the exposure protocols employed [133]. This protocol presents some disadvantages, particularly when using OVA, because a long-term challenge might lead to the development of tolerance to the allergen. The tolerance to the allergen corresponds to an adaptive process of the ASM that leads to a lower contraction in the presence of allergens. The increased tolerance might be related to the high mass concentrations of the aerosolized allergen used, which could overwhelm the clearance mechanisms. [122].

3.4.3. Mouse anatomy

This section aims to cover the physiology of mice which will be used in the development of the asthmatic model to be used for the study. Fig 3.1 shows the anatomy of the mouse upper airways and a brief explanation for each of the components is presented in this section [134].

Figure 3.1: Mice upper airways anatomy [134]

a) Pharynx and Epiglottis

The pharynx is connected to the nasal and oral cavities and contains the entrances to the Eustachian tube, the larynx and the esophagus. The epiglottis closes off the entrance to the larynx in order to prevent choking.

b) Larynx

The larynx extends from the pharynx to the trachea and the epiglottis is located at the border of the larynx and pharynx. The wall of the larynx is formed by respiratory epithelium from the inside through to the outside, which consists of a lamina propria rich in elastic fibres and glands, cartilages and vocal cords and loose connective tissue adventitia.

c) Trachea

The mouse trachea is a flexible tube connecting the larynx to the primary bronchi and containing several incomplete hyaline cartilage rings whose ends are joined by smooth muscle.

d) Lungs

The lungs of the mouse are covered by visceral pleura and like the lungs of the rat, they consist of an undivided left lung and a right lung divided into four lobes as observed in Fig 3.2. The primary bronchi (the division of the trachea) are the only bronchi in the mouse that contain cartilage and are lined by respiratory epithelium. Subsequent branches of the bronchial tree are the smaller intrapulmonary bronchi, the terminal bronchioles, and the respiratory bronchioles. As the airways get smaller their epithelium becomes more simplified and their walls become thinner with less connective tissue and smooth muscle.

e) Ventilation

The average mouse will have a normal breathing rate of around 150 breaths per minute and a tidal volume between 0.15 and 0.2 ml. Therefore using an approximation that the dead space will be 30 percent of the tidal volume (approximation used for humans), the dead space will be approximately 50 μ l.

Figure 3.2: Mice lower airways [134].

3.5. Asthma assessment techniques

To evaluate if the animal model has become asthmatic after the respective sensitization protocols, a number of techniques are available. In this section several techniques for the study of pulmonary function in mice are discussed.

3.5.1. Pulmonary function in mice - mechanical test

There are different techniques to assess pulmonary function in mice, which can be categorized as invasive and non-invasive [135].

Invasive techniques are normally used in anesthetized animals, due to the requirement of intubation, tracheotomy and expert handling. These techniques are used to measure pulmonary mechanisms in mice, and include the determination of parameters such as: lung resistance (R_L) and dynamic compliance (C_{dyn}) which are specific parameters to detect bronchoconstriction [135-137]. The determination of R_L and C_{dyn} can be done in tracheotomised mice; however this allows only one measurement per animal. Alternatively, orotracheal intubation of mice can be performed multiple times and allows for the measurement of the same variables [136], an scheme presented by Glaab et al of oreotracheal intubation and invasive plethysmography is presented in Fig 3.3. Another technique to assess respiratory function corresponds to low-frequency forced oscillation technique; This technique was initially used in humans and larger animals and produces estimates of lung impedance (Z) which is considered the most detailed measurement of pulmonary function currently available [135].

Figure 3.3: Invasive plethysmograph [136]

Non-invasive plethysmographic methods to monitor pulmonary function are preferred for long-term serial study designs, as well as for screening large numbers of conscious mice. The plethysmograph is a device used to measure changes of volume in the lungs. This instrument is usually used to measure functional residual capacity (FRC) of lungs and also the total lung capacity. In asthma dose-response studies, this technique is used to measure bronchoconstriction that is reflected in the enhanced pause parameter (Penh) [135], which is a unit-less index of AHR. There are two types of plethysmography: whole-body plethysmography (WBP) where the mice are placed in a closed chamber and the pressure fluctuations that occur during the breathing cycle are recorded; and the head out body plethysmograph where the mice are placed with the head outside of the plethysmograph. Both techniques present advantages over invasive techniques, particularly that the mice can be awake during measurements and repetitive measurements are possible. However the trade-off is a greater uncertainty about the exact magnitude and localization of bronchoconstriction and how much of the allergen is delivered to the airways, although none of the in vivo techniques can assess how much of the allergen reaches the target airways. An example of non-invasive technique is shown in Fig 3.4.

Figure 3.4: Non-invasive methods: Whole-body plethysmography [135]

A non-invasive technique such as the WBP seems to be a more practical approach for the present studies, due to the fact that asthma attacks occur in conscious subjects and relatively often. However, there are considerable differences in accuracy compared to invasive procedures. In some cases invasive and non-invasive techniques must be performed in parallel to fully understand the phenomena under study.

Considering all the information above and the requirements for the experimental protocols, it was decided to proceed with a more invasive approach using R_L and C_{dyn} , which are considered one of the best parameters to evaluate bronchoconstriction. In order to obtain these parameter also other set of respiratory parameters need to be measured.

3.5.2. Pulmonary Resistance Parameters

Considering that the methodology selected for this study is based on the measurement of R_L and C_{dyn} as indicators of level of bronchoconstriction, others parameters also need to be measured in order to obtain them. This section will cover all the pulmonary resistance parameters and explain how they are measured and calculated [135, 136, 138].

a) Tidal air flow

Measurement of the airflow as the mouse breathes is accomplished with the use of a pneumotachograph meter, which has a flow restriction in middle similar to a venturi tube as observed in Fig 3.5. The pressure difference across this constriction is translated to a low pressure transducer and the data analysed on a computer. This signal from the transducer corresponds to the tidal airflow (V) through the breathing cycle of the mouse.

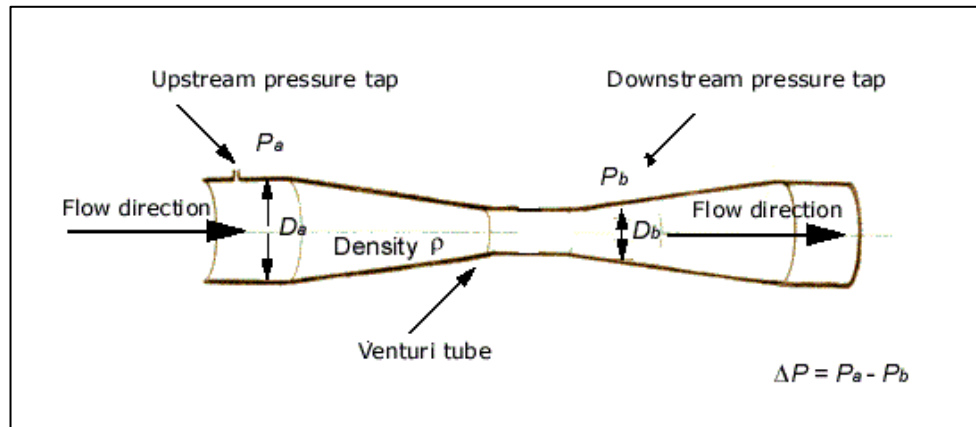


Figure 3.5: Scheme for venturi.

b) Tidal Volume (T_v)

When the tidal flow rate is known over a particular period, say one breathing cycle. The tidal volume (T_v) of the mouse as observed in Fig 3.6, can then be found by simply integrating the tidal flow over the specific time period. Software can be used to continuously monitor the tidal air flow, and continuously calculate the tidal volume as the mouse keeps breathing and as the tidal air flow changes.

c) Tracheal pressure (T_p)

This is the change in pressure observed and recorded at the level of the animal mouth during the breathing process (inspiration – expiration)

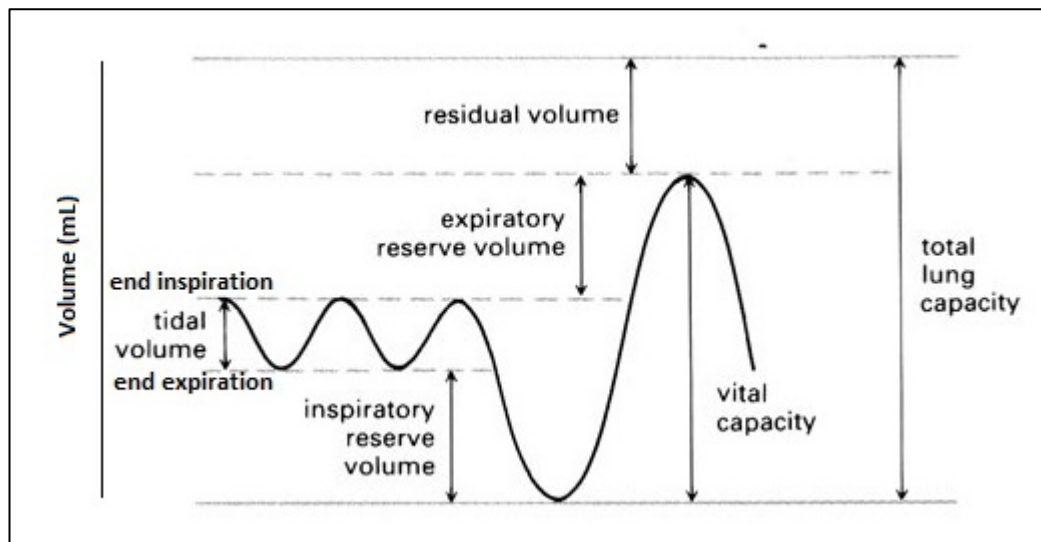


Figure 3.6: Lung volumes occurring during breathing.

d) Transpulmonar Pressure (P_{tp})

Transpulmonar pressure (P_{tp}) corresponds to the difference of the pressures registered at the level of the lungs before inspiration and at the end of expiration.

Measuring the transpulmonar pressure (P_{tp}) however, is a complicated task. In order to obtain this measurement, a fluid filled catheter is inserted into the esophagus of the mouse to the level of the mid-thorax [136]. This tube must then be connected to a pressure transducer. The way this works is that, when the tube is inserted at just the right location in the esophageal tube, as the lungs expand and contract, the fluid in the tube is displaced, which will cause a volume change in the tube, which in turn will give a pressure reading through the transducer that corresponds to the transpulmonar pressure of the mouse. Placing the esophageal tube in just the right location along the trachea is essential and can only be achieved by experimentation, adjusting the location until a maximum value is reached.

The data from the transducer is then sent to a computer, which can then continually monitor the difference in the pressures occurring during breathing, which will give out the reading of transpulmonary pressure.

e) Dynamic Compliance (C_{dyn})

Dynamic compliance (C_{dyn}) is calculated as tidal volume over transpulmonary pressure, from the end of the previous cycle to the end of the present respiratory cycle [14]. Using relevant software and programming, the computer can determine C_{dyn} when P_{tp}, and T_v are known.

$$C_{dyn} = T_v / P_{tp} \quad (Eq. 3.1)$$

f) Pulmonary Resistance (R_L)

Pulmonary resistance (R_L) is the opposition of the respiratory tree to air flow. A person who is undergoing an asthmatic attack will have narrow airways and will therefore have a larger pulmonary resistance due to the larger opposition to flow. This is why R_L is essential when carrying out studies on mice, as it gives insight into whether a certain treatment for asthma will reduce R_L or have no effect.

When all of the parameters discussed above are known, the R_L can be found as follows:

$$R_L = P_{tp} / \text{Flow} \quad (Eq. 3.2)$$

Determining the pulmonary resistance of mice during spontaneous breathing, after anaesthetisation and intubation is essential in the study of implementing a solution to asthma. Knowing the pulmonary resistance before and after an aerosol challenge, as well as before and after a solution is applied to the mouse will determine if the airways begin to relax and expand, and will confirm if a specific treatment is working.

3.5.3. Airways response - Chemical evaluation

Not only mechanical assessments can be performed to observe AHR and changes on the airways, chemicals test also can report successfully sensitization of the animal models. Some of these techniques evaluate immune response (ELISA) or cellularity changes in the airways (BAL), which in the case of increased IgE levels in serum and the presence of WC (white cells) in airways would indicate a successful sensitization.

a) ELISA (IgE determination)

Enzyme-Linked Immunosorbent Assays (ELISA) are the most widely used type of assay. They have evolved from viral lysate tests to tests containing recombinant protein and synthetic peptide antigens [49, 50]. This technique is widely used to determine levels of different antibodies present in the different fluids of live organisms when a disease is present [139-141], i.e. high levels of IgE are commonly observed in asthmatic subjects [105, 106, 110, 118].

b) Broncho-alveolar lavage (BAL)

Bronchoalveolar lavage (BAL) is a minimally invasive procedure performed during flexible fiberoptic bronchoscopy to obtain a sample of alveolar cells. Analysis of BAL cell counts, cytology, and culture provides insights into immunologic, inflammatory, neoplastic, and infectious processes occurring at the alveolar level [142, 143]. The presence of increased cellularity not typically observed in BAL from healthy airways is considered a good marker of pathology on the airways.

3.6. Pilot group

As first stage of the project it was decided to develop an acute asthmatic model using a classic Ovo-albumin (OVA) based sensitization protocol, with two stages of exposure to the allergen and with addition of adjuvant at one of the stages. This was done in order to study how asthmatic airways behave under different experimental conditions, such as contraction induced by chemicals and relaxation induced by drugs and mechanical oscillations in physiological and non-physiological ranges. The strain selected for purposes of this study was one of the most reactive mouse strains known for respiratory studies; the mouse strain Balb/c [108, 109, 144-146]. This strain is widely used to study airways responsiveness and it has been observed that female mice in the age range of 8 – 12 weeks are more reactive to the exposure to allergen than males and other mice strains.

3.6.1. Experimental group

Two groups of mice 1) asthma model and 2) control group were prepared in order to test the acute model and obtain the first set of data. These two groups were formed in order

to test *in vitro* the effect of mechanical oscillations on pre constricted airways alone and in combination with bronchodilators.

a) Control (healthy) Group

This group was only under controls of weight and general health. It did not go through any injection or nebulization of the allergen. Table 3.1 presents the details for the protocol presented in Fig 3.7.

Table 3.1: Details of sensitization protocol for control group.

| Protocol details | |
|-------------------------|--|
| Mice | BALB/c; Female; 8-12 Weeks old |
| Allergen | None |
| Adjuvant | None |
| Anesthetic | Ketamine and Xylazine |
| Challenge | Ach (10^{-2} M) |
| Via of Administration | None |
| Sensitization (Fig 3.5) | <p>Days</p> <p>0 Control of weight and general health.</p> <p>7 Control of weight and general health.</p> <p>14 Control of weight and general health.</p> <p>Days</p> <p>24 Control of weight and general health.</p> <p>28 Control of weight and general health.</p> <p>32 Control of weight and general health.</p> <p>Day</p> <p>33 Experimental protocol</p> |

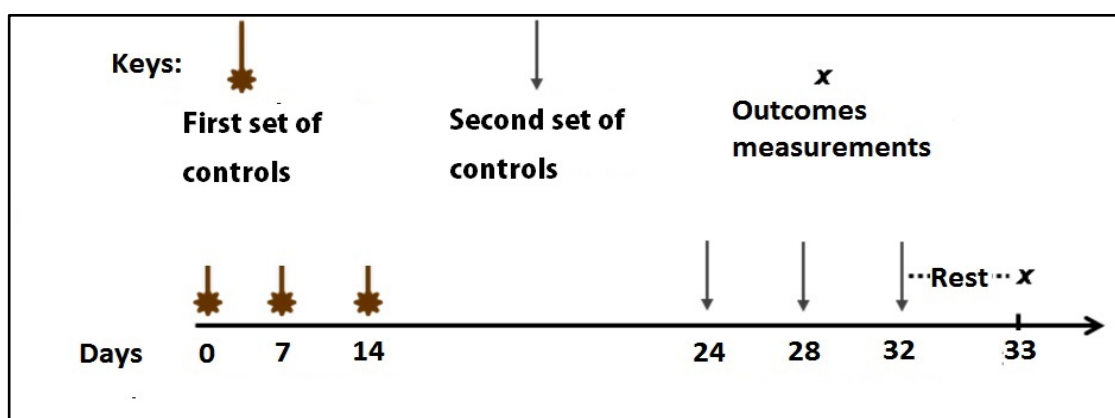


Figure 3.7: Control protocol, the weight and the behavior of the mice was checked on day 0, 7 and 14 and later on 24, 28 and 32 before the experimental protocols.

b) Acute asthmatic model

This model is a short term sensitization protocol, which will be close to one month in duration, using OVA as allergen (allergen). The allergen will be prepared in the presence of alum which acts as an adjuvant, increasing the immunological response of the mouse. The allergen will be administrated via intraperitoneal injection and nebulisation. With this model the objective is to observe the short term response of ASM to the allergen such as inflammation markers and initial changes in ASM. Table 3.2 presents the details for the sensitization protocol presented in Fig 3.8.

Table 3.2: Details of sensitization protocol for asthmatic group.

| Protocol details | |
|--------------------------------|--|
| Mice | BALB/c; Female; 8-12 Weeks old |
| Allergen | OVA |
| Adjuvant | Alum (Aluminum hydroxide) |
| Anesthetic | Ketamine and Xylazine |
| Challenge | Ach (10^{-2} M) |
| Via of Administration | Intraperitoneal (i.p.) and Inhalation (inh.) |
| Sensitization (Fig 3.6) | <p>Days</p> <p>0 Injection of OVA at 10µg diluted sodium chloride 0.9% (saline) + 1mg aluminum hydroxide mixture (i.p.).</p> <p>7 Injection of OVA at 10µg diluted sodium chloride 0.9% (saline) + 1mg aluminum hydroxide mixture (i.p.).</p> <p>14 Injection of OVA at 10µg diluted sodium chloride 0.9% (saline) + 1mg aluminum hydroxide mixture (i.p.).</p> <p>Days</p> <p>24 Aerial nebulization of Ova at 5% diluted in saline through the airways for 20 mi</p> <p>28 Aerial nebulization of Ova at 5% diluted in saline through the airways for 20 mi</p> <p>32 Aerial nebulization of Ova at 5% diluted in saline through the airways for 20 mi.</p> <p>Day</p> <p>33</p> |

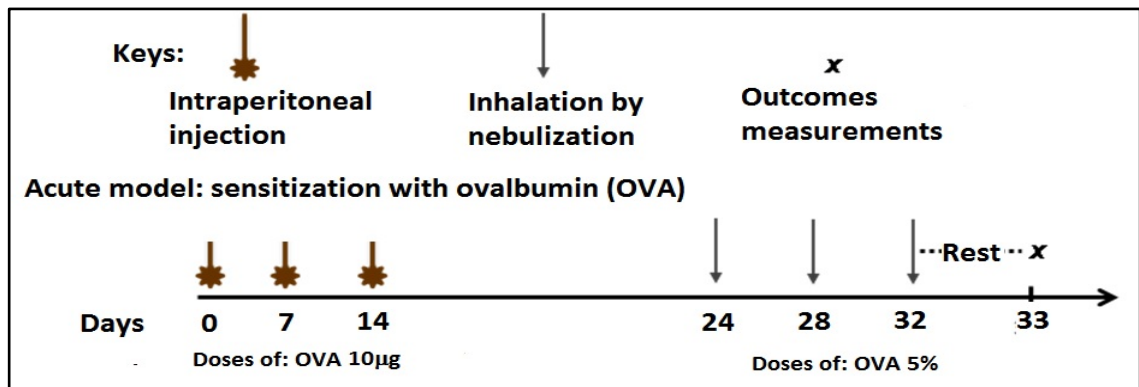


Figure 3.8: Sensitization protocol: The sensitization protocol was divided in two stages: first stage; induction of immunoresponse (injection of allergen) from day 0-14 and a Second stage; induction of AHR (nebulization of allergen) from day 24-32.

3.7. Selected Techniques to evaluate the model

The acute asthmatic was evaluated to determine if the sensitization process was successful. This was performed using different techniques, which evaluate AHR through bronchoconstriction using the respiratory parameters R_L and C_{dyn} and the increased immunological response with ELISA to determine IgE levels and bronchoalveolar lavage to observe cellularity changes in the airways. The combination of the mechanical parameters and chemical indicators provide a more reliable control to confirm the success of the sensitization protocol.

3.7.1. AHR / Plethysmography

Airway hyper responsiveness is measured in tracheotomized mice inside a custom-built thermoregulated Pneumotachograph/Plethysmograph setup. This system was developed and calibrated in house. Fig 3.9 shows a scheme of the modified plethysmograph (Details of plethysmograph and its modifications are presented in chapter 5).

The objective of this technique is to evaluate bronchoconstriction in the control, and sensitized animal model, by measuring the lung resistance and the dynamic compliance. These two parameters are considered as the most significant to evaluate bronchoconstriction in airways in this type of model. Through this technique we also expect to be able to evaluate the degree of AHR in both healthy and asthmatic mice.

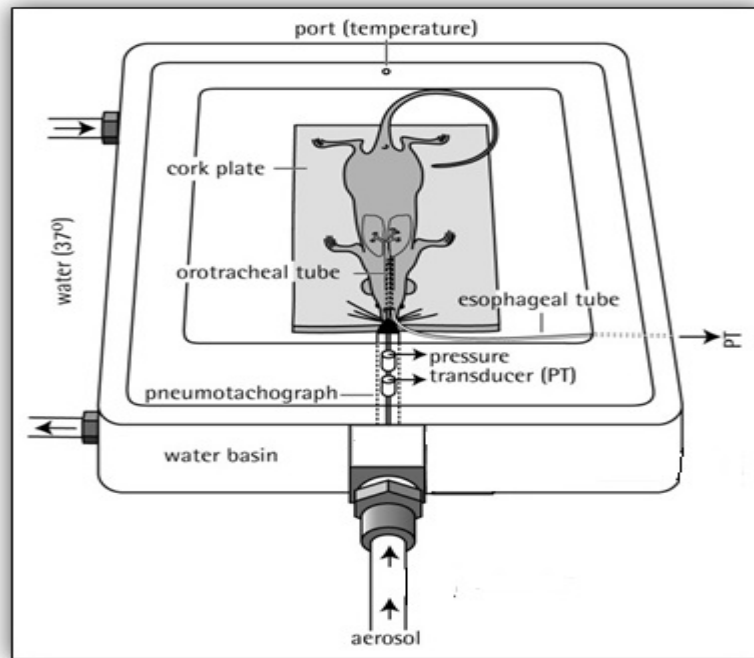


Figure 3.9: Sketch plethysmograph diagram (image modify from [136])

Protocol

Airway responsiveness is measured through the invasive determination of upper pulmonary resistance and the dynamic compliance (See section 3.5.2). Airway responsiveness is assessed as an increase in R_L after a challenge with aerosolized ACh in anesthetized and spontaneously breathing mice Balb/c. All the protocols were approved by the University of Auckland Code of Ethical Conduct (AEC) and performed in accordance with the Animal Welfare Act 1999 (attached in the appendix A).

- Mice are anesthetized with intraperitoneal injections of ketamine 40mg/kg and xylazine 10mg/kg (with minimal supplementations only if required).
- When anaesthesia was achieved, assessed by loss of the right and pinch toe reflex, the mice are placed on a plastic board and a quick surgical procedure was performed to reach the trachea (protocol detailed in chapter 4).
- Once the trachea is exposed a small hole is opened in between the trachea rings and a cannula is placed and fastened with silk thread.
- Following this the intubated spontaneously breathing mouse is placed in supine position in a thermo-controlled Plethysmograph/Pneumotacograph (Fig 3.10). This system has been designed to resemble the reference system used by Glaab et al [135,

136, 147]. Some modifications were made to the chamber (Size, inlets and outlets of the chamber) in order not only to fit mice but also rats (details of the system and its modification in chapter 5 sections 3 and 4), and similar transducers were used.

- The tracheal tube is connected directly to the pneumotachograph and the tidal flow is determined by the pneumotachograph which is connected to a differential pressure transducer.
- To measure transpulmonary pressure, a water-filled tube is inserted into the oesophagus to the level of mid thorax and coupled to a pressure transducer. The analogue signals obtained from this transducer were digitalized and recorded.

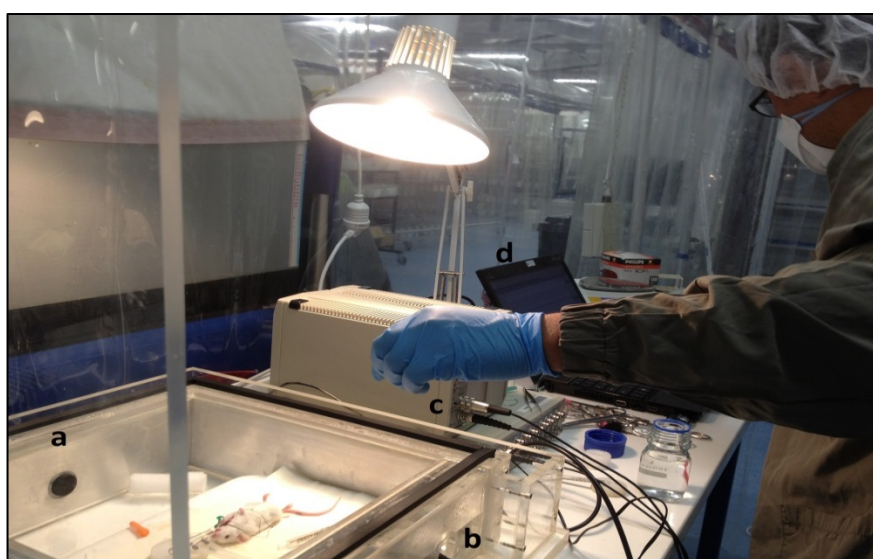


Figure 3.10: Overview plethysmograph and data acquisition system: a) testing chamber; b) pressure transducer; c) Data acquisition system; d) software.

- Different doses of bronchoconstrictor and bronchodilator are administered through the nebulizer which is connected to mouse lungs via the pneumotachometer. 5 ml of test solution (normal saline solution, or a specific concentration of Ach or ISO) is placed in the nebulizer tank (Fig 3.11).
- Each mouse was initially challenged for 2 min with saline solution. After 2 min of nebulisation, the nebulizer was switched off before recording the respiratory parameters for 10 min. The recording time corresponds also to a resting time for the animal since it will not undergo any additional treatment or manipulation during this time. After this, dose-responses for Ach and ISO were performed to determine optimal concentration of the drugs to be used).

- Airways responsiveness to Ach $10^{-2}M$ in all mice group was assessed to observe the response of ASM (this concentration was determined during the previous step and showed the higher contraction on the sensitized animals).
- This dose was tested several times and was administered before the addition of ISO (which was used to induce bronchodilation) as follows: nebulisation of Ach $10^{-2}M$ for 2 min followed by 2 min of rest; then nebulisation with ISO $10^{-6}M$ for 2 min followed by 2 min of rest; the previous step was repeated with ISO $10^{-5}M$, ISO $10^{-4}M$, ISO $10^{-3}M$, ISO $10^{-2}M$, ISO $10^{-1}M$ and ISO $1M$ and finally 2 min of nebulization of saline and 2 min of recovery.

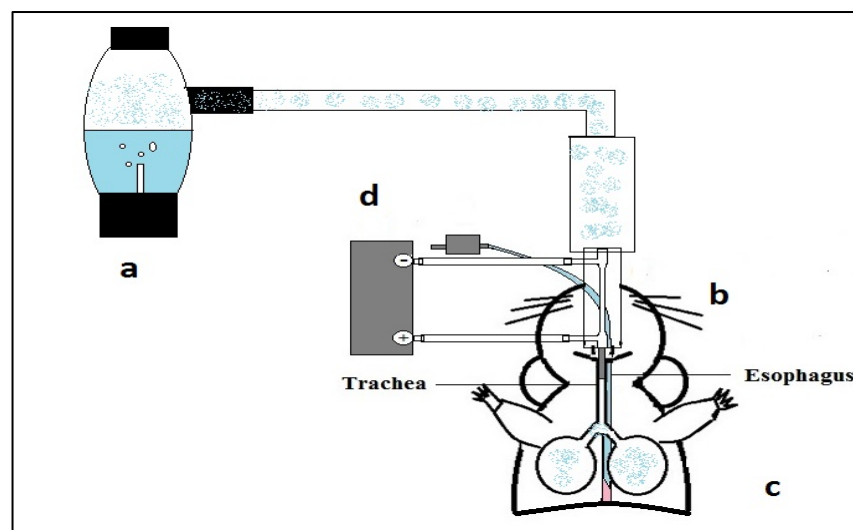


Figure 3.11: Scheme of connection of nebulizer and subject for drug delivery. a) Nebulizer and solution chamber for nebulization of drugs (ACh, ISO, saline); b) pneumotachograph; c) mice; d) pressure transducer.

3.7.2. ELISA (IgE)

As explained in chapter 2, in asthmatic models the levels of the antibodies IgE and IgG are increased. In order to confirm that our model is asthmatic the levels of these two antibodies were tested using a direct sandwich Enzyme Linked Immunosorbent Assay (ELISA) method. OVA-specific IgE levels will be determined in duplicate.

Protocol

- *Blood samples from the mice heart were obtained right after the experimental protocols and using coagulation and centrifugation, samples of serum were prepared from it and the stored at -80°C.*
- *Then IgE levels are quantify using the kit Mouse OVA-IgE ELISA from mdbioproducs (division of mdbiosciences) and compared between controls and sensitized.*

3.7.3. BAL

Bronchoalveolar lavage is a technique used to recover epithelial cells, proteins and leukocytes, which are normally present in the airways under pathological conditions. This technique involves successive lavages of the airways with physiological solutions. The volume of the mouse lung is small, so BAL in mice is generally performed with 1 ml syringes to infuse smaller volumes of fluid. Multiple infusions are required to obtain enough recovered fluid for multiple analyses. Once the BAL is successfully obtained, the cells are counted in neubauer chamber [148] and slides stained with hematoxylin and eosin are prepared to differentiate the white cells.

Protocol:

- *Lungs are cannulated in situ and washed with 1ml of saline (NaCl 0.9%) several times before collecting a representative sample of the airways.*
- *The solution collected from the lungs was placed into a cell chamber and observed at 40X for the presence of eosinophiles and epithelial cells and it was reported as follows:*

Presence of red cells (RC) and epithelial cells were observed and categorized as:

- + = *presence*
- ++ = *moderate presence*
- +++ = *plenty*
- (-) = *absence*

Slides were prepared from the BAL and stained with hematoxylin and eosin staining. White cells (WC) were counted and differentiated in a blinded fashion by counting 100 cells by light microscopy. The number of eosinophies was expressed as a % of the total WC.

3.8. Animal assessment

This section presents the data obtained from the different tests (Chemicals and mechanical) and their interpretation.

3.8.1. AHR

As shown in Fig 3.9 using R_L (cmH₂O/ml/sec) as indicator of bronchoconstriction *in vivo* a dose response test for Ach was performed. According to this, the best concentration to induce bronchoconstriction on our sensitized animals was of 10^{-2} M, even though 1M showed similar response (Fig 3.12), as per literature lowest concentration results in better practical results when combined with ISO [149], because higher concentrations tend to affect the response of the airways in the presence of ISO. Considering this finding, the concentration selected for future *in vivo* experiments will be Ach 10^{-2} M. This concentration differs from the one used on the experiments *in vitro* which was of Ach 10^{-4} M (data no shown). This concentration was also determined using dose response tests prior to define the experimental protocols.

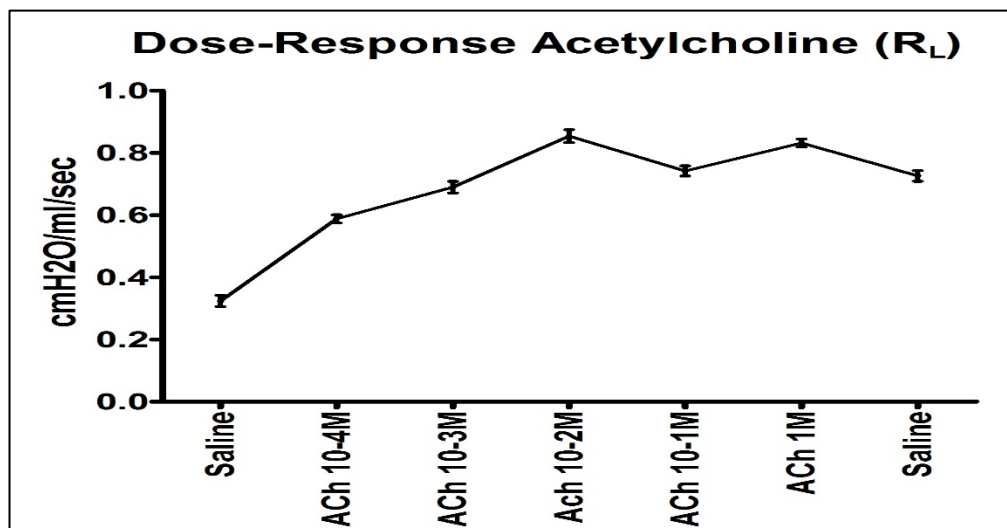


Figure 3.12: R_L for Ach dose-response asthmatic subjects: axis y corresponds to the value of R_L observed with the different experimental conditions presents in axis x ($n = 6$).

When similar dose response test was performed for ISO as shown in figure 3.13, it was found that several different concentrations provided similar reduction on the bronchoconstriction induced by Ach 10^{-2} M, these concentrations were 10^{-6} M, 10^{-5} M, 10^{-4} M and 10^{-1} M (Fig 3.13). Considering that all these concentrations reduce in similar manner the bronchoconstriction induced we decided to use the lower dose for our experiments, which was ISO 10^{-6} M

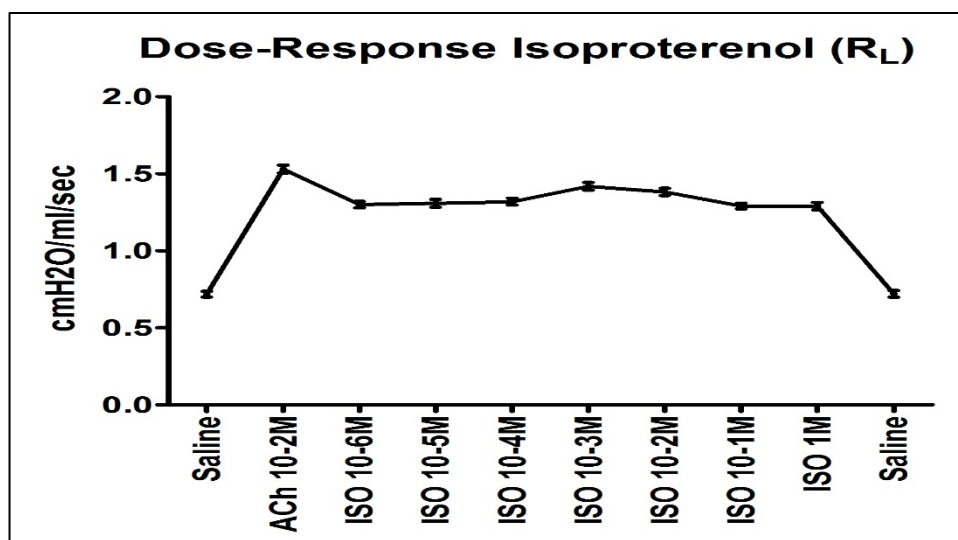


Figure 3.13: R_L for ISO dose-response asthmatic subjects: axis y corresponds to the value of R_L observed with the different experimental conditions presents in axis x ($n = 6$).

Using the concentrations mentioned and selected in the previous paragraphs a quick comparison between healthy and sensitized subjects was performed to observe any changes. We found using *t test* that sensitized airways were more responsive than healthy airways to Ach 10^{-2} M (p value < 0.01 vs p value 0.18 respectively as observed in figure 3.15) and that ISO 10^{-6} M was less effective to induce relaxation on precontracted airways from sensitized subjects when compared with healthy airways (p value 0.18 vs p value < 0.05 respectively as observed in figure 3.15) using same concentrations for Ach and ISO (Fig 3.14.). This behaviour was also observed later on in the *in vitro* tests (Data presented in chapter 4).

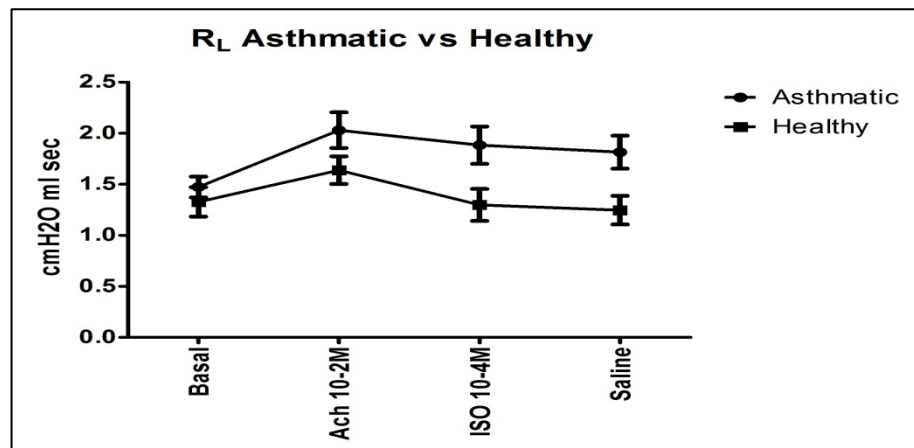


Figure 3.14: Comparison of R_L between asthmatic and healthy subjects. Axis y corresponds to the value of R_L observed with the different experimental conditions presents in axis x ($n = 6$).

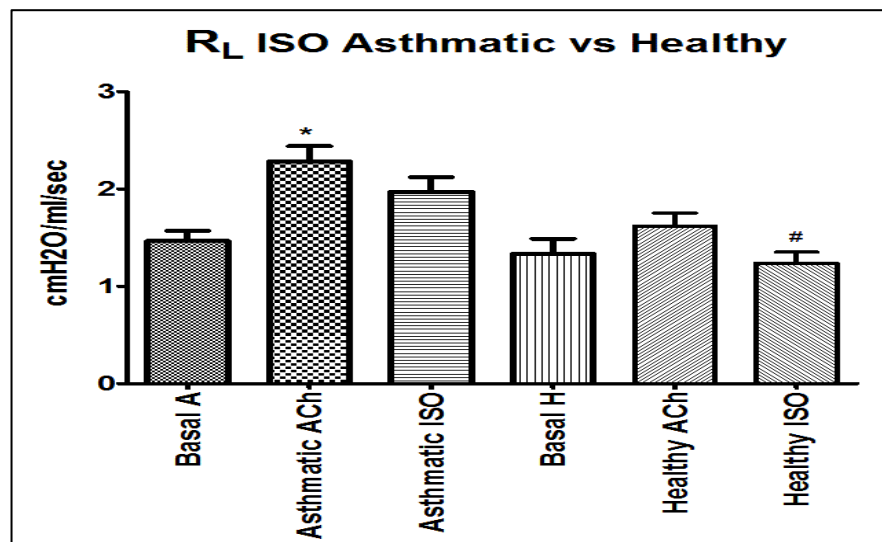


Figure 3.15: Comparison of R_L between asthmatic and healthy subjects. Axis y corresponds to the value of R_L observed with the different experimental conditions presents in axis x ($n = 6$) and its statistical significance (* or # = p value < 0.05).

3.8.2. BAL

When the BAL from the control mice was compared with the sensitized ones, it was found (as shown in Fig 3.16) that the BAL obtained from the sensitized airways showed increased presence of WC (white cells), RC (red cells) and epithelial cells in all the preparations (Fig 3.12; n=7) while in the slides prepared from BAL recovered from the healthy airways showed poor presence or completely absence of the same cellularity. A significant increase in eosinophiles in the slides from sensitized mice ($21 \pm 6\%$) was also observed when compared with controls ($3 \pm 1\%$).

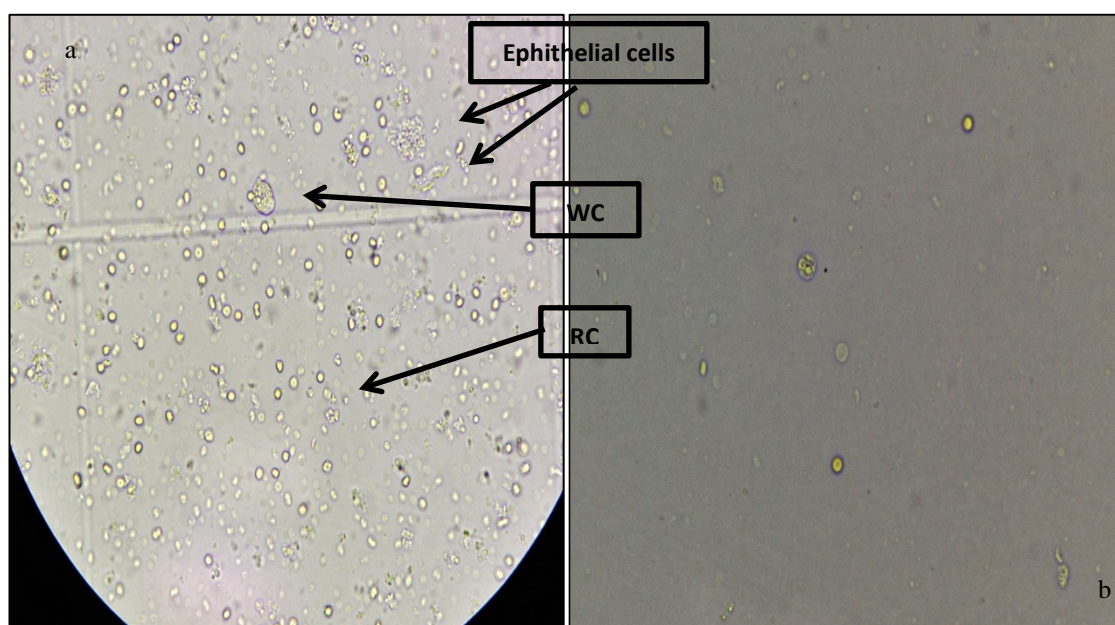


Figure 3.16: BAL images a) sensitized animals, b) control (healthy) animals: Epithelial cells, WC (white cells) and RC (red cells)

3.8.3. ELISA

In order to analyse the data obtained from the healthy and sensitized mice a standard curve with known concentrations for OVA IgE was. The standard concentration curve shown in Fig 3.17 was built using the following concentrations: 7.8, 15.6, 31.2, 62.5, 125, 250, 500ng/mL. Table 3.3 shows concentration and optical density (OD) for each commercial standard prepared. These standards were provided by mdbioproducts and prepared just before of the experiment, from a concentrated stock of 2500 ng/mL, prior to the testing of the serum samples obtained from the healthy and sensitized mice for the study. The standards were placed in the ELISA plate with samples obtained for each

animal and the same protocol to determine the concentration IgE was applied for samples and standards (commercial protocol ELISA).

Table 3.3: OD for each concentration of the commercial standards.

| OVA IgE Concentration (ng/mL) | Optical density for commercial standards |
|-------------------------------|--|
| 7.8 | 0.04085 |
| 15.5 | 0.0342 |
| 31.2 | 0.0338 |
| 62.5 | 0.06505 |
| 125 | 0.14025 |
| 250 | 0.6883 |
| 500 | 1.60535 |

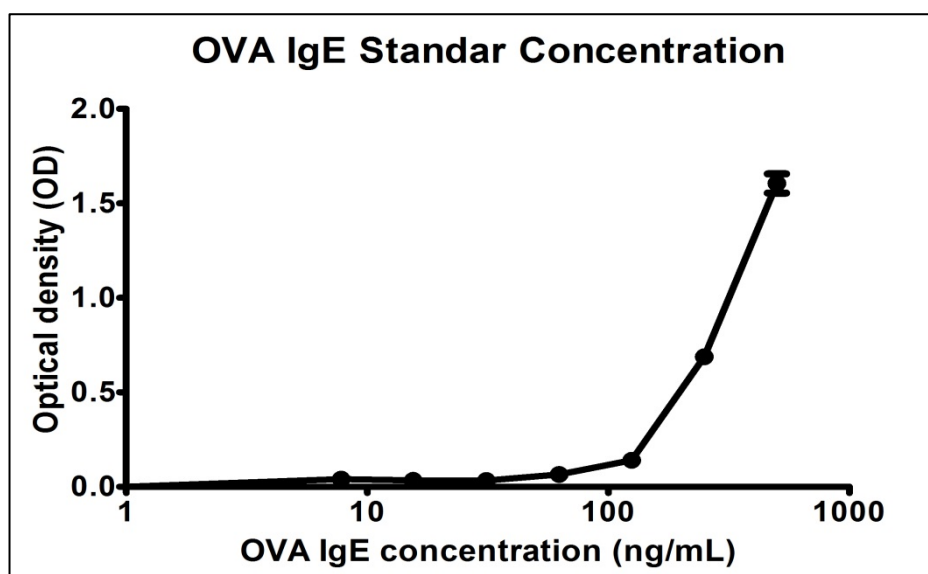


Figure 3.17: ELISA OVA IgE Standar concentration curve: axis y corresponds to the optical density for each concentration, and axis x corresponds to the concentration of each standard. a) 7.8, b) 15.6, c) 31.2, d) 62.5, e) 125, f) 250, g) 500 ng/mL

Once the OVA IgE concentration curve was obtained, it was easy to spot the concentration of the levels for OVA IgE in our samples using the reference curve and

comparing the data with the absorbance obtained in the serum samples from healthy and asthmatics.

The absorbance obtained from the healthy and asthmatic groups was 0.032 ± 0.02 and 0.141 ± 0.03 respectively ($n=11$). The absorbance for both groups was compared and analysed with a *t test* obtaining a statistical significance with a *p value* of 0.039 as shown in figure 3.18.

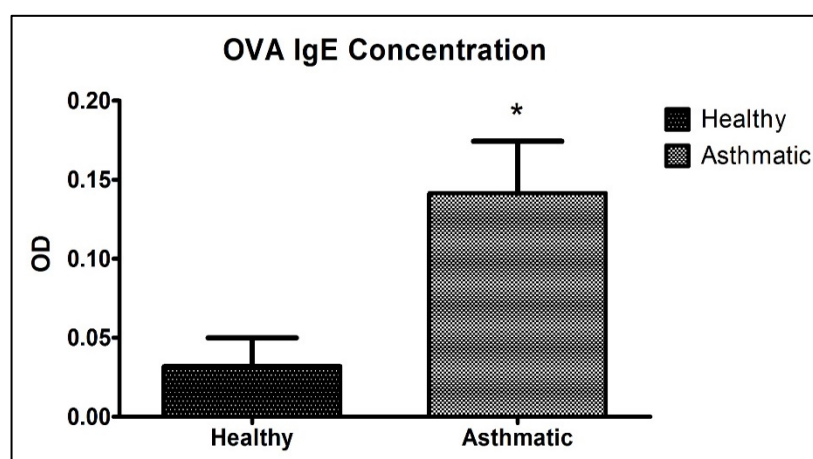


Figure 3.18: BAL concentration a) sensitized animals, b) control (healthy) animals (*p value* < 0.05; *n* = 11).

After this the absorbances obtained for the experimental samples were plotted against the known concentrations (presented in standard curve Fig 3.13), allowing us to calculate the OVA IgE levels in our samples. The Mean concentration for healthy and sensitized mice is presented in table 3.4.

Table 3.4: Details of OD for each group tested (healthy and asthmatics) and IgE concentration for samples.

| Healthy | | Asthmatic | |
|---------|-------|-----------|---------|
| OD | ng/mL | OD | ng/mL |
| 0.032 | 6.110 | 0.141 | 125.668 |

3.9. Closure

The data obtained shows increased response (hyper responsiveness) to ACh and reduced response to ISO in asthmatic subjects when compared to control (healthy) subjects. Besides these findings, changes in cellularity in BAL and differences on IgE levels were also observed. All these findings indicate that we are in presence of subjects with hyper reactive airways and that our sensitization protocol to develop an acute asthmatic model is working as expected, exhibiting some typical features of asthma. With this information, we can now proceed to test mechanical oscillations on sensitized airways and compare their effect with healthy airways *in vitro* (first step) and afterwards *in vivo* (second step). This step is important because most of the knowledge in the area (asthma) and oscillations has been built based on studies ASM from healthy airways, leaving a gap of important information that we are aiming to fill.

Chapter 4

In vitro experimental investigation

4.1. Introduction

Previous work [10, 11, 16, 81-83, 98, 101, 150], including that from IBTec has shown that *in vitro* oscillations induce relaxation of pre constricted airway smooth muscle (ASM) from healthy subjects (mice, pigs, bovine, etc), and to the best of our knowledge only physiological oscillations have been tested in asthmatic airways *in vivo* or *in vitro* [7]. In order to establish the mechanism via which these oscillations work on asthmatic airways, as well as to narrow down the range of oscillations that have potential in inducing relaxation in these type of subjects (if there is any), it was decided to focus on two types of experiments. The first set of experiments focussed on *in vitro* investigations using intact tissue (trachea rings) from asthmatic and healthy mice. The second set of experiments focussed on applying oscillations to the animals' breathing, using anaesthetized asthmatic and healthy mice. In order to conduct these experiments, two different approaches were used to deliver the oscillations based on the sample type and method of delivery: for the *in vitro* experiments, mechanical length oscillations were applied directly to the tissue; the second set of experiments focussed on *in vivo* testing by applying oscillations during the animal's breathing cycles.

The first stage focussed on the *in vitro* experiments and is explained in detailed through this chapter, describing first how the tissue was obtained and selected, after this a description of the *in vitro* set-up and programs used for the experiments, an explanation of the concept of optimal diameter, a presentation of a pilot study performed on healthy airways with its results and findings, and finally the comparison of healthy and asthmatic airways with its results and conclusions. The main purpose of this protocol is to determine how airways *in vitro* from healthy and asthmatics subjects respond to superposed oscillations during an induced asthmatic attack.

4.2. Tissue acquisition

Prior to the dissection and acquisition of the tissue a physiological salt solution (PSS: composition in mM: 110 NaCl, 0.82 MgSO₄, 1.2 KH₂PO₄, 3.39 KCL, 2.4 CaCl₂, 25.7 NaHCO₃ and 5.6 Glucose) was prepared with Millipore MilliQ 18 MΩ water. The solution was bubbled for 5-10 min with a gas mix of 95% O₂/5% CO₂, pH was then measured to assure physiological ranges (pH 7.35 – 7.45) and placed in a PSS reservoir which was continuously bubbled.

Tissues were acquired from mice strain C57 from KODE laboratories (AUT, New Zealand) as third product (discarded tissue from their experiments). The experiments were not subject to ethical approval requirements at AUT. Each trachea was obtained from the mice within 30 min after they were culled. Connective tissue was then removed and trachea rinsed with PSS solution.

4.3. In vitro set-up

A tissue testing set-up from Aurora Scientific Inc. was acquired and assembled (Dual-mode lever system, model no 300C). A system diagram of the set-up is given in Figure 4.1. Each of the components shown in the diagram will be briefly discussed below.

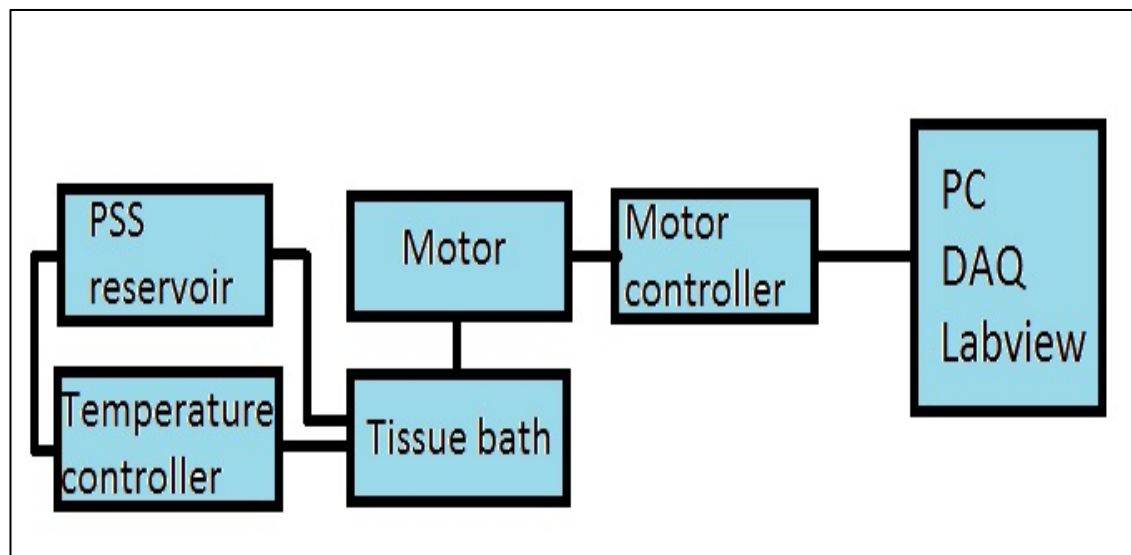


Figure 4.1: System diagram of tissue testing set-up.

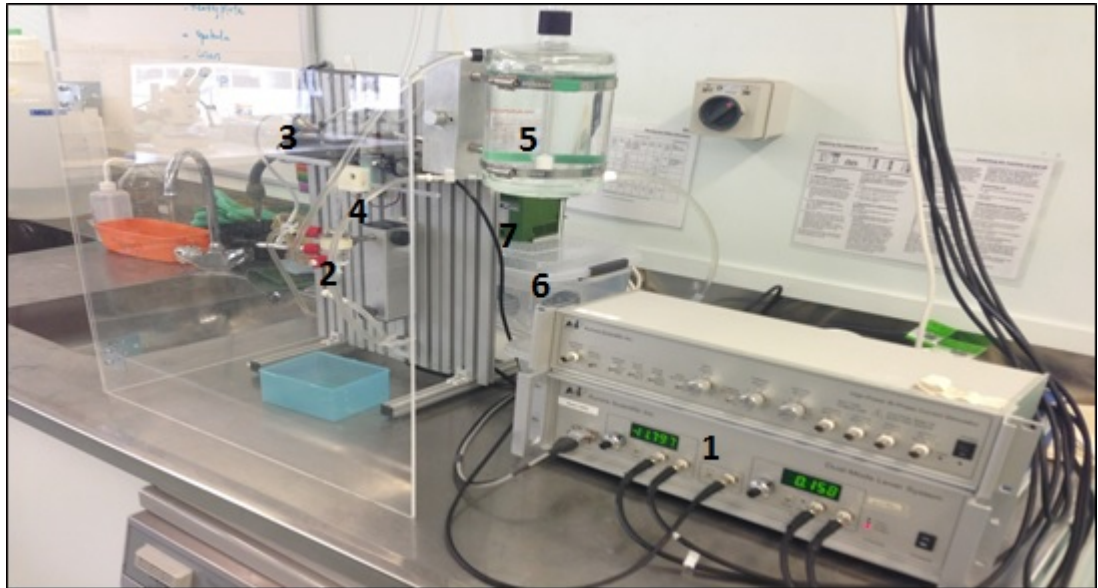


Figure 4.2: Caption of in vitro testing set-up: 1) Dual-mode lever system (Aurora scientific inc); 2) Tissue bath (5ml water jacket reservoir); 3) muscle lever (the tissue is fix to this lever arm that generate oscillations and register changes in tension); 4) Bottom glass hook (tissue is fixed at this point); 5) 1L water jacketed reservoir for physiological solution; 6) Heater, pump, and water reservoir (to maintain all the system under physiological temperature 37°C).

- Tissue Bath (Fig 4.2): This consists of a 5 ml water jacketed reservoir with inlets and outlets for flow of temperature regulated fluid. A gas bubbler for bubbling with 95% O₂/ 5% CO₂ is inserted in the bottom connector and an entry valve and exit valve are mounted at the top and bottom of the bath, respectively. The bath can be vertically moved relative to the dual mode motor. The tissue was suspended vertically using silk attached to steel hook wires, one connected to the motor, another to a screw operated clamp.

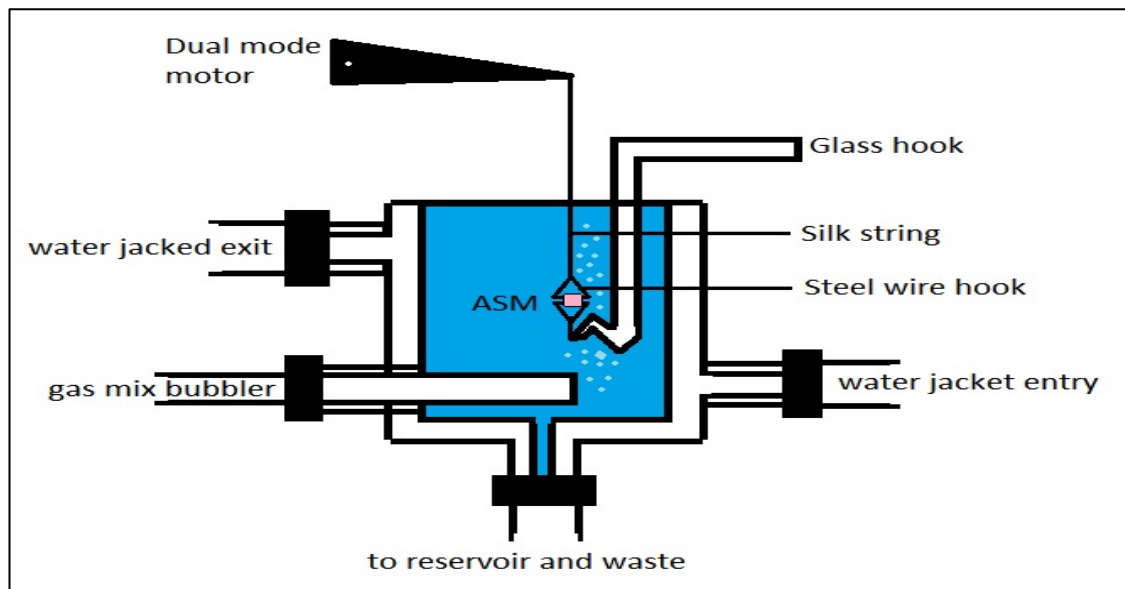


Figure 4.3: Tissue bath, with all the accessories, inlets and outlets.

- Reservoir: An ^L water jacketed reservoir is filled with PSS and connected to the tissue bath. The fluid flow to the tissue bath is regulated by a 2 way valve.
- Temperature control: A circulating temperature controller (B.Braun Thermomix 1419) is attached to both the PSS reservoir and the tissue bath. While the described experiments were performed at physiological temperature (37 °C), the temperature controller was primarily used as a fluid pump to warm up the reservoir fluid, which was stored at 4 °C.
- Dual mode motor and controller (Fig 4.2): A Cambridge 300C dual mode motor and controller provide switchable length (0-3 mm range) and force (0-500 mN) control of the tissue by analogue input signal or through dial operation on the controller. The controller also provides an analogue output force and length signal with variable amplification (1-10 x) with a maximum output range of - 10 to 10 V on both channels with total ranges equal to the input ranges.
- The system was controlled through a Data Acquisition Card (NI 6024E) using National Instruments Labview (version 6.0).

4.4. Programs

For data acquisition of the force and length signal and the generation of the force and length signal three programs were used (programs are presented on appendix), which were previously developed by IBTEc (details of the programs in appendix B).

- ***Converter.vi*** : Initial Labview data acquisition programs saved data in a .SCL format. This program converted the files into .txt format to enable it to be read in MS Excel® or MATLAB®.
- ***ASM_Length.vi*** : This file can perform all the tasks of *acquire_signal.vi*. However, it also allows for imposing superimposed protocols. The time, force and length data are stored in two types of files: *high_res* data acquired at a sampling rate of 3000 per second and *low_res* data acquired at a sampling rate of 100 per second. This program was used for conducting preliminary experiments with superimposed oscillations.
- ***Low_res_signal.vi*** : This is the most developed program that can conduct all the tasks of the aforementioned programs. In addition to that, it also allows for time tracking of any set of oscillations as an indication to the user. It also saves two versions of a file (high and low resolution) according to the date of the experiment conducted.
- ***SUBVI_button_timer.vi*** : This SUBVI is used in *ASM_length.vi* and *Low_res_signal.vi* that provides feedback to the oscillation loops to be started after a certain time.

The force and length data from the Labview program were analysed in MATLAB® (appendix C) and GraphPad Prism®.

4.5. Reference diameter (D_o)

To minimize variability of the tissue behaviour between the ring tracheas, a reference diameter was determined. Most of the studies on ASM use isolated strips tissue for their experiments and an optimal length of the tissue is determined preceding the experimental protocols. However, due to the size of the tissue sample (mice trachea), a less invasive approach with a segment of the trachea (2mm) was used, thus leaving the ASM untouched. Considering that trachea corresponds to a cylindrical element (which was measured cross sectional to assure that it was circular) and the reduction during constriction or increase of the ASM length during different experimental conditions changes the whole diameter of this element we decided to refer to it as Optimal diameter rather than Optimal length. Therefore, when optimal diameter is referred to here, it is calculated in the same manner as the optimal length of the muscle. Several different approaches for defining reference length or diameter (ring trachea) have been suggested in literature [151], but none of them have been proven as an ultimate protocol to define it. Unlike skeletal muscle, ASM does not possess a constant optimal length for force generation (as presented in chapter 2). However it is assumed that it does possess a length range at which it can adapt to a stable optimal force generating capacity. The purpose of a reference diameter (D_o) procedure is to find the present optimal muscle length for maximum force generation. This will minimise the subsequent force changes by continuous length adaptation. The approach used in this study corresponds to a direct search for optimal ASM length or diameter. This is the most common approach [152-154] and it involves a series of stretch, equilibration, contraction and relaxation cycles, and the reference diameter, D_o is defined as the diameter at which the difference between the active force and the prior relaxed force stabilises and generates the maximal contraction from one contraction to the next.

Do protocol:

Repeated cycles of stretch and contraction were induced using ACh at a concentration of $10^{-4}M$ (this concentration was determined using curves of dose-response) and rinse until the maximum contractile force (force during contraction – passive force) is reached (Fig 4.4). Subsequently the airway was allowed to stabilize at D_o for 30 minutes.

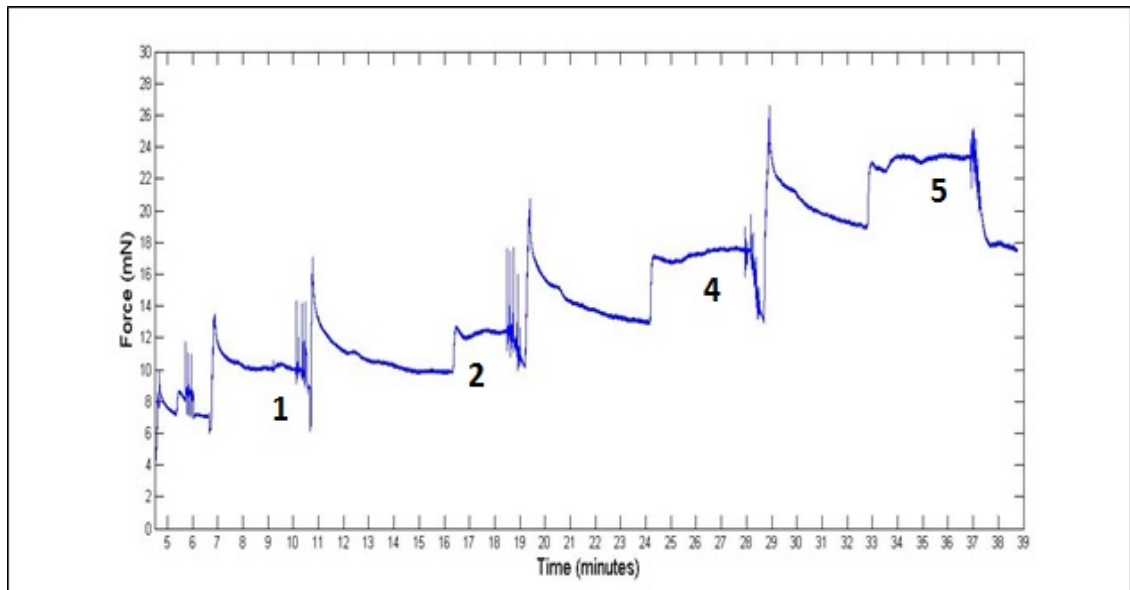


Figure 4.4: Example of determination for optimal diameter. In the caption the last contraction obtained which corresponds to number 5 was not bigger than the previous number 4, so optimal diameter was considered reached.

4.6. Pilot study experiments (healthy airways)

As mentioned in chapter 2 testing mechanical oscillations on pre constricted healthy airways is the point of start for the experiments, before moving and testing on sensitized airways. In order to do this, intact airways from mice C57 (tissue acquisition as explained in section 4.2) were used for two set of experiments at this stage.

1. The first set of experiments consisted in to test the relaxation effect of different known relaxant agents of the pre constricted healthy airways such as breathing oscillations, ISO or breathing in combination with ISO. The objective of these experiments was to compare later on effect of SILO with these agents.
2. The second set of experiments focused on SILO using frequencies of 10, 20 and 30Hz and amplitude of 1%. SILO (these values were previously used by our group in porcine airways), which were imposed over breathing oscillations and analysed. The animals selected for this set of experiments were mice, because they are widely used in respiratory studies and because of their small size, easy manipulations and literature supporting them as a good model (Chapter 3). The strain used was mice C57, and the tissue was acquired as explained in section 4.2.

Protocol:

- *For each testing protocol the tracheas were first constricted with ACh $10^{-4}M$ (concentration was calculated using curve of dose-response for the drug) until a stabilized contractile force was found.*
- *Subsequently, to address the first set of experiments after the plateau with ACh was reached, breathing, ISO or breathing plus ISO were used to test their relaxant effect under static conditions as follows:*
 - *Breathing oscillations (4%/2.7Hz). An amplitude of 4% was selected for TO using as reference of Hughes et al [80] and other groups that have used range of TO between 2-8% in different species including mice [81, 82, 155] and the frequency of 2.7Hz was calculated as the breathing frequency of the mice using ~163 cycles per minute, and followed by 5min of recovery.*
 - *ISO $10^{-6}M$ (concentration was calculated using curve of dose-response for the drug), followed by 5min of recovery.*
 - *ISO + Breathing oscillations, followed by 5min of recovery.*
- *Subsequently, to address the second set of experiments after the plateau with ACh was reached, breathing, or breathing + SILO were used to test their relaxant effect under static conditions as follows:*
 - *Breathing oscillations (4%/2.7Hz), followed by 5min of recovery.*
 - *Breathing + SILO (1%/10Hz), followed by 5min of recovery.*
 - *Breathing + SILO (1%/20Hz), followed by 5min of recovery.*
 - *Breathing + SILO (1%/30Hz), followed by 5min of recovery.*
- *The trachea is rinsed repeatedly with PSS solution after each protocol and allowed to recover prior to a subsequent test. Examples of the records obtained for these experimental protocols are presented in Fig. 4.5.*

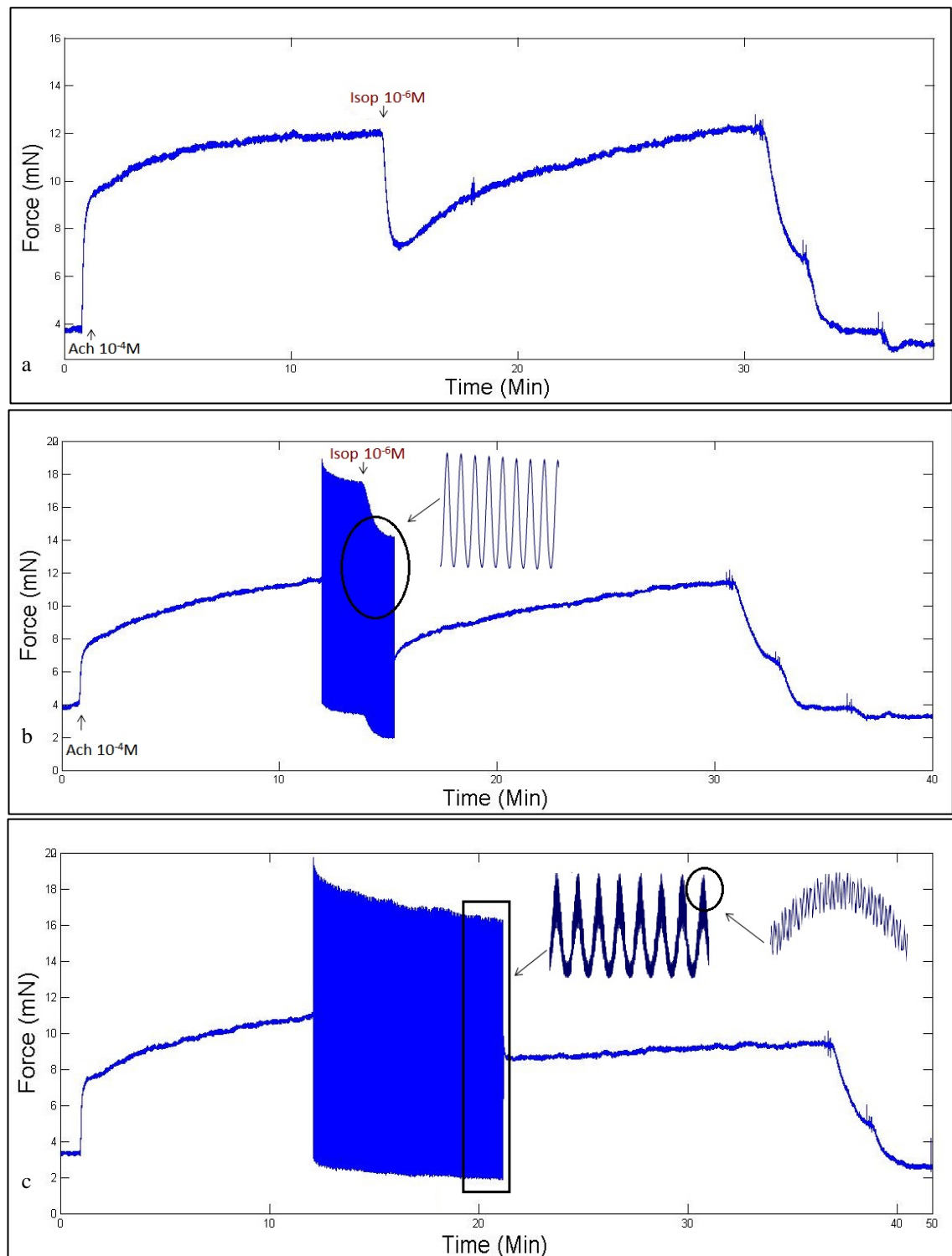


Figure 4.5: Experiments type. a) Relaxation induced using just ISO ($10^{-6}M$); b) relaxation induced by ISO in combination with tidal oscillations (4%:2.7Hz); c) relaxation induced by tidal oscillations in combination with superimposed oscillations (1 and 1.5%: 5, 10, 15 and 20Hz)

4.7. Data reduction

The tissue was rejected when the active force development after the stabilization period was less than 60% of the peak of the active force obtained at the end of the *Do* procedure, because this reduction of the active force could indicate deterioration of the tissue (ASM) through the protocols. However was common to observe increasing in the peak of active force with time, especially if the tissue was allowed to rest long enough.

4.8. Relaxation

The percentage of relaxation (%R) was calculated as the percentage of total force reduction (b) observed after 5 minutes after the application of ISO and/or oscillations relative to the force observed prior to these agents, which corresponds to the plateau (a) (eq. 4.1).

$$\%R = \frac{(a-b)}{a} \quad (Eq. 4.1)$$

Fig 4.6 presents the results obtained with breathing, ISO 10^{-6} M and ISO combined with breathing oscillations, which resulted in peaks of 47.8 ± 9 , 55.7 ± 5 and 61.8 ± 5 % respectively (n = 6). Even though it seems to show a trend of increasing relaxation compared with just ISO or breathing, the results were not statistically significant when analysed with ANOVA or *t* test (n = 6; p value > 0.05). Data was analysed using Graphpad Prism 5.0™.

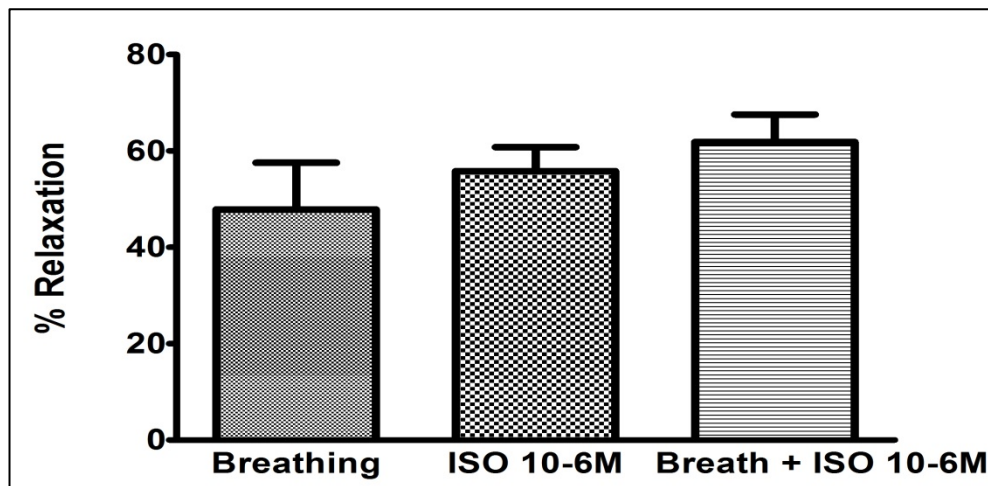


Figure 4.6: Effect of Isoproterenol and the combined effect of ISO and mechanical oscillations equivalent to breathing on contractile force, represented as % relaxation on Y axis (n=6).

Figure 4.7 presents the results of the relaxation obtained with mechanical oscillations equivalent to breathing, which induces $47.8 \pm 9\%$ (n = 6) of reduction in force of contraction (relaxation observed) and compare it with the imposition of SILO with frequencies of 10, 20, 30 Hz on the breathing equivalent oscillation which presents a reduction in force of contraction of 32.8 ± 4 , 23.9 ± 4 and $35.5 \pm 7\%$ of relaxation respectively.

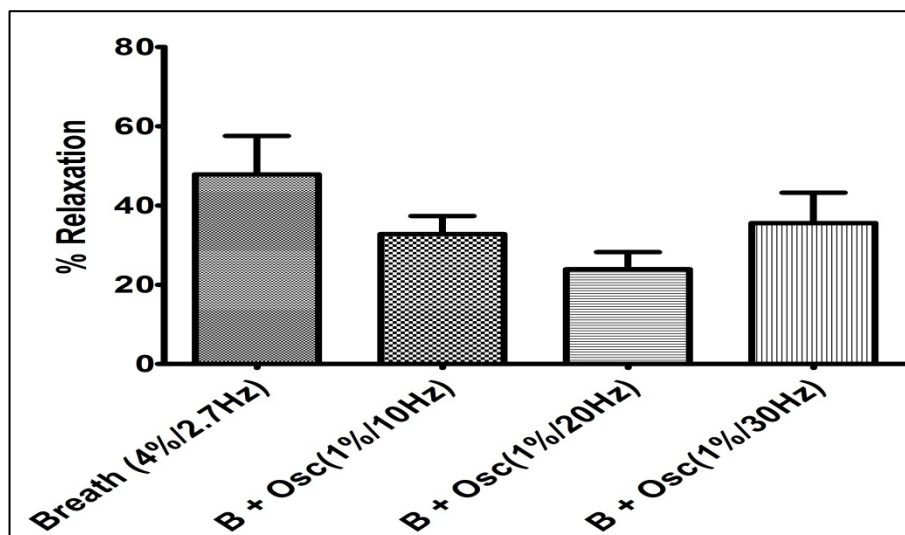


Figure 4.7: Effect of mechanical oscillations equivalent to breathing with and without superimposed length oscillations on contractile force (n=6).

4.9. Breathing, ISO and SILO

The results presented in Fig. 4.6 show that the imposition of breathing oscillations has a bronchorelaxant effect in pre constricted airways, which reinforce the findings in healthy ASM [7, 10, 16, 81-84, 98, 150, 156]. It was also observed that the bronchorelaxant effect of ISO seems to increase when combined with these types of mechanical oscillations as reported previously by Gump [10]. It is believed that the force reduction observed when mechanical oscillations were applied could be the result of length oscillations acting directly on the bridge dynamics thus disrupting them (more details in Chapter 1). Even though other components of the airways such airway wall constituents, cartilage and lung parenchyma could be participating, only ASM is considered an active component and principal target of oscillations and literature seems to support the idea that oscillations are affecting directly the crossbridge [10, 83]. Furthermore Fig 4.7 shows that when SILO in the range of 10-30 Hz were added to breathing oscillations, the relaxation of ASM from healthy airways was lower than the one obtained with breathing oscillations alone, This is contrary to what was expected, but these findings are not conclusive because ASM from asthmatic subjects seems to respond differently to oscillations [7]. It is believed that biochemical changes and alterations in the dynamic properties of ASM occurring during the development of the disease could be responsible for increasing the ASM resistance to the dilating influence of breathing and deep inspiration [81, 102, 104, 157, 158].

4.10. Healthy and asthmatic airways

As reported in the previous section the results indicate that breathing oscillations induce relaxation in healthy tissues, and the relaxation observed with ISO increases when combined with breathing [10]. On the other hand, superimposed oscillations in the range of frequency between 10-30Hz seemed to increase the force of contraction rather than further relax the precontracted airways. It has been reported by other authors the different behaviour between asthmatic and healthy airways [7, 158]. Therefore, different values of frequency and amplitude for SILO need to be tested.

For the comparison between airways from healthy and asthmatic subjects a new set of experiments was designed, and also a different strain of mice was used. The former was obtained through the artificial induction of asthma on mice strain Balb/c, females, 8-12

weeks old, using an acute model for the experiments (more information of sensitization protocol in chapter 3).

4.11. Tissue acquisition

Once healthy and sensitized animals groups for the experiments were ready, they were euthanized using a CO₂ overdose and dissection was only started after the mouse did not present any reflex (ocular and foot) or pain response, and the breathing had stopped. As presented in Fig. 4.8, the mouse was placed on a square plastic surface and its extremities were fixed to the plastic square using rubber bands to facilitate dissection. The area of the neck was cleaned (hair removal); a clean vertical cut was performed in the area using scissors, in order to expose the trachea.

Using a pair of tweezers, the pre-tracheal muscles were dissected and moved from the sagittal plane to the sides, allowing the observer to find the trachea below them. The trachea is a tube, composed of ASM, cartilage rings, and surrounded by connective tissue. Once the trachea was reached, a couple of clean cuts at the level of the thyroid gland and before the bifurcation to the lung were performed, obtaining a trachea of around 4-8 mm length. The latter was then placed onto a Petri plate with PSS for further dissection, and the mice were rolled into absorbent paper and placed into the freezer at -20°C to be discarded afterwards. The trachea was cleaned by removing vascular and connective tissue, measured, and smaller trachea rings of 2-3 mm length were obtained. The obtained trachea ring was mounted onto the system (explained in detail later in the chapter) using homemade steel wire hooks, while taking care that the hooks were placed in the cartilage zone and were not touching the ASM, which could damage the muscle and alter the force generation during the experiments.

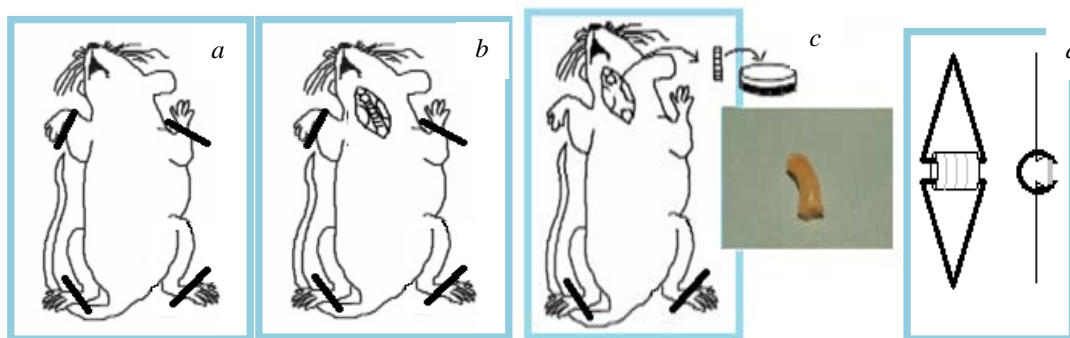


Figure 4.8: a) Anesthetized mice is placed in plastic square; b) Pre tracheal muscles are dissected in order to expose the trachea; c) The trachea is removed from mice and cleaned from surroundings tissue ; d) Dissected trachea is cut into smaller pieces (2-3mm) and mounted onto wire hooks leaving the ASM untouched.

4.12. Experiments

Two sets of experiments were conducted at this stage. The first set of experiments consisted on testing the relaxant effect of breathing oscillations, ISO and Breathing in combination with ISO on healthy and asthmatic airways, in order to compare and test their effectiveness between the different airway types. A second set of experiments was focused on the effect of SILO on healthy and asthmatic airways. For these experiments some changes in the parameters used for SILO were made: frequencies of 5, 10, 15 and 20Hz and amplitudes of 1 and 1.5% were used, this is because, it has been observed that not only frequency affects the behaviour of ASM response to oscillations, but also amplitude does [9, 11, 82].

Protocol:

- For each testing protocol the tracheas were first constricted with ACh $10^{-4}M$ (concentration was calculated using curve of dose-response for the drug) until a stabilized contractile force was found.
- Subsequently, to address the first set of experiments after the plateau with ACh was reached, breathing, ISO or breathing plus ISO were used to test their relaxant effect under static conditions as follows:
 - Breathing oscillations (4%/2.7Hz). An amplitude of 4% was selected for TO using as reference of Hughes et al [80] and other groups that have used a range of TO between 2-8% in different species including mice [81, 82, 155] and the frequency of 2.7Hz was calculated as the

- breathing frequency of the mice using ~163 breathing cycles per minute, and followed by 5min of recovery.*
- *ISO 10^{-6} M (concentration was calculated using curve of dose-response for the drug), followed by 5min of recovery.*
 - *ISO + Breathing oscillations, followed by 5min of recovery.*
- *Subsequently, to address the second set of experiments after the plateau with ACh was reached, breathing, or breathing + SILO were used to test their relaxant effect under static conditions as follows:*
 - *Breathing oscillations (4%/2.7Hz), followed by 5min of recovery.*
 - *Breathing + SILO (1%/5Hz), followed by 5min of recovery.*
 - *Breathing + SILO (1%/10Hz), followed by 5min of recovery.*
 - *Breathing + SILO (1%/15Hz), followed by 5min of recovery.*
 - *Breathing + SILO (1%/20Hz), followed by 5min of recovery.*
 - *Breathing + SILO (1.5%/5Hz), followed by 5min of recovery.*
 - *Breathing + SILO (1.5%/10Hz), followed by 5min of recovery.*
 - *Breathing + SILO (1.5%/15Hz), followed by 5min of recovery.*
 - *Breathing + SILO (1.5%/20Hz), followed by 5min of recovery.*
 - *The trachea was rinsed repeatedly with PSS solution after each protocol and allowed to recover prior to a subsequent test. All oscillation amplitudes were calculated as percentage of D_0 .*

4.13. Relaxation

The %relaxation was calculated in the same manner as previous experiments and the statistical analysis was performed using Graphpad Prism 5.0™, considering a normal distribution of the data and using a paired *t*-test for each dose of treatment (% amplitude, Hz and ISO), also tests for non-normal distribution of the data were considered for the analysis its analysis. Fig 4.9 shows the data obtained when breathing, ISO and ISO combined with oscillations were applied in precontracted airways from healthy airways and compare them with the data obtained from asthmatic airways. The relaxation observed with ISO seems to increase in this mice strain (Balb/c) when combined with breathing oscillations (as observed previously with mice C57), compared to just ISO ($\sim 43 \pm 8.3\%$ and $57 \pm 9.30\%$ respectively), but this effect is

missing in asthmatic airways (ISO + Breathing $\sim 3 \pm 1.85\%$ and just ISO $6 \pm 3.16\%$; P value Fig 4.9). Also the effectiveness of breathing oscillations, ISO at 10^{-6}M and both agent combined was observed to be significantly reduced in asthmatic airways when compared to the effect of the same concentration on healthy airways as presented in table 4.1.

Table 4.1: Column stats for response of airways from healthy and asthmatic airways to breathing, ISO and ISO + breathing.

| % Relaxation | | | | | |
|---------------------|-----------------------|---------------------------------|-----------------------------------|--|--|
| Breathing (healthy) | Breathing (asthmatic) | ISO 10^{-6}M (healthy) | ISO 10^{-6}M (asthmatic) | Breath + ISO 10^{-6}M (healthy) | Breath + ISO 10^{-6}M (asthmatic) |
| 47 ± 9 | 5 ± 1 | 43 ± 8 | 3 ± 1 | 57 ± 2 | 6 ± 3 |
| P value < 0.05 | | P value < 0.05 | | P value < 0.05 | |

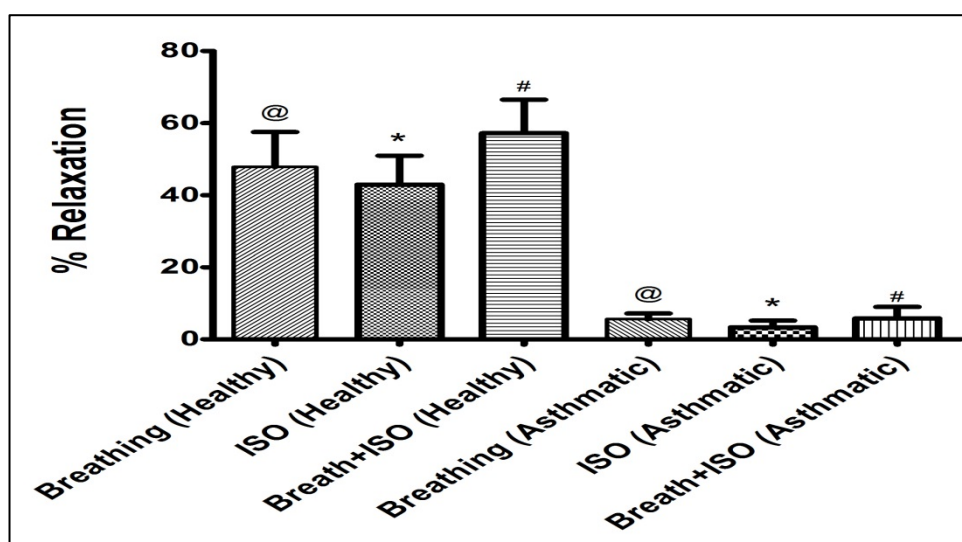


Figure 4.9: Compared effect of Isoproterenol and the combined effect of ISO and mechanical oscillations equivalent to breathing on contractile force on healthy and asthmatic airways. @, * and # indicates statistical significance between the means of the effect of breathing, ISO and Breathing + ISO on healthy airways and effect of the same experimental condition asthmatic airways respectively ($n=6$, p value < 0.05).

When the effect of SILO with an amplitude of 1% at frequencies of 5, 10, 15 and 20Hz on breathing equivalent oscillations were analysed and compared with breathing

oscillations alone on asthmatic airways, a variety of responses presented in Fig 4.10 were observed, with increased relaxation for some of the frequencies and reduction in relaxation for others (with statistical significance only for 10Hz, p values presented in table 4.2).

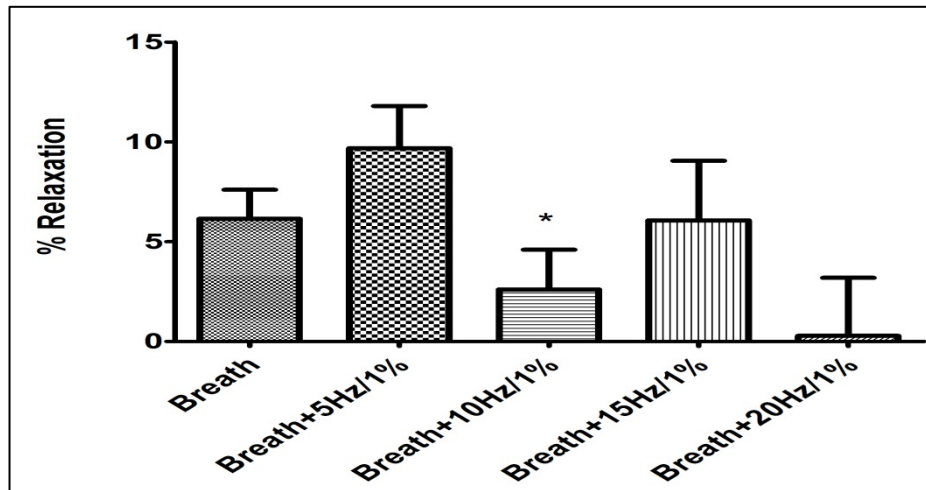


Figure 4.10: Effect of mechanical oscillations equivalent to breathing with and without superimposed length oscillations (1% amplitude) on contractile force. * indicates statistical significance for the mean of SILO at 10 Hz when compared to the mean to breathing alone (n=7).

Table 4.2: Statistical significance table for the effect of mechanical oscillations equivalent to breathing with and without superimposed length oscillations (amplitude 1%) on contractile force. Yellow box indicate statistical significance.

| P value comparison table for 1% of amplitude: "Are means signif. different? (P < 0.05)" | | | | | | | |
|---|------------|--------------|------------|--------------|------------|--------------|------------|
| Treatment 1 | | Treatment 2 | | Treatment 3 | | Treatment 4 | |
| 5Hz | | 10Hz | | 15Hz | | 20Hz | |
| Wilcoxon (#) | t test (*) | Wilcoxon (#) | t test (*) | Wilcoxon (#) | t test (*) | Wilcoxon (#) | t test (*) |
| 0.1875 | 0.1525 | 0.0547 | 0.036 | 0.4063 | 0.4868 | 0.1094 | 0.1074 |

But when the effect of the SILO with amplitude of 1.5% at frequencies of 5, 10, 15 and 20 Hz overlapped on breathing equivalent oscillations were analysed and compared to breathing oscillations alone (on asthmatic airways) the pattern observed was completely different (Fig 4.11), with increased relaxation for all the frequencies at 1.5% of $\sim 16 \pm$

2.07, 8 ± 3.39 , 20 ± 9.14 and $14 \pm 8.39\%$ respectively. Presenting statistically significance for all the parameters tested as presented in table 4.3.

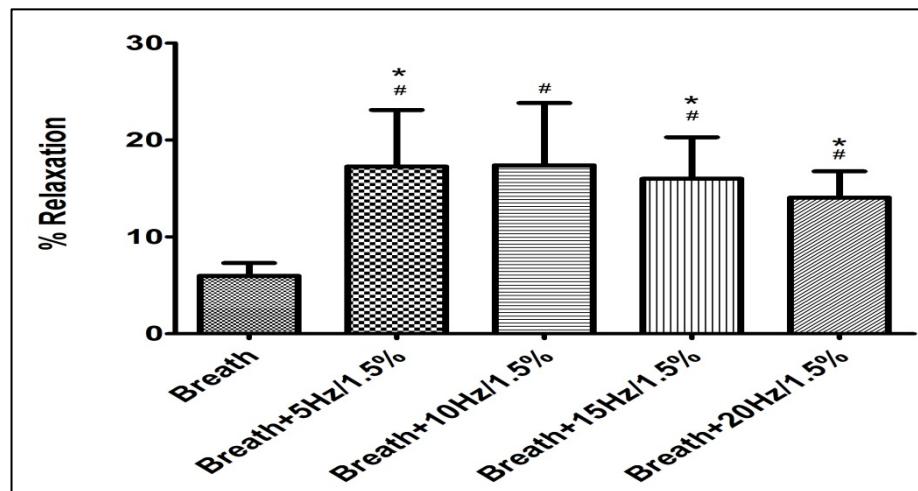


Figure 4.11: Effect of mechanical oscillations equivalent to breathing with and without superimposed length oscillations (1.5% of amplitude) on contractile force. * indicates statistical significance for the means of the effect of SILO when combined with breathing and compared with the effect of breathing alone using Wilcoxon; # indicates statistical significance between the means of the effect of SILO when combined with breathing and compared with the effect of breathing alone using t test on asthmatic airways (n=7).

Table 4.3: Statistical significance table for the effect of mechanical oscillations equivalent to breathing with and without superimposed length oscillations (amplitude 1.5%) on contractile force. Yellow boxes indicate statistical significance.

| P value comparison table for 1.5% of amplitude: "Are means signif. different? (P < 0.05)" | | | | | | | |
|---|------------|--------------|------------|--------------|------------|--------------|------------|
| Treatment 1 | | Treatment 2 | | Treatment 3 | | Treatment 4 | |
| 5Hz | | 10Hz | | 15Hz | | 20Hz | |
| Wilcoxon (#) | t test (*) | Wilcoxon (#) | t test (*) | Wilcoxon (#) | t test (*) | Wilcoxon (#) | t test (*) |
| 0.0156 | 0.0369 | 0.0078 | 0.0555 | 0.0547 | 0.0482 | 0.0234 | 0.0327 |

When SILO were compared with ISO alone on asthmatic airways, they showed similar observed patterns to those compared with breathing alone. When ISO was compared with SILO of 1% amplitudes only 5Hz showed statistically significant increased relaxation (Fig 4.12).

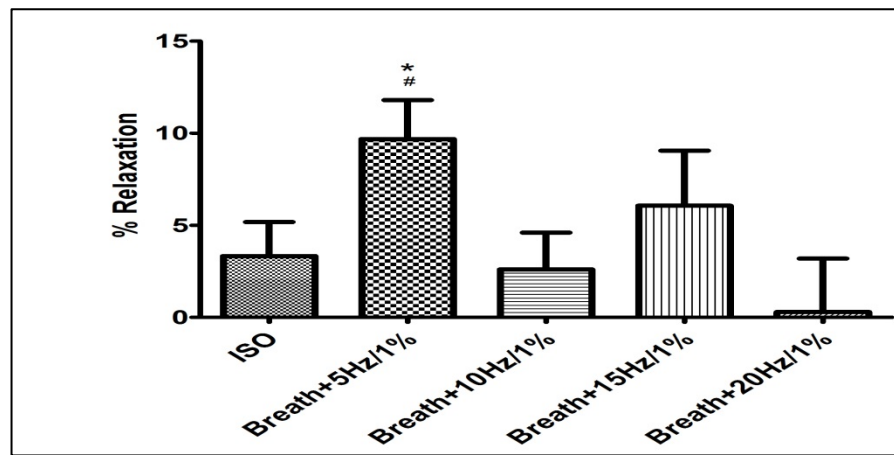


Figure 4.12: Effect of ISO compared with mechanical oscillations equivalent to breathing + superimposed length oscillations (1% of amplitude) on contractile force. * indicates statistical significance for the mean of SILO at 5 Hz when compared to the mean to the effect of ISO alone (n=7).

When SILO at 1.5% were compared with ISO alone, similar increased relaxation patterns were observed when compared to breathing alone, with statistical significance for all the frequencies tested as presented in Fig. 4.13.

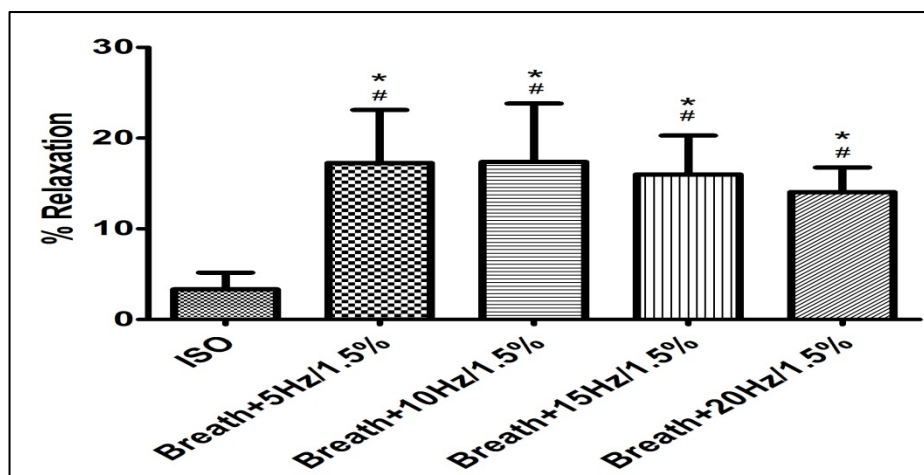


Figure 4.13: Effect of ISO compared with mechanical oscillations equivalent to breathing + superimposed length oscillations (1.5% of amplitude) on contractile force. * indicates statistical significance for the means of the effect of SILO when combined with breathing and compared with the effect of ISO alone using Wilcoxon; # indicates statistical significance between the means of the effect of SILO when combined with breathing and compared with the effect of ISO alone using t test on asthmatic airways (n=7).

4.14. Closure

The results here show that the imposition of breathing oscillations has a bronchorelaxant effect in both of the healthy strains of mice tested (C57 and Balb/c), which reinforces previous findings in ASM tissues [7, 10, 16, 81-83, 98, 99, 101, 156, 159], and the bronchorelaxant effect of ISO seems to increase when combined with mechanical oscillations similar to breathing (2.7Hz/4%) in healthy airways, but the relaxant effect of breathing, ISO and breathing + ISO is significantly lower in asthmatic airways. This may be due to airway changes or adaptation of the ASM during the development of the disease [81, 102, 104, 157, 158].

Furthermore, even when superposed oscillations with a frequency in the range of 10-30Hz and an amplitude of 1% were not more effective than just breathing or ISO to induce relaxation on healthy airways, the superimposition of oscillations with amplitude of 1.5% and frequencies in the range of 5-20 Hz on breathing oscillations alone increase the relaxation of the asthmatic airways compared with oscillations equivalent to both breathing and ISO alone. The superimposition of mechanical oscillations with amplitude of 1% in the same range does not result in similar findings; on the contrary a reduction in relaxation of asthmatic airways was observed with the only exception of 5Hz when compared with mechanical oscillations equivalent to breathing alone.

If SILO of 1.5% of amplitude overlapped to breathing patterns can still induce relaxation in pre-constricted asthmatic airways where tidal oscillations have failed as observed in the results, these could corroborate the theory that the effector (crossbridge) remain the same as its components (myosin and actin) and it could be disrupted though mechanical oscillations. This data in addition to previous data published by our team in healthy airways [83] seems to indicate that the relaxation of the ASM in healthy and asthmatic airways is closely related to the crossbridge rate (speed of attachment) and this could be disrupted by changes on amplitude and frequency independently. These findings need to be tested and probed under *in vivo* conditions in order to advance in the direction of a possible new therapy to treat asthmatic attacks.

Chapter 5

In vivo experimental setup

5.1. Introduction

As *in vitro* tests give some indication and knowledge about ASM behaviour, little knowledge is available on their *in vivo* response. The primary objective of this research is to determine the *in vivo* response of asthmatic airways to mechanical length oscillations. The purpose of this chapter is to summarize and explain the methodology for the *in vivo* experiments. It covers the selected methods, parameters to evaluate pulmonary function, construction of *in vivo* setup, calibration, and selection, construction and explanation of oscillation device.

Determining the respiratory function of laboratory mice *in vivo* is of great interest due to the important role that these animals play in biomedical, toxicological and pharmacological research. When conducting respiratory research on allergic airway disease, mice have been found to be the preferred species to use in experimentation due to their well characterised genome and immune system, short breeding periods, the availability of inbred and transgenic strains, suitable genetic markers, the ability to readily induce genetic modifications and their relatively low maintenance costs [109, 112, 115, 118, 144, 145, 160-162].

Due to the small size of the airways in mice, measurement of their pulmonary function presents some challenges. However, in recent years, considerable progress has been made in developing methods to measure the lung function in mice. As a result, several invasive and non-invasive lung function techniques have been developed to characterise the phenotype of experimental models of lung disease.

Each approach used to measure lung functions represents a compromise between accuracy, non-invasiveness and convenience. Therefore there is a relationship between the invasive measurement technique and its resulting accuracy. Usually the less invasive a measurement is, the less likely it is to produce consistent, reproducible and meaningful data.

5.2. *Experimental layout*

As previously explained in chapter 3, to assess *in vivo* pulmonary functions in mice different techniques are available. These normally are separated into two categories invasive and non-invasive. This section summarizes and discusses the selected methodology for our *in vivo* experimental protocols.

Invasive and non-invasive techniques are available to study respiratory physiology, both with some advantages and disadvantages. These methods are sometimes used alone and other times combined for more accurate results. In order to obtain more reliable results and allow more control over the overall manipulations it was decided for this study to use an invasive approach. The selected technique is based on plethymography with tracheal intubation and oesophageal cannulation. This methodology allows us to measure different respiratory parameters such as tidal volume (T_v) and transpulmonar pressure (P_{tp}), which are associated with the dynamic elasticity of the airways and are used for the determination of dynamic compliance (C_{dyn}), and also other parameters such as flow and tracheal pressure (T_p) which are associated with resistance of the airways and are used to calculate other important parameter which is lung resistance (R_L). R_L and C_{dyn} are considered specific parameters to evaluate bronchoconstriction during the experimental protocols.

In order to measure the bronchoconstriction level using the parameters of R_L and C_{dyn} , a plethysmograph custom built based on the setup used by Glaab et al [136] was developed and built. The experimental layout presented in figure 5.1 consists of two units: animal containment and measuring components. The animal containment unit consist of a testing chamber custom built and a thermo regulated bath. On the other hand the measuring components unit consist of pressure transducers and amplifiers; Drugs delivery system: Jet Nebulizer for the allergens and drugs; and Data acquisition system (Labchart). These elements are explained in more details in the following sections.

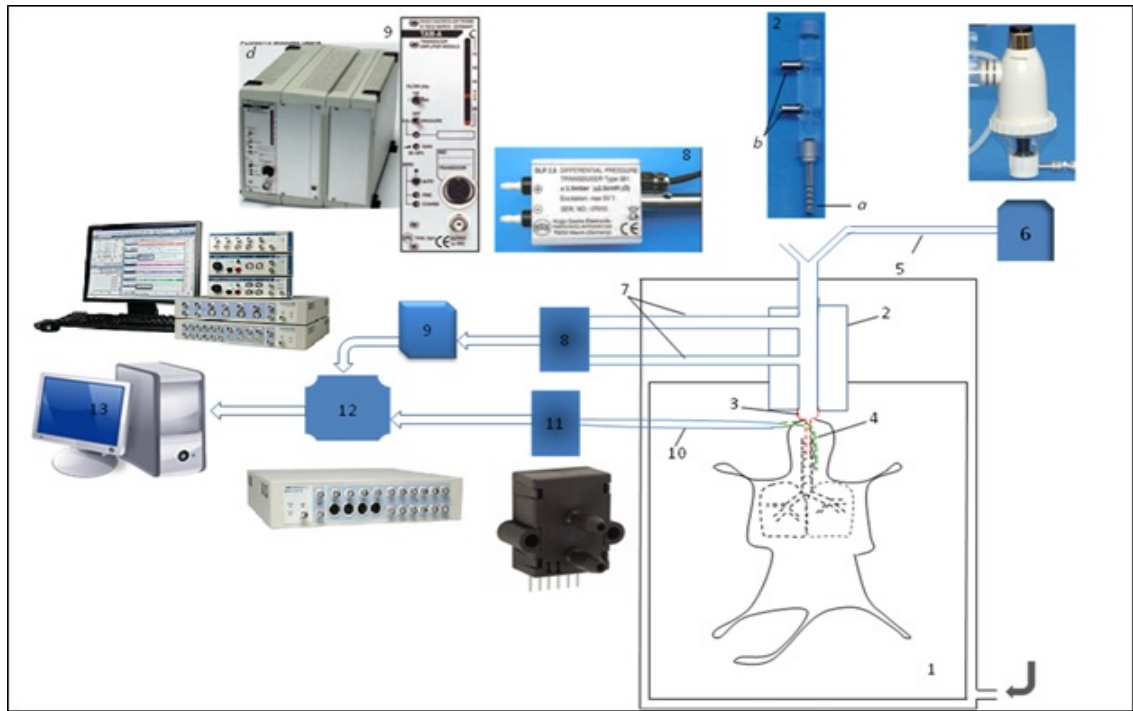


Figure 5.1: 1) Thermostated plexiglas chamber; 2) Pneumotachometer; 3) Tracheal cannula; 4) Oesophageal catheter; 5) Tube supplying the nebulised solution; 6) Nebulizer; 7) Connection pipes; 8) Differential pressure transducer; 9) Tam-A Transducer amplifier (c) and Plugsys amplifier module (d); 10) Connection pipe; 11) Honeywell pressure transducer; 12) 16 channels data acquisition board Labchart; 13) Computer with data acquisition Labchart.

5.3. Animal containment

This section covers in detail the containment elements of the set-up and explains how they connect with each other.

5.3.1. Testing chamber

The chamber has three major requirements: an appropriate size in order to fit different animal body sizes inside such as mice or rats; provide suitable environmental conditions; and allow to connect the measurement components with the experimental subject in a comfortable manner for subject and equipment using front and back inlets. The chamber was design using Computer Aided Design (CAD) modelling (Fig 5.2 and 5.3), in order to have a fully visual aspect of the device and to ensure that all the designed dimensions will come together to form the finished product, for the construction CNC machining was used as the files could be used directly and the result were very accurate components.

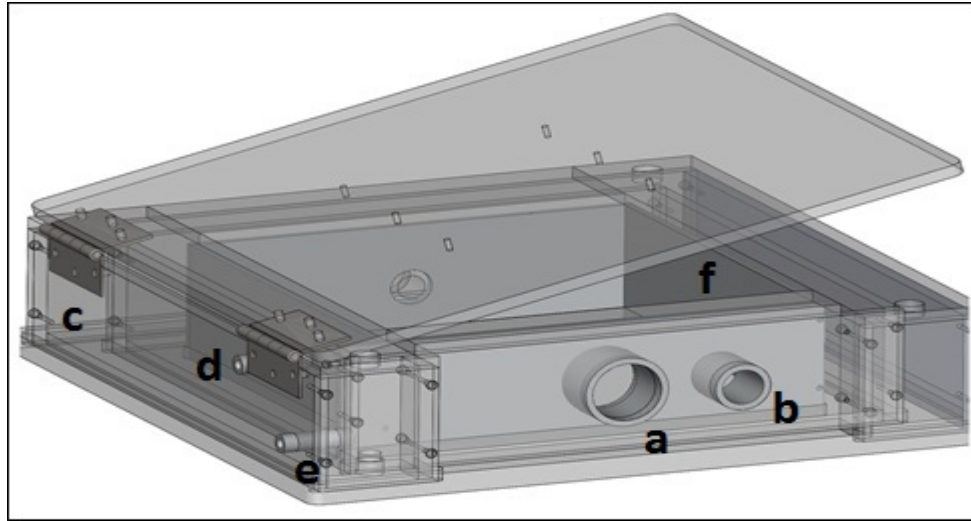


Figure 5.2: Front of testing chamber: a) front inlet for Pneumotacograph, b) front inlet for eosophagal cannula, c) Inner basin for warm water, d) Side inlet for warmed water, e) side outlet for water, e) insulation.

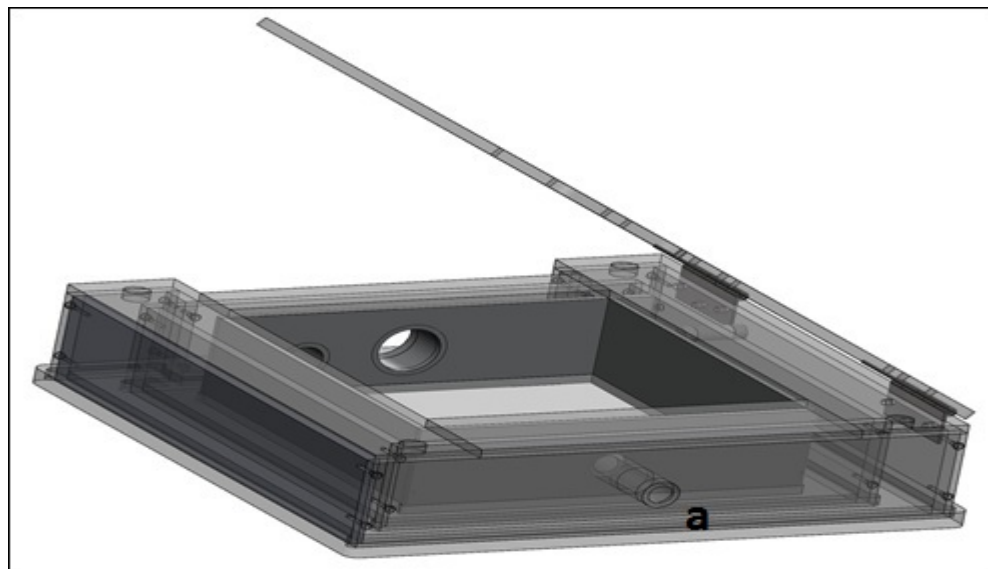


Figure 5.3: back of testing chamber: a) inlet for temperature probe.

The chamber was built from acrylic sheets of 1mm thickness, with external dimensions of 520 x 480 x 15 cm (Wide x Long x height) and internal dimensions of 300 x 300 x 14 cm with 4 inlet/outlets. The testing chamber have an insulation system composed of one aluminium wall (6mm thickness) to reduce the heat loss, three acrylic walls (10 mm each of thickness each) separating the different compartments, an inner basin for warm water (30 mm thickness) and other external compartment for air (with a thickness of 30 mm) to improve the insulation (Fig 5.4).

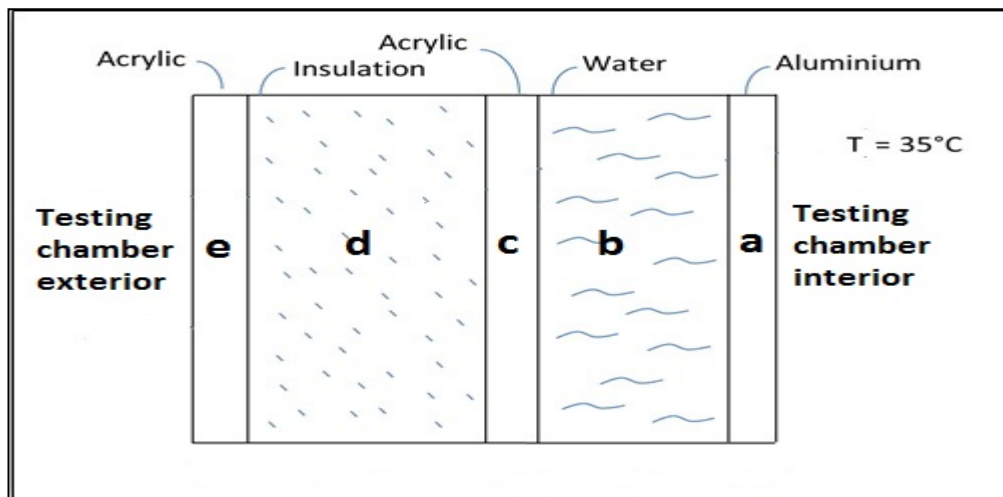


Figure 5.4: Insulation scheme: a) acrylic wall, b) water basin, c) acrylic wall, external insulation chamber and d) acrylic wall.

The inner basin for the warm water is connected through two lateral pipes to the thermo regulated bath allowing the entrance and exit of warmed water (37°C) to the system, in order to increase and maintain the chamber inner temperature in the range of 25-28 °C. All these arrangements have the final goal of maintaining the anesthetized subject comfortable and under physiological temperature during the whole experimental protocols in order to keep it alive.

5.3.2. Thermo regulated bath.

The thermo regulated bath is composed of a plastic container of 10Lts for the water and a heating and circulating water pump from Grant instruments (Cambridge Ltd; serial number 51333; volts 200-250). The pump heat the water up to 37°C and pumps it into the inner basin of the acrylic chamber through the lateral pipes of it (as shown in Fig 5.5), the temperature was controlled using a typical glass thermometer.

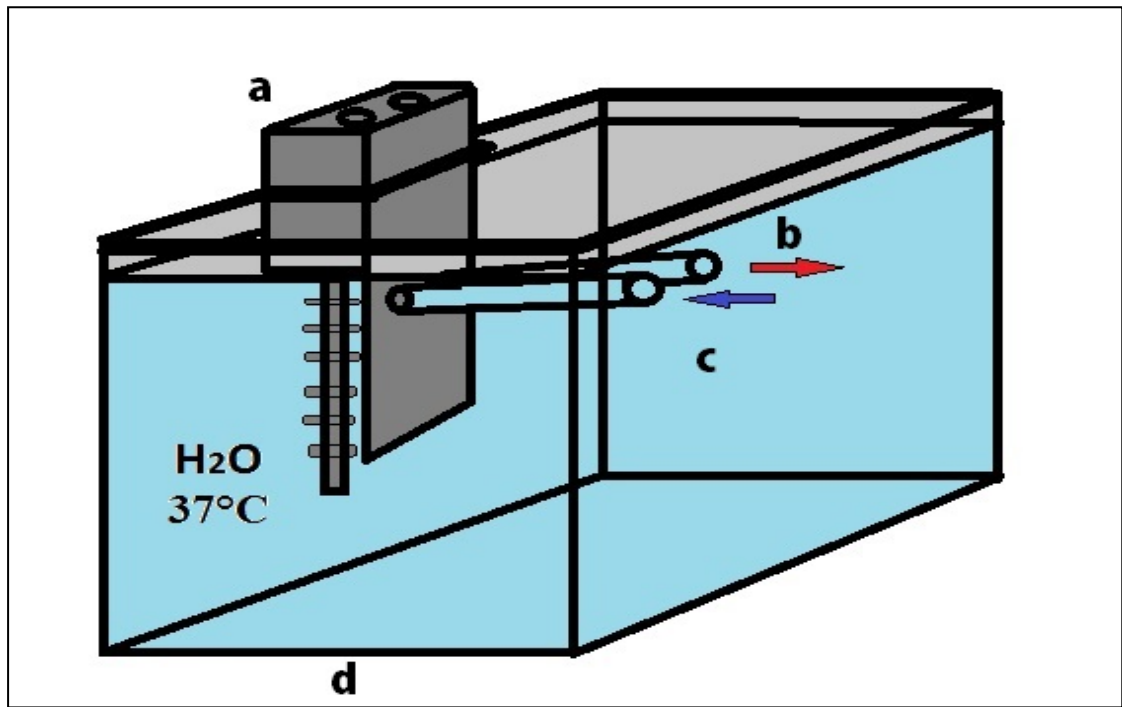


Figure 5.5: Thermo regulated bath: a) heat pump, b) outlet for warm water, c) return inlet for water from the chamber, d) Plastic container.

5.4. Measurement components

The measurement components are the different elements used to determine T_v , Flow, P_{tp} and T_p . These parameters are used to calculate R_L and C_{dyn} (as shown in Fig 5.6) as explained in detail in chapter 3. The elements used to obtain these respiratory parameters were: a) Pneumotachograph and tracheal cannula; b) Differential Pressure transducer for T_p ; and c) Differential pressure transducer for P_{tp} ; and d) Esophageal cannula.

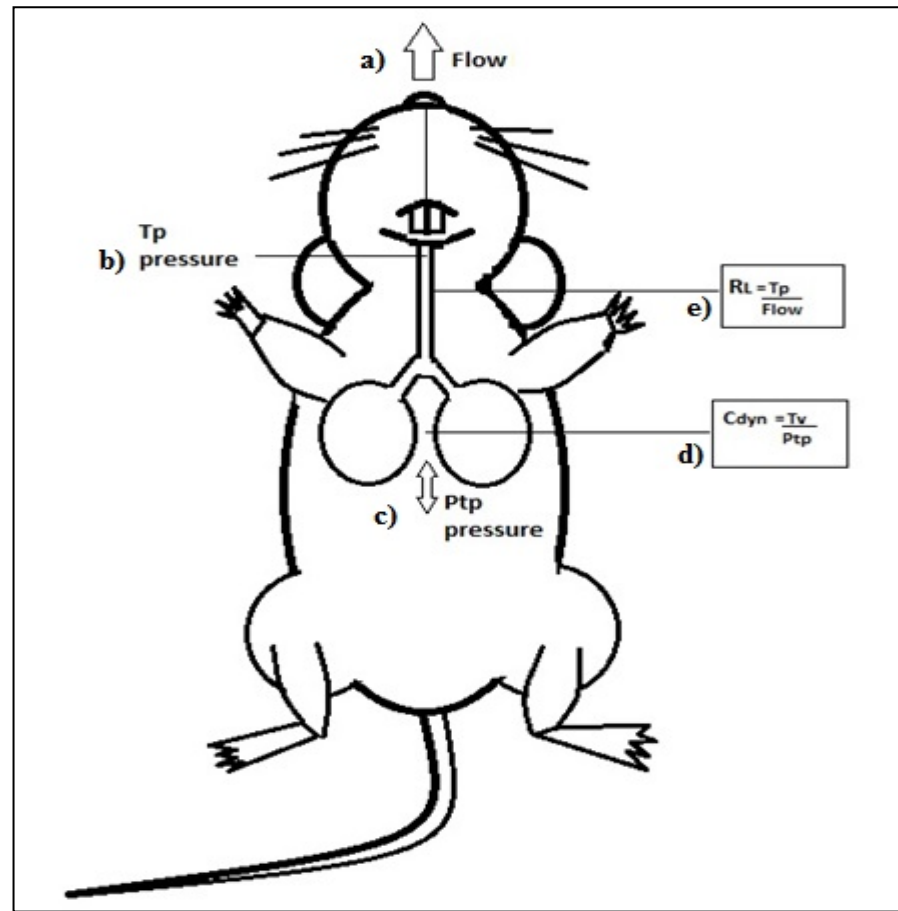


Figure 5.6: Respiratory parameters: a) Flow; b) T_p pressure (tracheal); c) P_{tp} pressure (transpulmonar); d) R_L (lung resistance); C_{dyn} (dynamic compliance) [138].

5.4.1. *Pneumotachometer and tracheal cannula*

The pneumotachometer and tracheal cannula are used to cannulate the trachea during the experimental procedures by keeping the airways open. The pneumotachometer through the connection with the DLP 2.5 differential pressure transducer also allows the measurement of pressure changes to occur at the level of the mice trachea and to measure the air flow and tidal volume occurring during the breathing process. The pneumotachograph shown in figure 5.7 was sourced from Harvard Apparatus from the United States by a New Zealand company called Alphatech Systems and its specifications are presented in table 5.1 (HSE-Pneumotachometer PTM Type 378/0.9 For Mice, P/N 73-0981).

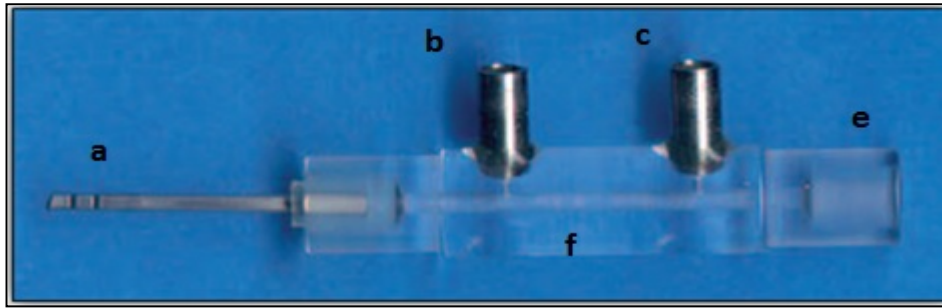


Figure 5.7: HSE-Pneumotachometer PTM Type 378/0.9 For Mice: a) Tracheal cannula, b) outlet to measure pressure at level of the mouth (before resistance), c) outlet to measure atmospheric pressure (after resistance), e) outlet for air and f) reduction of diameter of the tube (resistance).

Table 5.1: Pneumotachograph specifications

| Specification | Mice | Rats |
|--------------------------|-------------------------------------|---------------------------------------|
| Nominal sensitivity | 10 mmH ₂ O for 27 ml/sec | 10 mmH ₂ O for 10.5 ml/sec |
| Nominal flow range | ±27 ml/sec | ±10.5 ml/sec |
| Flow resistance (approx) | 0.4 mmH ₂ O/ml/sec | 1.0 mmH ₂ O/ml/sec |
| Dead space (approx) | 50 µl | 25 µl |

5.4.2. Low Differential Pressure Transducer (Air Flow & Tidal Volume)

This pressure transducer is used to register the T_p , T_v and flow (Fig 5.8). This differential pressure transducer was selected due to its ability to maintain accuracy of readings at low pressures which is essential for measuring the tidal airflow and tidal volume. The transducer was sourced from Hugo Sachs in Germany and its specifications are presented in table 5.2 (Differential Low Pressure Transducer DLP 2.5, P/N 73-3882)

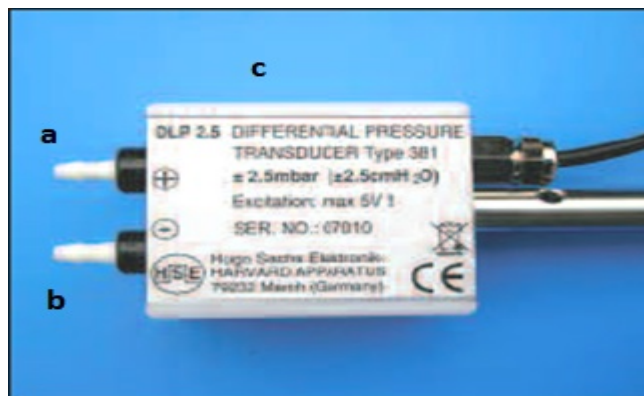


Figure 5.8: DLP 2.5 Differential pressure transducer: a) inlet for pressure signal from the mouth, b) inlet for pressure signal from environment, c) differential pressure transducer.

Table 5.2: DLP 2.5 Differential pressure transducer specifications

| Specification | Value |
|------------------------|---|
| Overpressure | $\pm 2.5\text{cm H}_2\text{O}$ |
| Natural frequency | 250cm H ₂ O |
| Measuring system | Full bridge |
| Pressure cavity volume | 120mm ³ |
| Excitation voltage | 5VDC |
| Thermal zero shift | $\pm 1.5\%$ FS (-25 to 85°C) |
| Sensitivity | 65 to 67 mV/cm H ₂ O at 5 V excitation |
| Linearity | $\pm 0.25\%$ FS |
| Weight | 190g |

In order to gain useful readings from the pressure transducer outputs, the signals was needed to be amplified using a TAM-A transducer amplifier module (P/N 73-0065) provider from the same company that provide the differential pressure transducer. The amplified signal is send through the 16 channels board, which transmit the data to the Labchart software for its analysis. In order to power the amplifier, a PLUGSYS Minicase was also required (Fig 5.9) to house and provide the power to the amplifier module, its technical specifications are presented in table 5.3.



Figure 5.9: TAM-A transducer amplifier module and PLUGSYS Minicase type 609

Table 5.3: TAM-A amplifier specifications

| Specifications | Description |
|------------------------|--|
| Bridge Supply Voltage | +5V / 50 mA max. |
| Transducer Input | 6-pin socket with screw lock (binder, Amphenol Tuchel) Differential input circuit, input impedance $10^{10} \Omega$ |
| Gain | Selectable Ranges by Internal Jumper: 0.2 to 10, 0.4 to 20, 1 to 50, 2 to 100, 4 to 200, 10 to 500, 20 to 1000, 100 to 5000, 200 to 10000. Fine Adjustment Through 10-Turn Trimmer |
| Bridge Balance | Through 10-turn trimmer coarse adjustment and electronic autozero by push button (LED for error if autozero is not possible) |
| Signal Output | <ul style="list-style-type: none"> On front panel through BNC socket ± 10 V pulsatile filtered or mean signal output internally selectable. Through bus connector to PLUGSYS measuring system through links ± 10 V pulsatile filtered and mean signal voltage. |
| Output low-pass filter | <ul style="list-style-type: none"> Selectable by switch on front panel for pulsatile output signal: 1, 100, 300 Hz. Selectable by internal jumper for mean output signal: 0.1, 0.3 Hz. |
| Analog indication | TAM-A LED bar graph 20 LEDs (+13/-7) for visual check on the signal sensitivity approx. 1 V/LED TAM-D 3 1/2-digit LED display |
| Electrical calibration | Selectable by switch on front panel: <ul style="list-style-type: none"> 0 V output signal with switch in position '0'. Positive or negative calibration output voltage adjustable with 10-turn trimmer if switch is in position 'CAL'. |
| Power supply | +5 V through connector from PLUGSYS bus system |
| PLUGSYS width | 2 slot units |

5.4.3. Oesophageal catheter

The oesophageal catheter was required to measure the Ptp. The catheter was made of PE tubing (PE 90) and a blunt 20 g needle (as shown in Fig 5.10). The needle body is covered by a silicone tubing with ID = 3 mm and OD = 5 mm. The PE tubing had a length of 120mm and the tip was bevelled at 45°. Two oval holes were incised into the PE tubing at about 3 and 8 mm from the tip using a micro spring scissor or a scalpel. The holes were opposite sides and had a size of about 2 mm by 1 mm. The PE tubing was mounted on the 20 g blunt needle with the silicone tubing sleeve. The silicone tubing was used to maintain the needle into the oesophagus and the blunt 20 g needle was connected to the differential pressure transducer. The catheter was filled with saline solution and changes on the position of the column of saline were registered by pressure transducer as result of changes of pressure at mid thorax [136].

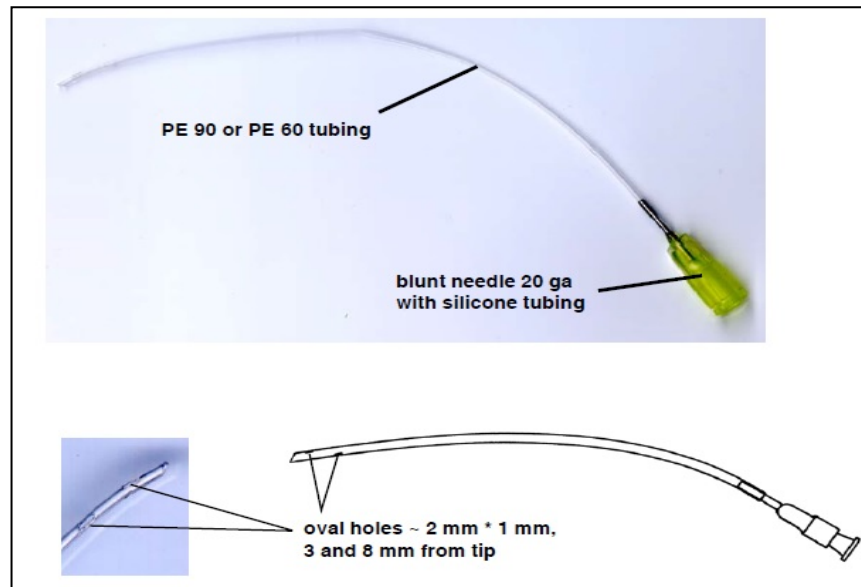


Figure 5.10: Eosophagal catheter (obtained from data sheet)

5.4.4. Pressure Transducer (Oesophageal Pressure)

This pressure transducer is required to measure the Ptp once that it is connected to the filled Oesophageal catheter. This pressure transducer is shown in figure 5.11 and it was selected due to its ability to maintain accuracy of readings at low pressures (± 1 psi), which is essential for measuring the change of pressure occurring between the lungs at mid thorax (as shown in Fig 5.12 and 5.13). The transducer was sourced from Honeywell S&C (P/N HSCSAAN001PDAA5), and its technical specifications are presented in table 5.4.

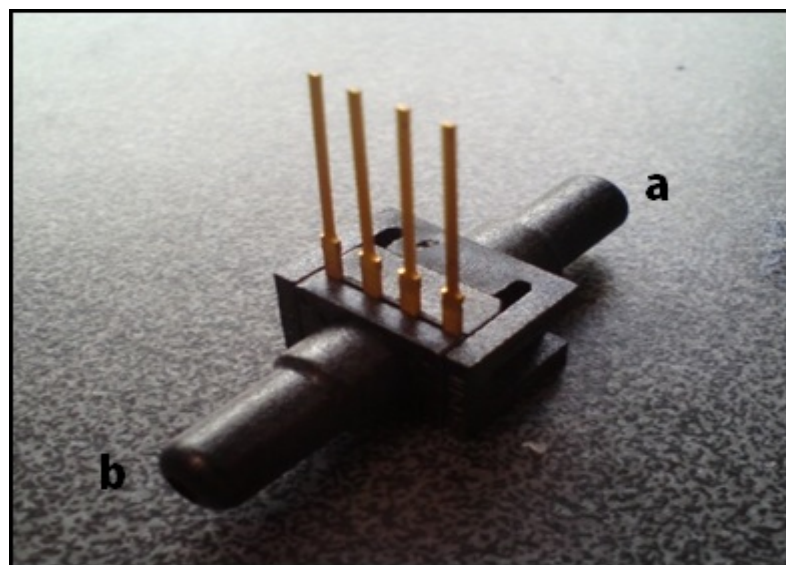


Figure 5.11: Sensor technics model 26PC0050D6A: a) Inlet for pressure signal from mid thorax, b) inlet for pressure signal from the environment.

Table 5.4: Sensor technics pressure transducer specifications [19]

| Specification | Value |
|------------------------------|-------------------------|
| Operating pressure | 0-50 cmH ₂ O |
| Sensitivity | 240 μ V/mbar |
| Full-Scale span - Minimum | 10.5mV |
| Full-Scale span - Typical | 12.0mV |
| Full-Scale span - Maximum | 13.6mV |
| Response time | 1 ms |
| Repeatability and hysteresis | ± 0.2 |

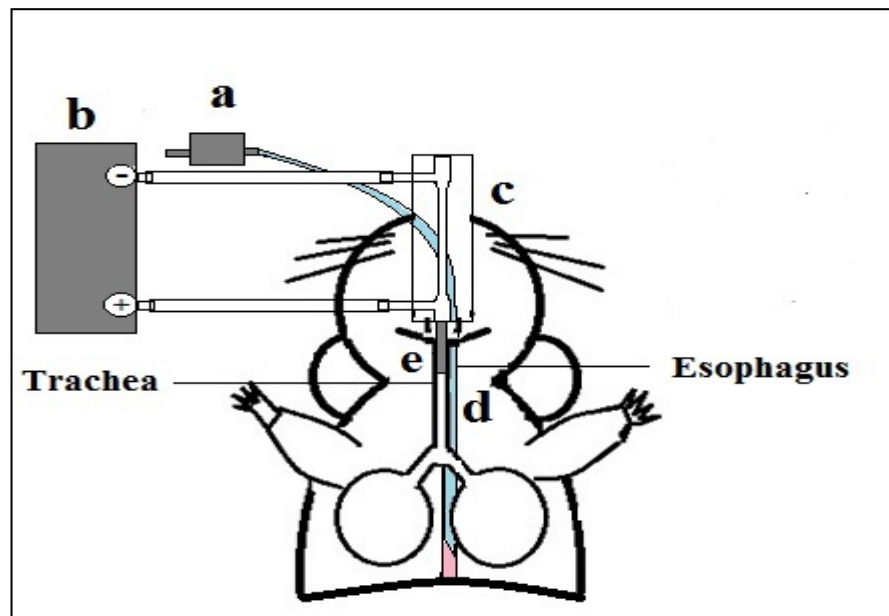


Figure 5.12: Scheme of location for esophageal catheter and tracheal cannula. a) Pressure transducer; b) Differential pressure transducer; c) Pneumotachograph (venturi); d) esophageal catheter (located at mid thorax through the oesophagus); e) Tracheal cannula.

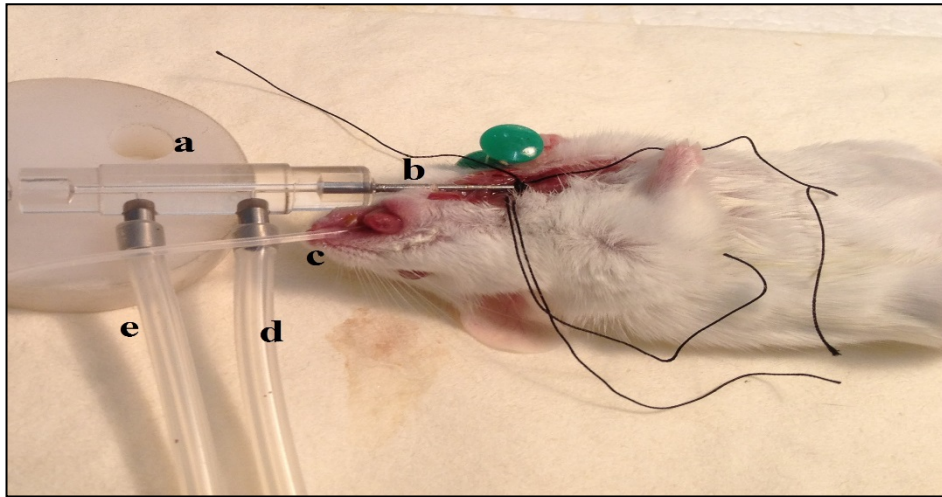


Figure 5.13: Location of tracheal cannula and oesophageal catheter: a) Pneumotachograph (venturi); b) Tracheal cannula; c) oesophageal catheter; d) Tracheal pressure and e) atmospheric pressure.

All these measuring elements mentioned above corresponds to the whole measuring set-up that integrate the plethysmograph, but also was required to develop for the project an oscillation device to deliver the oscillations into the airways *in vivo*.

5.4.5. Powerlab 16Ch and Labchart 7.0

The system selected to record the data and process it was The PowerLab 16/30 (overview of setup in Fig 5.14). This is a high-performance data acquisition system suitable for a wide range of research applications that require up to 16 input channels. The unit is capable of recording at speeds of up to 400 000 samples per second continuously to disk, and is compatible with instruments, signal conditioners and transducers supplied by ADInstruments, as well as many other brands. In addition to standard single-ended BNC inputs, the PowerLab 16/30 features 4 differential Pod ports that allow for direct connection of Pod signal conditioners and appropriate transducers. Both pressure transducers are attached to the board using coaxial connectors into ports 1 and 7.



Figure 5.14: Powerlab 16/30 and cds for Chart scope and Chart Pro

The PowerLab 16/30 works with the ADInstruments software LabChart, which is a flexible and easy tool to work with. This software brings several templates which could be used for different physiological experiences. The template for spirometry was used to develop the final program for the experiments of this study. This template has the option of automatically setting channels to register flow (L/s), Tidal Volume (L), Minute Ventilation (L/min). This template was modified for purposes of the study and 9 channels were activated and set as shown in table 5.5 as follows: Ch1) Voltage; Ch2) T_p ; Ch3) Flow; Ch4) Volume; Ch5) Minute ventilation; Ch6) Tidal volume; Ch7) P_{tp} ; Ch8) RL and Ch9) C_{dyn} . In order to obtain these two last parameters, specific equations for each of them were added into their respective channels settings (equations presented in chapter 3). The pressure transducer were physically connected to the board using coaxial cables/connectors as follows: DLP 2.5 Differential pressure transducer to Ch1 and Sensor technics model 26PC0050D6A to Ch7 to register the voltage changes signals, which were converted into data pressure changes (these signals were previously calibrated using the protocol explained in detail in section 7). These readings were useful to determine parameters such as T_v , Flow, T_p , and P_{tp} , and indirectly to measure RL and C_{dyn} in real time as shown in figure 5.15.

Table 5.5: Channels and unit used for the readings.

| Channel | Parameter measured and unit |
|----------------|------------------------------------|
| Ch1 | Voltage |
| Ch2 | Tp (mmH ₂ O) |
| Ch3 | Flow (L/s) |
| Ch4 | Volume (L) |
| Ch5 | Minute Ventilation (L//Min) |
| Ch6 | Tv (L) |
| Ch7 | Ptp (mmH ₂ O) |
| Ch8 | RL (mmH ₂ O/L/s) |
| Ch9 | Cdyn (L/mmH ₂ O) |

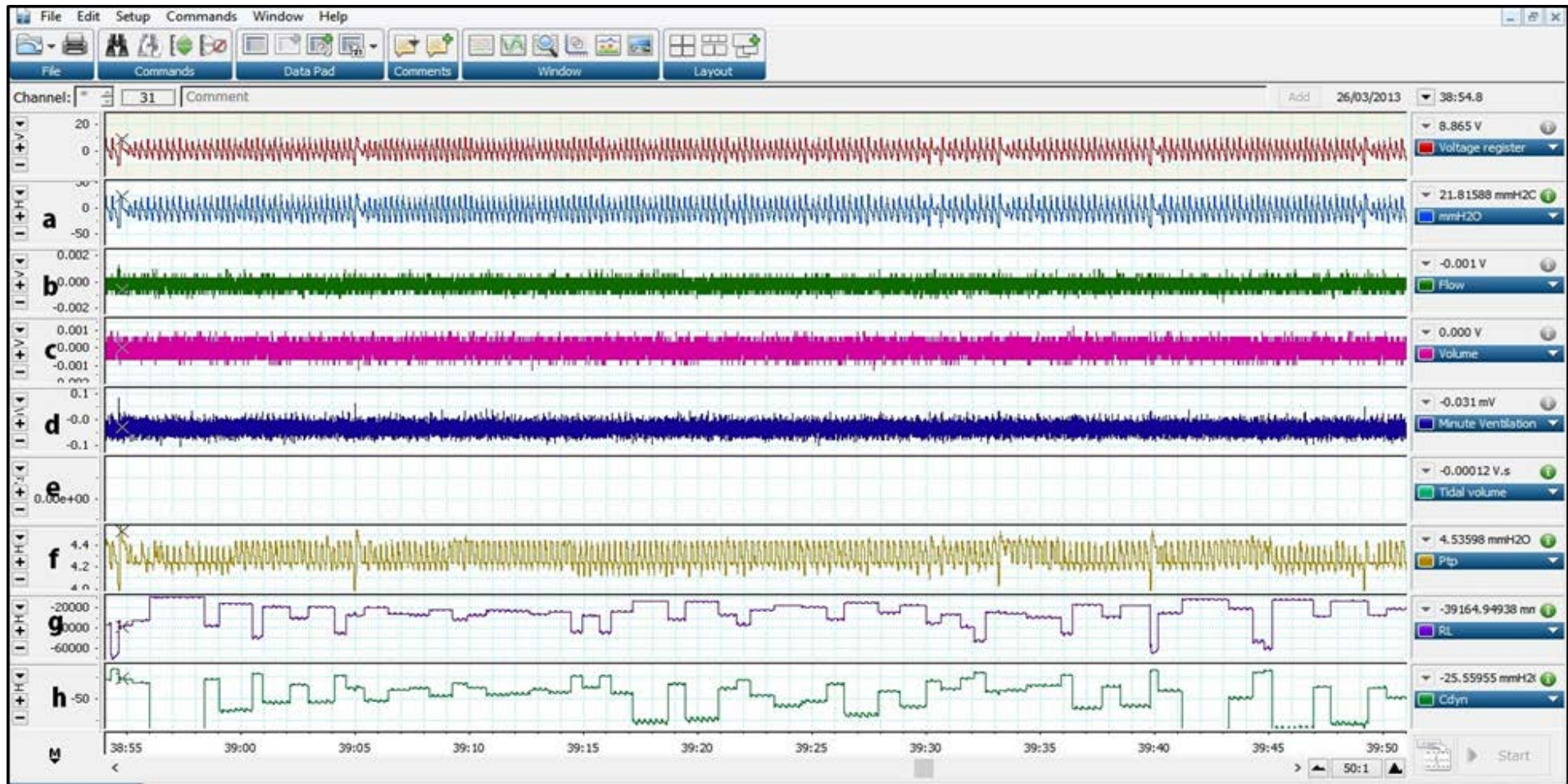


Figure 5.15: Labchart program: a) Tracheal pressure (T_p , mmH₂O); b) Flow L/s; c) Volume (L); d) minute ventilation (ml/min); e) Tidal volume (T_v , L); f) Transpulmonary pressure (P_{tp} mmH₂O); g) Lung Resistance (R_L , mmH₂O/L/s) and h) Dynamic compliance (C_{dyn} , L/mmH₂O).

5.5. *Drugs and allergen delivery system*

This section covers the details of the jet nebulizer used for the drug and allergen delivery and the accessories needed in the experiments.

5.5.1. *Nebulization system for the drugs and allergen*

In order to sensitize and deliver drugs into the airways of the animal models for sensitization a nebulizer was required. For purposes of this study a jet nebulizer from Harvard apparatus was acquired (P/N 73-1963). This aerosol jet nebulizer required an operating pressure of approximately 1.5 bar (22 psi) from a compressed air source (Fig 5.17, a). This pressure was supplied using an AMPRO air brush compressor with a working range of 15-50 psi (Fig 5.17, b), which was fixed to the pressured required by the jet nebulizer. All of the particles generated by the jet nebulizer are 10 μm or less in size with 60% of the particles being 2.5 μm or less. The data presented below in the figure 5.16 shows the particle sizes obtained when 5 ml of a 0.9% saline solution was nebulized with a gas inlet pressure of 1.5 bar (data obtained from data sheet).

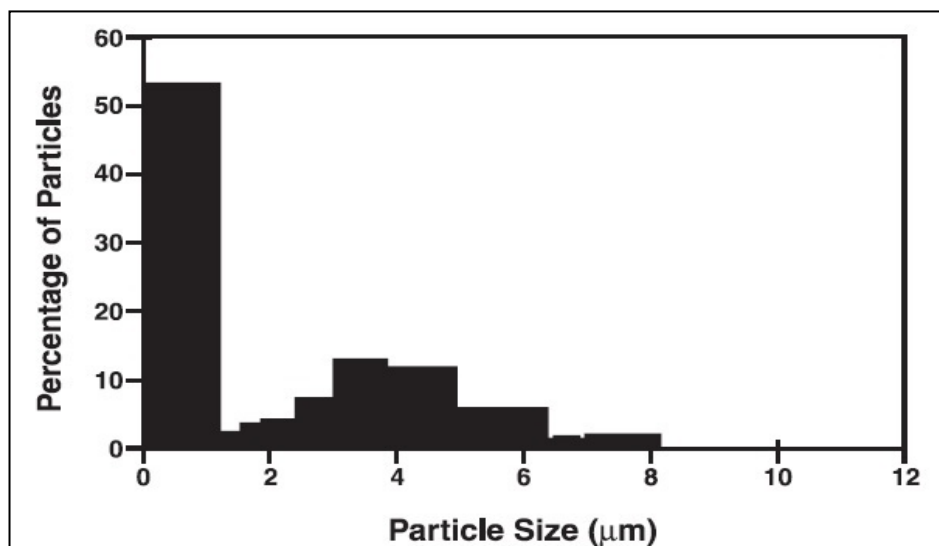


Figure 5.16: Particle size chart (from datasheet provided for jet nebulizer).

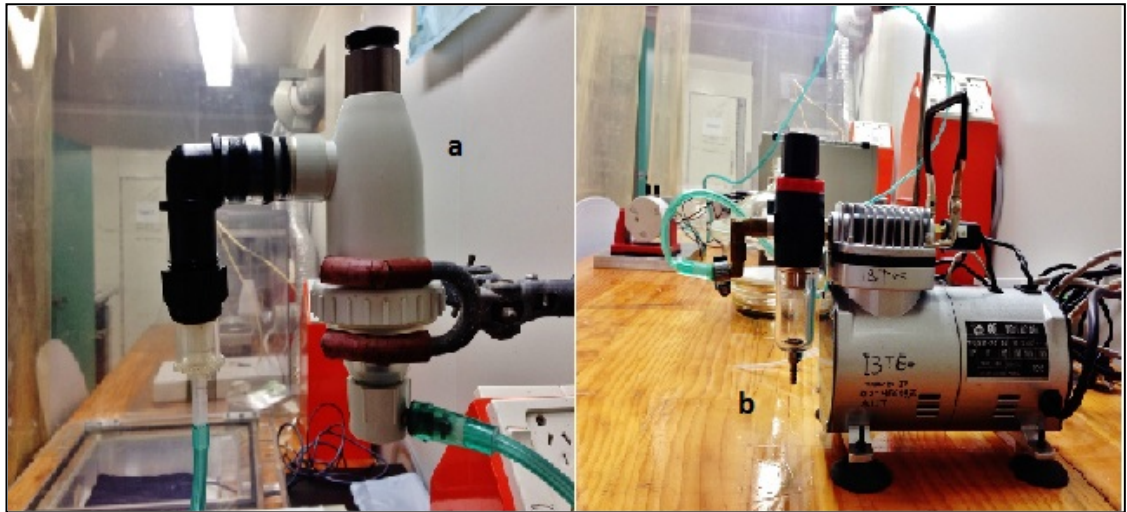


Figure 5.17: Nebulization setup: a) Jet nebulizer from Harvard apparatus; b) AMPRO air brush compressor.

5.6. Pressure oscillation setup

In order to establish how these oscillations work on asthmatic airways a device to deliver superposed oscillations into the airways during spontaneous breathing was also required for the study. The most commonly used methodologies to induce oscillations on animal experimentation are electromagnetic shakers, pressure-volume changes [163, 164], or acoustic waves (from speakers) [165].

For purposes of this study a device based on pressure-volume oscillations was built (Fig 5.18 and 5.19). It was considered that this type of oscillations were the most direct approach to deliver the oscillations to be tested and also the less invasive of all those mentioned before. This device involved the use of: a) arbitrary waveform generator (Hewlett Packard); b) LDS PA25E power amplifier; c) a shaker Model V203 (Ling Dynamics System LTD); d) a 10ml plastic chamber with one inlet and one outlet, e) a piston built with silicone connected to the shaker and placed into the chamber, and f) a sturdy base to maintain the device in a fixed position. The device was capable of generating pressure changes, which were induced using a waveform generator that create the waveform desired and which was sent to the shaker and the piston, generating displacement of the piston inside of the sealed chamber. The working range for amplitude/frequency of the device is 50-700mV/0.001-100Hz respectively. The device was tested with an initial frequency of 3Hz (close to the 2.7Hz calculated for the breathing patterns of the mice, which corresponds to the breathing frequency of mice (~163 per minute, [166]) to 20Hz that corresponds to the maximal frequency tested

during the tissue testing (*in vitro*). A Large range of amplitudes were tested (50mV – 1.3V) in order to have a wide range of pressure values to choose from for the experiments. The maximal volume changes expected with the current piston will be in between 100-200 μL , which is equivalent to the physiological volumes observed in the breathing process of the mice (tidal volume: 150 μL /per breathing cycle).

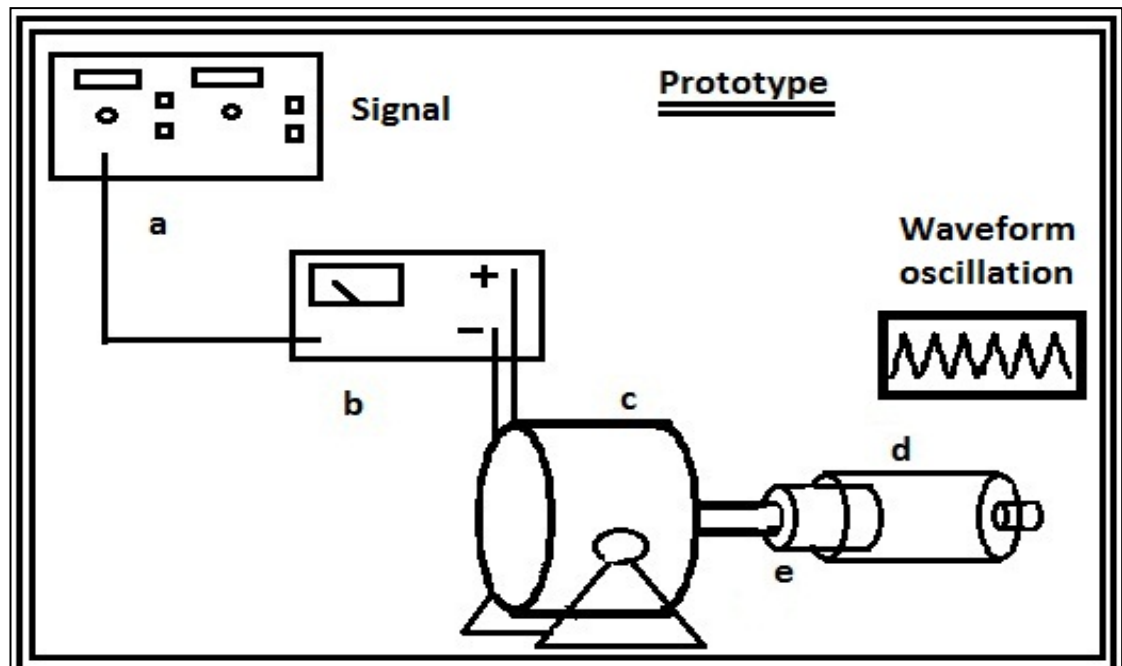


Figure 5.18: a) waveform generator; b) Power amplifier; c) shaker; d) chamber; e) piston.

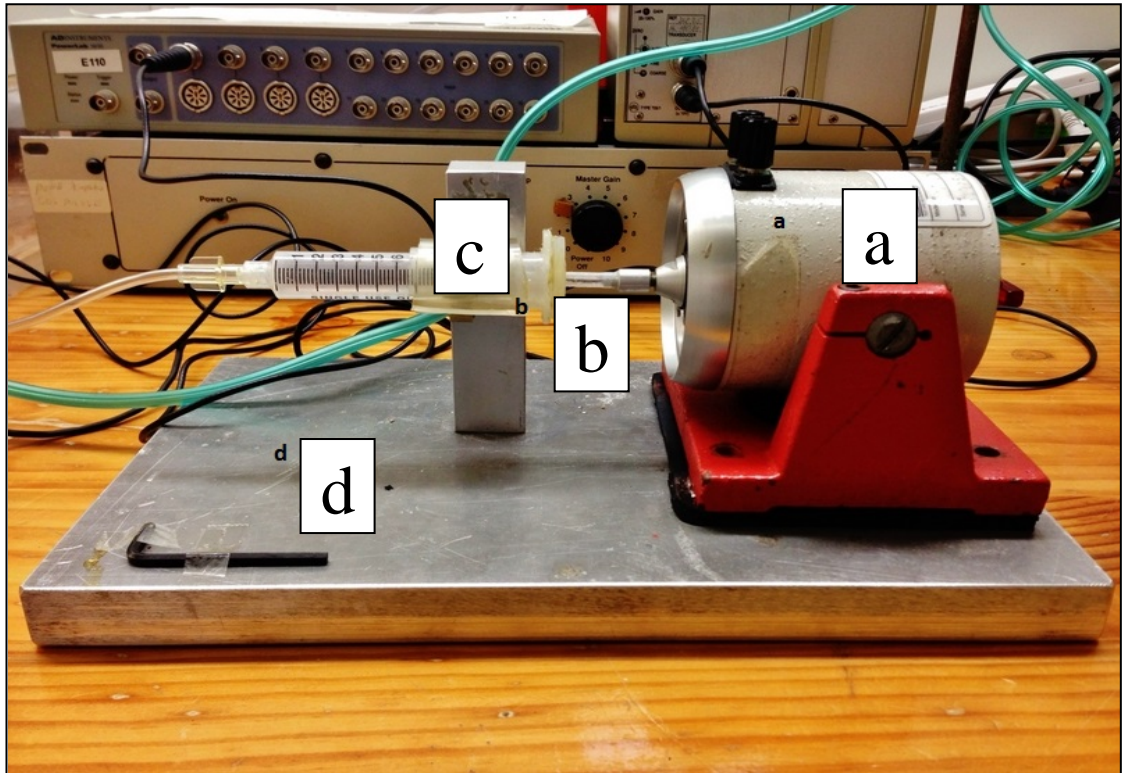


Figure 5.19: Pressure oscillation setup: a) Shaker, b) Chamber, c) Piston and base.

5.7. Calibration of devices and oscillation setup

This section cover the calibration and standardization of the pressure transducers for tracheal and oesophageal pressure, and oscillation device.

5.7.1. Calibration Low Differential Pressure Transducer

Before its use, the differential pressure transducer was tested and calibrated once all the equipment was put together. The calibration process was performed using the pressure transducer connected through a plastic pipe to water manometer (as shown in Fig 5.20) and it was calibrated using changes of 1mmH₂O per time (9 points) and the protocol was repeated at least three times. The data was registered using Labchart and the results obtained from the calibration were tabulated and plotted in table 5.6 and figure 5.21 respectively.

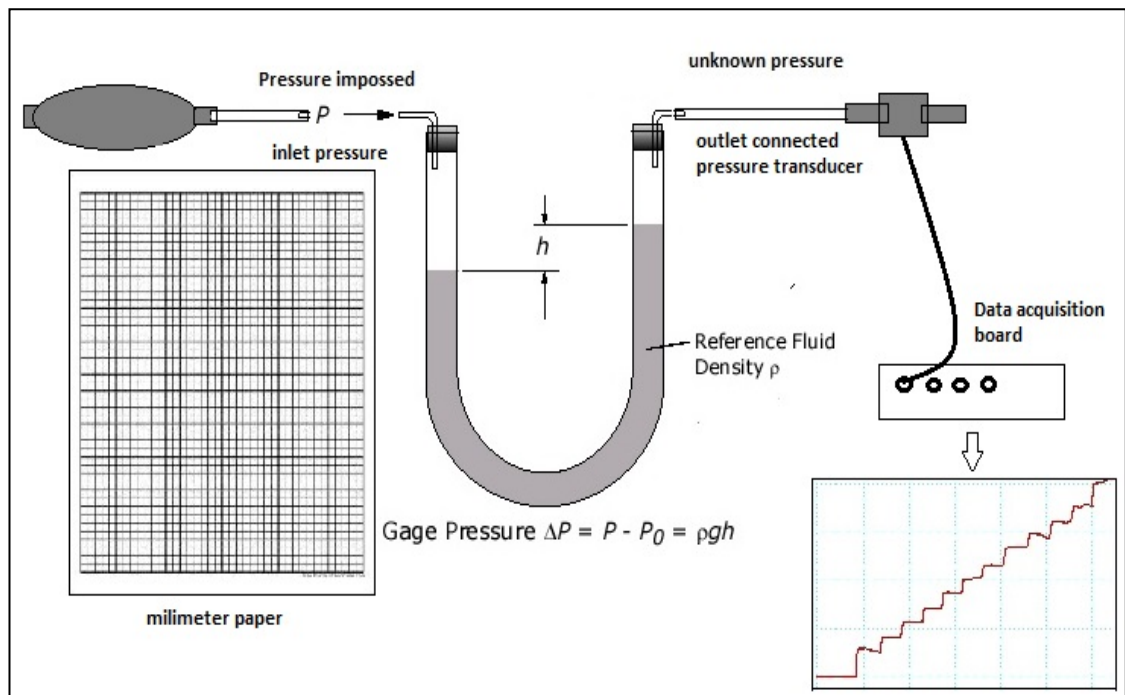


Figure 5.20: Water manometer used for calibration curve for pressure transducer for T_p .

Table 5.6: Pressure data obtained with differential pressure transducer for T_p .

| Tracheal Cannula | | | | |
|--------------------|--------|--------|--------|--------|
| Calibration dots | | | | |
| mmH ₂ O | 1 | 2 | 3 | Mean |
| 1 | 2.1435 | 2.2167 | 2.2983 | 2.2195 |
| 2 | 2.4868 | 2.6014 | 2.5518 | 2.5467 |
| 3 | 2.9201 | 2.9275 | 2.8353 | 2.8943 |
| 4 | 3.2682 | 3.2895 | 3.1140 | 3.2239 |
| 5 | 3.7006 | 3.5802 | 3.3832 | 3.5547 |
| 6 | 3.9850 | 3.7993 | 3.7413 | 3.8419 |
| 7 | 4.1229 | 4.0835 | 4.1869 | 4.1311 |
| 8 | 4.4772 | 4.3037 | 4.5015 | 4.4275 |
| 9 | 4.7487 | 4.5048 | 4.9264 | 4.7266 |

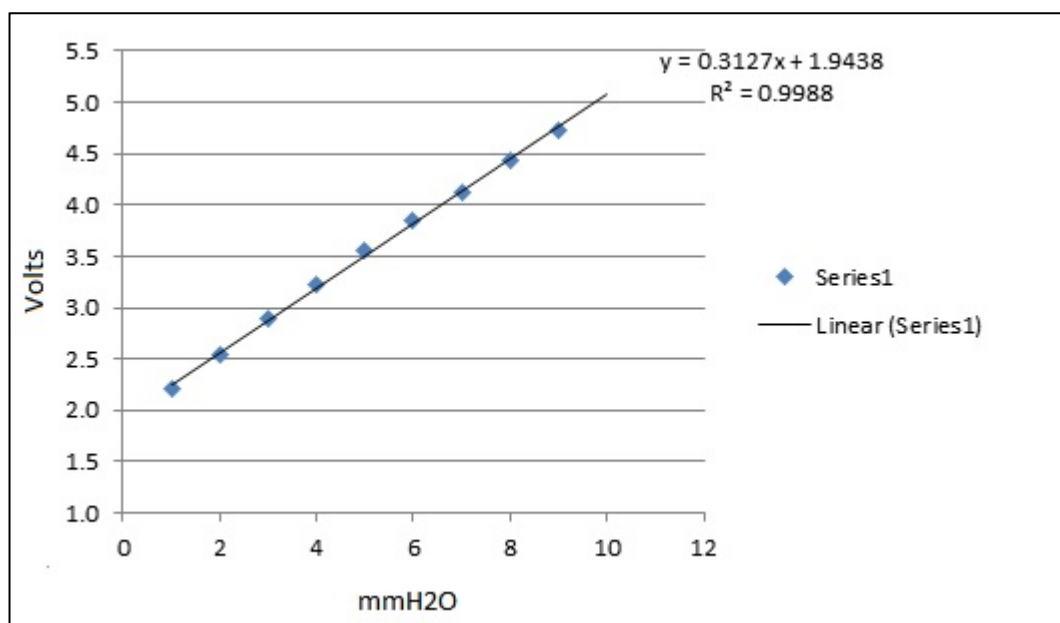


Figure 5.21: Calibration curve for pressure transducer for T_p .

5.7.2. Calibration Pressure Transducer (Oesophageal Pressure)

Before its use, the differential pressure transducer acquired from Honeywell was also tested and calibrated. The calibration process was performed following the same procedure described for the low pressure transducer in the previous section. The data was registered using a Labchart and the results obtained from the calibration were tabulated and plotted in table 5.7 and figure 5.22 respectively.

Table 5.7: Pressure data obtained with differential pressure transducer for P_{tp} .

| Oesophageal Cannula | | | | |
|---------------------|--------|--------|--------|--------|
| Calibration dots | | | | |
| mmH2O | 1 | 2 | 3 | Mean |
| 1 | 0.0050 | 0.0050 | 0.0041 | 0.0047 |
| 2 | 0.0088 | 0.0087 | 0.0082 | 0.0086 |
| 3 | 0.0131 | 0.0120 | 0.0118 | 0.0123 |
| 4 | 0.0181 | 0.0172 | 0.0179 | 0.0177 |
| 5 | 0.0216 | 0.0225 | 0.0220 | 0.0220 |
| 6 | 0.0264 | 0.0272 | 0.0274 | 0.0270 |
| 7 | 0.0317 | 0.0318 | 0.0311 | 0.0315 |
| 8 | 0.0368 | 0.0363 | 0.0350 | 0.0360 |
| 9 | 0.0413 | 0.0395 | 0.0403 | 0.0404 |
| 10 | 0.0459 | 0.0431 | 0.0445 | 0.0445 |

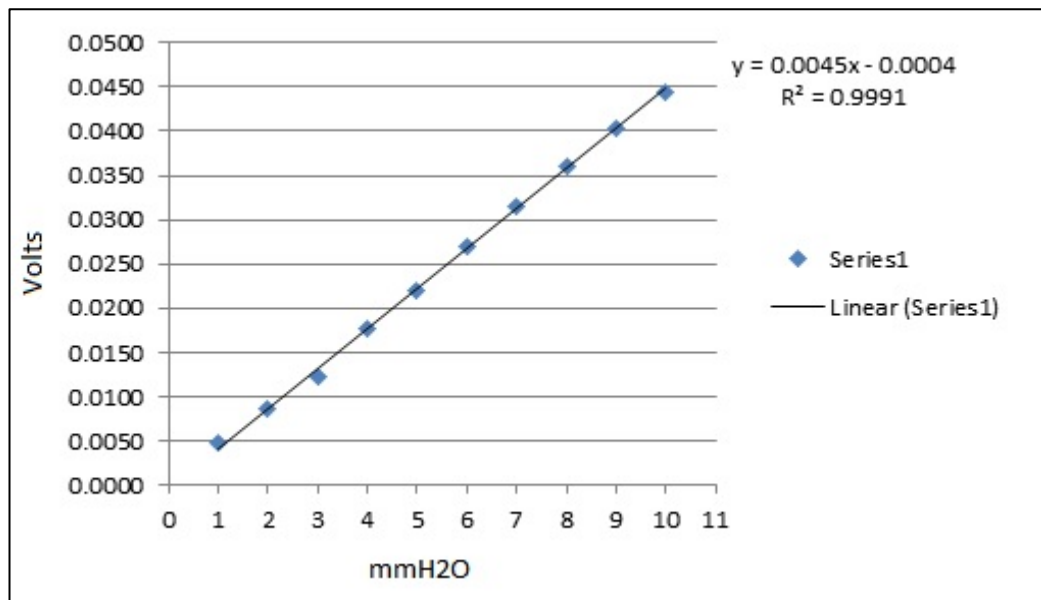


Figure 5.22: Calibration curve for pressure transducer for Ptp.

5.7.3. Calibration of oscillation setup

Before its usage the pressure oscillation setup was required was calibrated. Different frequencies in the range of 3-20 Hz were tested with amplitudes varying from 50mV – 1.3 V and pressures observed were tabulated and presented in table 5.8. These tests were performed to determine the range of work of the setup and useful amplitude range for the experiments of this study. The range of frequencies was selected based on the consideration of frequencies used during the *in vitro* stage and the range of amplitudes were varied while the tests were performed.

Table 5.8: Pressure observed with device.

| Voltage | cmH ₂ O | | | | |
|---------|--------------------|--------|-------|-------|-------|
| | 3Hz | 5Hz | 10Hz | 15Hz | 20Hz |
| 50mV | 0.393 | 0.318 | 0.071 | 0.064 | 0.134 |
| 60mV | 0.473 | 0.417 | 0.346 | 0.078 | 0.177 |
| 70mV | 0.523 | 0.445 | 0.431 | 0.261 | 0.191 |
| 80mV | 0.636 | 0.572 | 0.495 | 0.332 | 0.325 |
| 90mV | 0.742 | 0.65 | 0.594 | 0.396 | 0.403 |
| 100mV | 0.813 | 0.756 | 0.678 | 0.431 | 0.431 |
| 200mV | 1.71 | 1.632 | 1.512 | 1.052 | 1.053 |
| 300mV | 2.685 | 2.614 | 2.403 | 1.674 | 1.682 |
| 400mV | 3.717 | 3.604 | 3.335 | 2.353 | 2.311 |
| 500mV | 4.812 | 4.657 | 4.275 | 3.025 | 2.961 |
| 600mV | 5.712 | 5.526 | 5.095 | 3.668 | 3.569 |
| 700mV | 7.017 | 6.671 | 6.155 | 4.395 | 4.289 |
| 800mV | 7.766 | 7.547 | 7.024 | 4.968 | 4.841 |
| 900mV | 8.833 | 8.487 | 7.886 | 5.639 | 5.477 |
| 1V | 9.667 | 9.151 | 8.621 | 6.233 | 6.049 |
| 1.1V | 10.769 | 9.957 | 9.413 | 6.911 | 6.756 |
| 1.2V | 11.964 | 10.791 | 10.19 | 7.59 | 7.321 |
| 1.3V | 3.752 | 3.413 | 3.166 | 2.233 | 2.169 |

The pressure changes obtained with the system were recorded using the same program that was used for the experimental protocols which was Labchart and it was expresses in cmH₂O. The pressure range observed with the frequencies and amplitudes mentioned on the previous paragraph was between 0.06 cmH₂O for 15Hz/50mV and 11.96 cmH₂O for 3Hz/1.2V.

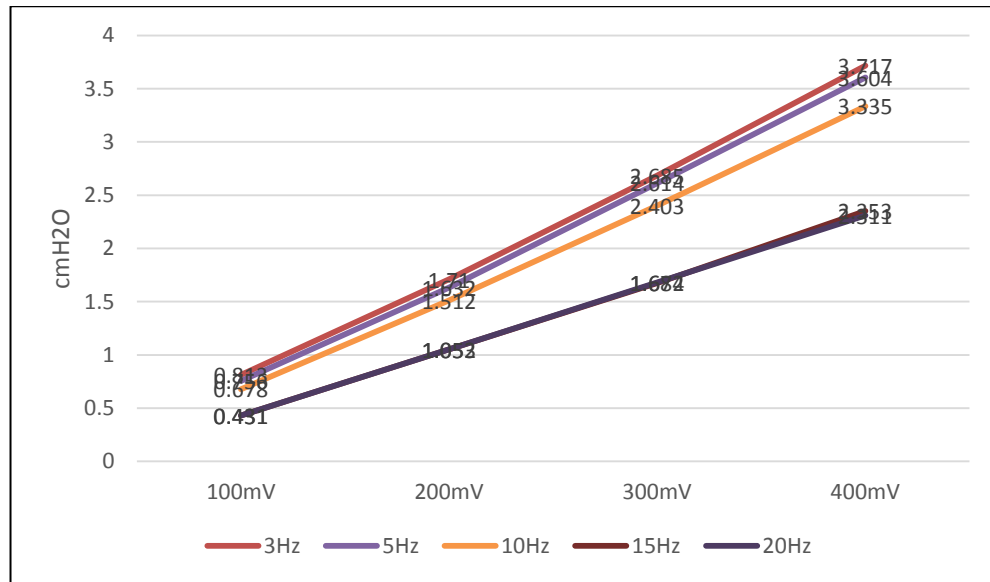


Figure 5.23: Pressure observed with device.

Considering the results obtained from the combination of the amplitudes and frequencies mentioned in the previous paragraph and table 5.8, and also considering values of pressure oscillations used for other groups [163] the range of pressure selected for the study was in the range of 0.5 cmH₂O – 4 cmH₂O as shown in figure. This range of pressure which will be applied to the airways in form of superposed oscillations during spontaneous breathing includes amplitudes between 100 – 400 mV within the same frequencies used in the *in vitro* experiments 5, 10, 15 and 20Hz (chapter 4).

5.8. Testing *in vivo*

Once all the equipment described in this chapter was tested and calibrated, it was time to test these oscillations on the animal models to see if these types of superposed oscillations were effective under *in vivo* conditions.

During the plethysmography, the animals were anaesthetised and intubated with tracheal cannula and oesophageal catheter (the procedure was described in detail in the first part of the protocol from chapter 3 section 7). Unique doses of bronchoconstrictor (Ach 10⁻²M), and bronchodilator (Isoproterenol 10⁻⁶M) were used for the protocol to induce contraction and relaxation of the airways (respectively). These drugs were administered as a mist using the jet nebulizer (Presented in Fig 5.17). The jet nebulizer was indirectly connected to the mouse lungs via the duo pneumotachometer-tracheal cannula. Five ml of testing solution (normal saline solution, or a specific concentration

of Acetylcholine and Isoproterenol) was placed in the nebulizer tank (depending of the protocol).

Protocol:

- *Each mouse is initially challenged for 5 min with saline solution to obtain a basal reading, and after 5 min of nebulisation, the nebulizer will be switched off before recording the respiratory parameters for 10 min. The recording time corresponds also to a resting time for the animal since it will not undergo any additional treatment or manipulation during this time.*
- *Then an unique dose of Acetylcholine is administered to induce bronchoconstriction according to the following sequence: nebulisation of Acetylcholine $10^{-2}M$ for 2 min.*
- *Then the bronchorelaxation will be tested by administration of unique dose of ISO (Data presented in chapter 3) during 2 min followed by 5 min of rest.*
- *After these steps have been recorded the sequence would be repeated from the baseline with saline and superimposed pressure oscillations will replace ISO.*

Four sets of superposed oscillations were tested after contraction was induced using Ach $10^{-2}M$:

- *First set with a frequency of 5Hz and amplitudes of 100, 200, 300 and 400mV with 2 min per amplitude and after that 5 min of rest and saline.*
- *After these steps have been recorded the sequence would be repeated from the baseline with saline.*
- *Second set with a frequency of 10Hz and amplitudes of 100, 200, 300 and 400mV with 2 min per amplitude and after that 5 min of rest and saline.*
- *After these steps have been recorded the sequence would be repeated from the baseline with saline.*
- *Third set with a frequency of 15Hz and amplitudes of 100, 200, 300 and 400mV with 2 min per amplitude and after that 5 min of rest and saline.*
- *After these steps have been recorded the sequence would be repeated from the baseline with saline.*
- *Finally a fourth set with a frequency of 20Hz and amplitudes of 100, 200, 300 and 400mV with 2 min per amplitude and after that 5 min of rest and saline.*

- *After these steps have been recorded the sequence would be repeated from the baseline with saline.*

5.9. Closure

All the equipment and devices presented and explained through this chapter are the tools that facilitate the work to determine how the airways previously constricted using bronchoconstrictors such as ACh (simulation an asthmatic attack) from sensitized and healthy subjects behave *in vivo* in presence of oscillations. Once all the components were tested, calibrated and put together, it was time to test the mechanical oscillations imposed onto the airways in the form of pressure oscillations *in vivo* using the animal models developed for this purpose and following the protocol presented in the previous section.

Chapter 6

In vivo experimental investigation

6.1. Introduction

The purpose of this chapter is to present the *in vivo* experimentation, experimental results, a quick comparison of the raw data between healthy and asthmatics subjects, their statistical data analysis and discussion. In this chapter also a comparison is made between the findings observed during the *in vitro* phase of the research.

6.2. *In vivo* Testing

Once all the pieces of the equipment presented in chapter 5 were tested and calibrated, it was time to use them on the animal models. The main objective was to investigate the effect of superposed oscillations on the lung performance of asthmatic subjects.

The test protocol was given in chapter 5 and it consists of:

Protocol:

Basal (saline)

- *During the plethysmography, the animals are anaesthetised and intubated with tracheal cannula and oesophageal catheter.*
- *Each mouse is initially challenged for 5 min with saline solution.*
- *After the previous step the nebulizer is switched off and the respiratory variables for 10 min were recorded as basal.*

ISO

- *An unique dose of Acetylcholine ($10^{-2}M$) using the jet nebulizer is administered to induce bronchoconstriction for 2min (different times for the duration were tested initially, but 2min was selected due to the fact that the airways were stable after 2 min and allowed to perform different protocols in the same experimental procedure).*
- *The bronchorelaxation is tested by administration of unique dose of ISO (Data presented in chapter 3) during 2 min followed by 5 min of rest.*

- After these steps have been recorded the sequence is repeated from the baseline with saline and superimposed pressure oscillations replace ISO.

ISO was tested only in order to compare with the effect of SILO and response of airways.

Superposed oscillations

- First set with a frequency of 5Hz and amplitudes of 100, 200, 300 and 400mV with 2 min per amplitude and after that 5 min of rest and saline.
- After these steps have been recorded the sequence is repeated from the baseline with saline and a second set using 10Hz, a third set using 15Hz and a fourth set of 20Hz using the same ranges of amplitudes were performed.

6.3. Experimental data

The changes of pressure were recorded in real time using software Labchart 7.0 (see appendix) from ADInstruments (details in chapter 5). This program in combination with the plethysmograph is capable to provide the data for Tv, Flow, Tp, Pp which were directly measured using channel 1-7 and through an addition of equations (presented in chapter 3) in the remaining two channels (Channel 8 and 9), R_L and C_{dyn} were indirectly calculated. All changes of pressure are recorded and measured peak to peak (breathing cycle; ($P_{max} - P_{min}$)) from a representative segment of the register for the response of the airways to each and different experimental conditions. The values for each cycle in the segment chosen were summarized and divided for the total number of cycles occurring in segment and this gives the mean for pressure fluctuations (\bar{X}) for each of these segments selected was presented in a graph (Eq. 6.1).

$$\bar{X} = \frac{\sum (P_{max} - P_{min})}{n} \quad (Eq. 6.1)$$

Data obtained for the direct measurements: Tv, Flow, Tp and Ptp are presented in appendix D. This section shows the raw data obtained for the indirect variables R_L and C_{dyn} , which evaluate directly the level of bronchoconstriction in the airways studied.

The results for R_L are presented in Fig. 6.1, which are expressed as means for $R_L \pm \text{Std. error}$ (Axis y corresponds to R_L value obtained for each experimental condition presented in axis x). When the means for R_L obtained for healthy (controls) and the asthmatic mice (sensitized) were compared, differences on the response to the same concentration of Ach (10^{-2}M) was observed with a mean for R_L 1.62 ± 0.14 and $2.28 \pm 0.16 \text{ cmH}_2\text{O/ml/sec}$ respectively.

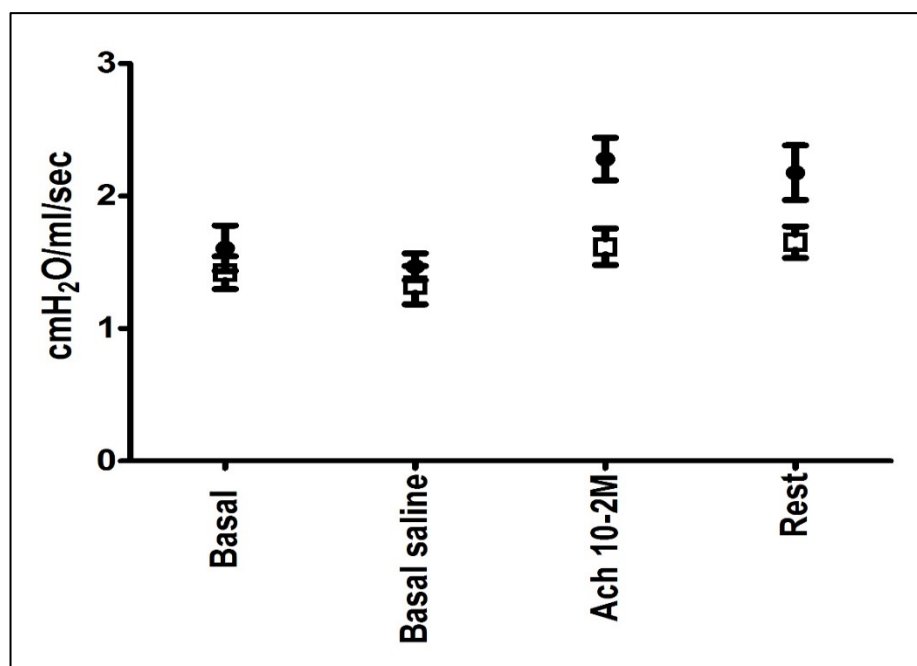


Figure 6.1: Comparison of the R_L response to ACh 10^{-2}M observed from healthy (control) and asthmatic (sensitized) subjects, axis y corresponds to R_L obtained for each experimental condition presented in axis x (\square = healthy; \bullet = asthmatic; $n=10$).

The results obtained for C_{dyn} are presented in Fig. 6.2 and are expressed as means for $C_{\text{dyn}} \pm \text{Std. error}$ (Axis y corresponds to the C_{dyn} value obtained for each experimental condition presented in axis x). When the means for C_{dyn} obtained for healthy (controls) and the asthmatic mice (sensitized) were compared, also differences on the response to the same concentration of Ach (10^{-2}M) were observed with a mean for C_{dyn} of 2.24 ± 0.40 and $1.79 \pm 0.81 \text{ ml/cmH}_2\text{O}$ respectively.

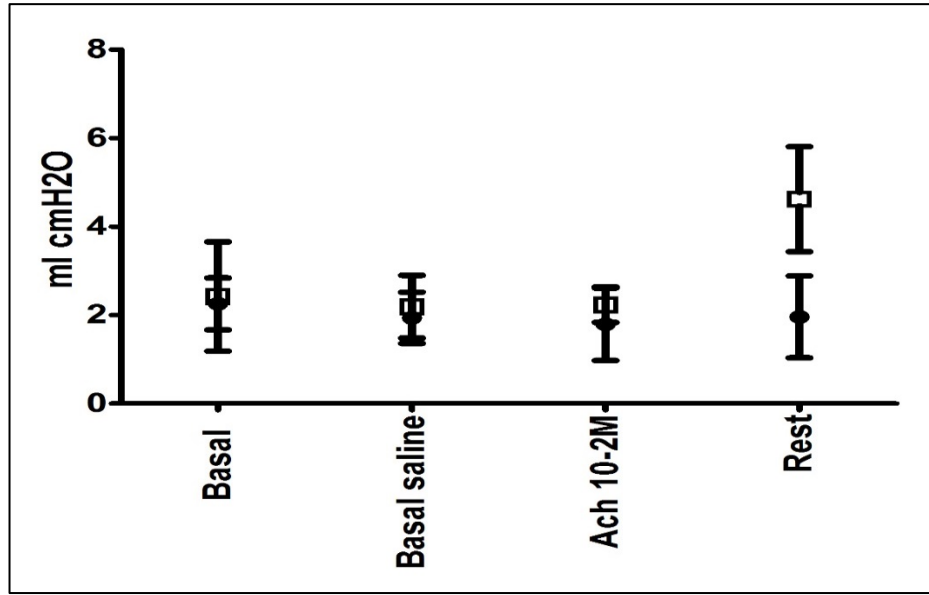


Figure 6.2: Comparison of the C_{dyn} response to ACh $10^{-2}M$ observed from healthy (control) and asthmatic (sensitized) subjects, axis y corresponds to C_{dyn} obtained for each experimental condition presented in axis x (\square = healthy; \bullet = asthmatic; $n=10$).

When the analysis was focus on the response of the precontracted airways to the different set of oscillations, it was found that each set of frequencies followed similar patterns inducing reduction of R_L obtained when the airways were previously stimulated with ACh $10^{-2}M$ (mimicking an asthmatic attack).

The results were expressed as means for R_L ; $C_{dyn} \pm$ Std. error and presented in the figures in this section. Table 6.1 shows the experimental data obtained for basal (no solution added), Saline, Ach and for the set of SILO at 5Hz, with amplitudes of 100, 200, 300 and 400 mV. This data was plotted and presented in figures 6.3 and 6.4 for comparison.

Table 6.1: experimental data for R_L and C_{dyn} for 5Hz data set (pre analysis)

| Experimental condition | $R_L \pm \text{Std. error}$ cmH ₂ O/ml/sec | $C_{dyn} \pm \text{Std. error}$ ml/cmH ₂ O |
|-------------------------------------|--|--|
| Basal | 1.61 ± 0.17 | 2.38 ± 0.64 |
| Basal Saline (NaCl 0.9%) | 1.46 ± 0.10 | 3.00 ± 1.40 |
| Ach (10^{-2} M) | 2.28 ± 0.16 | 1.97 ± 0.89 |
| 5Hz /100mV (0.7 cmH ₂ O) | 1.89 ± 0.10 | 2.04 ± 0.86 |
| 5Hz /200mV (1.6 cmH ₂ O) | 1.84 ± 0.14 | 2.99 ± 1.25 |
| 5Hz /300mV (2.6 cmH ₂ O) | 1.87 ± 0.16 | 1.74 ± 0.69 |
| 5Hz /400mV (3.6 cmH ₂ O) | 1.79 ± 0.07 | 2.09 ± 1.02 |

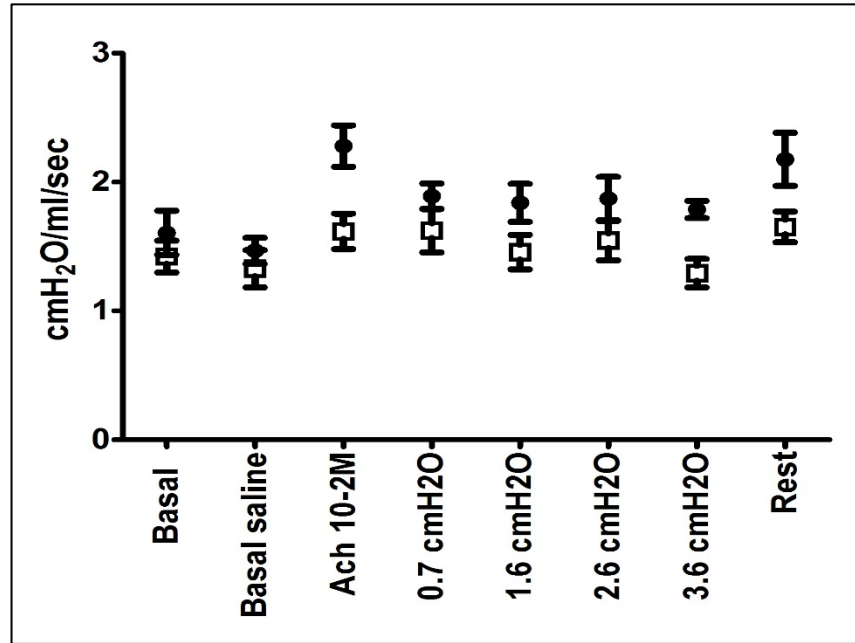


Figure 6.3: Changes of R_L observed as result of the application of SILO with 5Hz frequency and amplitudes in the range of 100 – 400 mV are presented in axis y for each experimental condition presented in axis x (□ = healthy; ● = asthmatic; n=10).

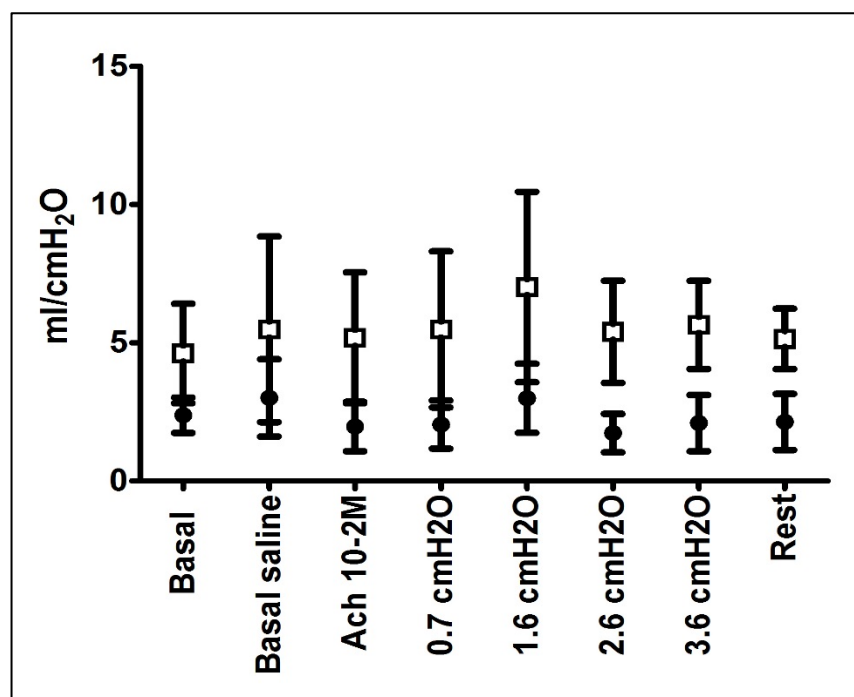


Figure 6.4: Changes of C_{dyn} observed as result of the application of SILO with 5Hz frequency and amplitudes in the range of 100 – 400 mV are presented in axis y for each experimental condition presented in axis x (\square = healthy; \bullet = asthmatic; $n=10$).

Table 6.2 shows the experimental data obtained for basal (no solution added), Saline, Ach and for the set of SILO at 10Hz, with amplitudes of 100, 200, 300 and 400 mV. This data was plotted and presented in figures 6.5 and 6.6 for comparison.

Table 6.2: experimental data for RL and C_{dyn} for 10Hz data set (pre analysis)

| Experimental condition | $R_L \pm \text{Std. error}$ cmH ₂ O/ml/sec | $C_{dyn} \pm \text{Std. error}$ ml/cmH ₂ O |
|--------------------------------------|--|--|
| Basal | 1.61 ± 0.17 | 2.38 ± 0.64 |
| Basal Saline (NaCl 0.9%) | 1.46 ± 0.10 | 3.00 ± 1.40 |
| Ach (10^{-2} M) | 2.28 ± 0.16 | 1.97 ± 0.89 |
| 10Hz /100mV (0.7 cmH ₂ O) | 1.89 ± 0.14 | 1.84 ± 0.82 |
| 10Hz /200mV (1.5 cmH ₂ O) | 1.83 ± 0.12 | 2.33 ± 1.13 |
| 10Hz /300mV (2.4 cmH ₂ O) | 1.88 ± 0.17 | 1.61 ± 0.69 |
| 10Hz /400mV (3.3 cmH ₂ O) | 1.80 ± 0.17 | 1.95 ± 0.92 |

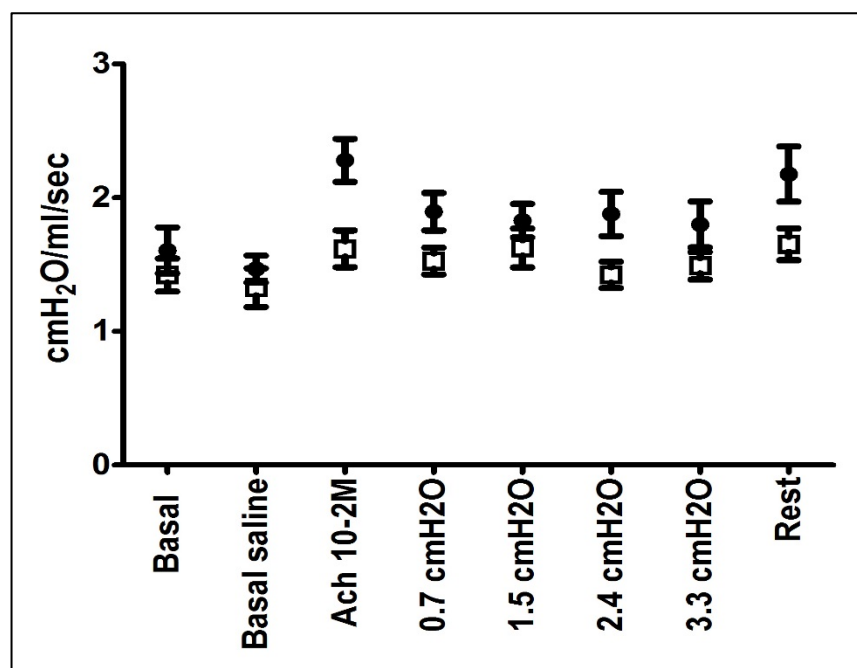


Figure 6.5: Changes of R_L observed as result of the application of SILO with 10Hz frequency and amplitudes in the range of 100 – 400 mV are presented in axis y for each experimental condition presented in axis x (□ = healthy; ● = asthmatic; n=10).

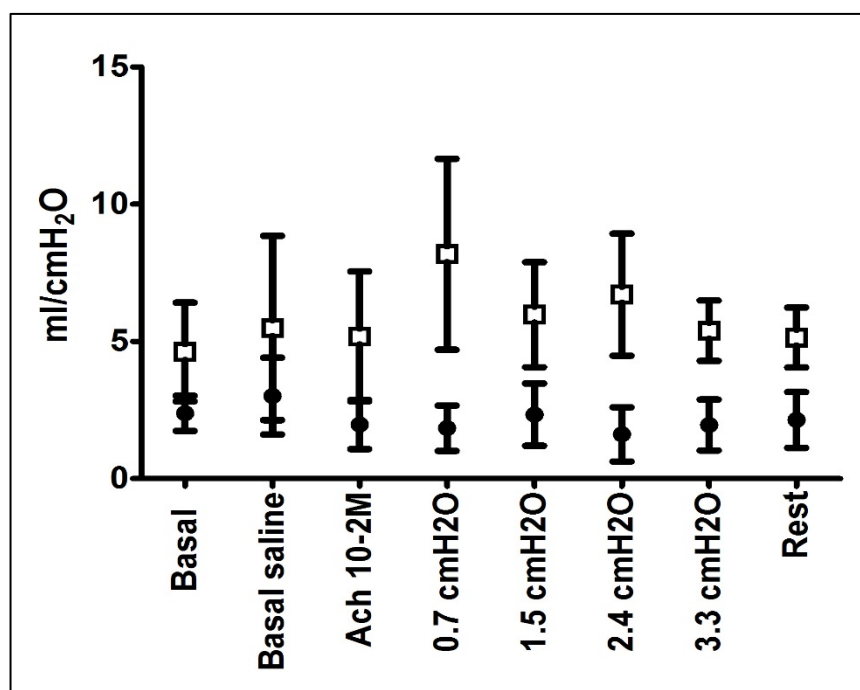


Figure 6.6: Changes of C_{dyn} observed as result of the application of SILO with 10Hz frequency and amplitudes in the range of 100 – 400 mV are presented in axis y for each experimental condition presented in axis x (□ = healthy; ● = asthmatic; n=10).

Table 6.3 shows the experimental data obtained for basal (no solution added), Saline, Ach and for the set of SILO at 15Hz, with amplitudes of 100, 200, 300 and 400 mV. This data was plotted and presented in figures 6.7 and 6.8 for comparison.

Table 6.3: experimental data for R_L and C_{dyn} for 15Hz data set (pre analysis)

| Experimental condition | $R_L \pm \text{Std. error}$ cmH ₂ O/ml/sec | $C_{dyn} \pm \text{Std. error}$ ml/cmH ₂ O |
|--------------------------------------|--|--|
| Basal | 1.61 ± 0.17 | 2.38 ± 0.64 |
| Basal Saline (NaCl 0.9%) | 1.46 ± 0.10 | 3.00 ± 1.40 |
| Ach (10^{-2} M) | 2.28 ± 0.16 | 1.97 ± 0.89 |
| 15Hz /100mV (0.4 cmH ₂ O) | 1.76 ± 0.17 | 2.46 ± 1.33 |
| 15Hz /200mV (1.1 cmH ₂ O) | 1.76 ± 0.17 | 1.23 ± 0.52 |
| 15Hz /300mV (1.7 cmH ₂ O) | 1.79 ± 0.17 | 1.76 ± 0.82 |
| 15Hz /400mV (2.4 cmH ₂ O) | 1.87 ± 0.21 | 2.44 ± 1.28 |

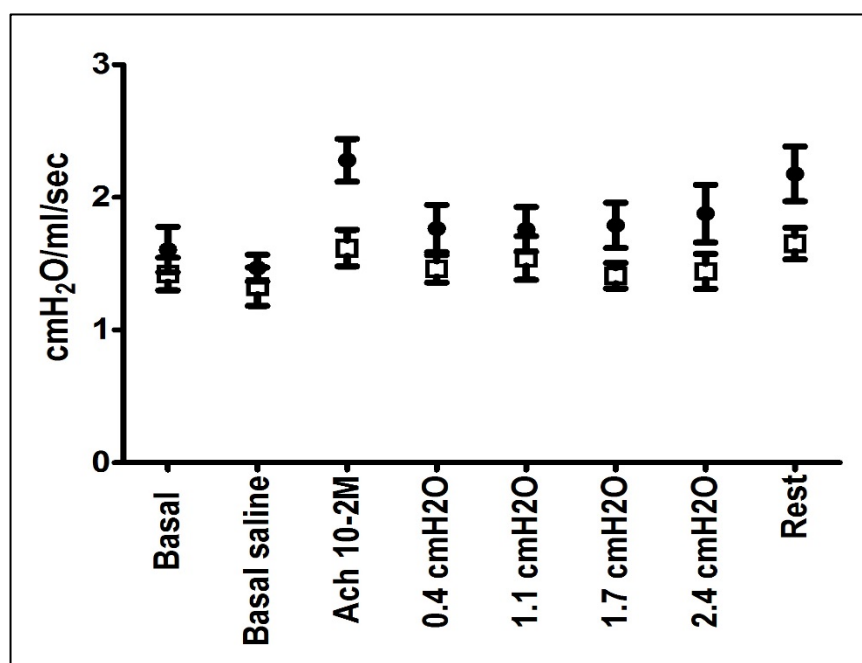


Figure 6.7: Changes of R_L observed as result of the application of SILO with 15Hz frequency and amplitudes in the range of 100 – 400 mV are presented in axis y for each experimental condition presented in axis x (□ = healthy; ● = asthmatic; n=10).

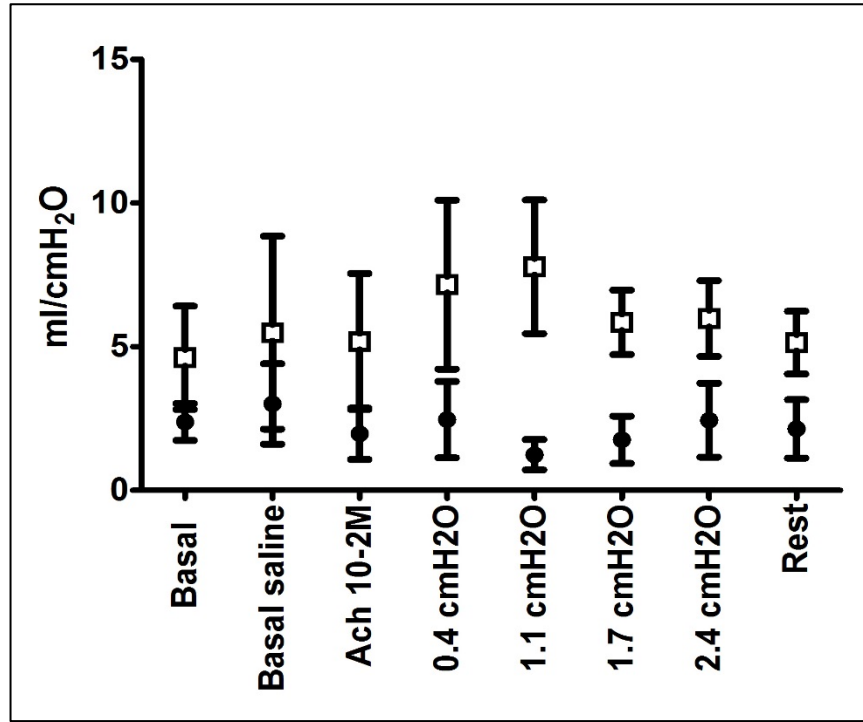


Figure 6.8: Changes of C_{dyn} observed as result of the application of SILO with 15Hz frequency and amplitudes in the range of 100 – 400 mV are presented in axis y for each experimental condition presented in axis x (□ = healthy; ● = asthmatic; $n=10$).

Table 6.4 shows the experimental data obtained for basal (no solution added), Saline, Ach and for the set of SILO at 20Hz, with amplitudes of 100, 200, 300 and 400 mV. This data was plotted and presented in figures 6.9 and 6.10 for comparison.

Table 6.4: experimental data for RL and C_{dyn} for 20Hz data set (pre analysis)

| Experimental condition | $R_L \pm \text{Std. error}$ cmH ₂ O/ml/sec | $C_{dyn} \pm \text{Std. error}$ ml/cmH ₂ O |
|--------------------------------------|--|--|
| Basal | 1.61 ± 0.17 | 2.25 ± 0.58 |
| Basal Saline (NaCl 0.9%) | 1.46 ± 0.10 | 2.77 ± 1.27 |
| Ach (10^{-2} M) | 2.28 ± 0.16 | 1.79 ± 0.81 |
| 20Hz /100mV (0.4 cmH ₂ O) | 2.01 ± 0.17 | 1.74 ± 0.81 |
| 20Hz /200mV (1.1 cmH ₂ O) | 2.09 ± 0.20 | 1.57 ± 0.62 |
| 20Hz /300mV (1.7 cmH ₂ O) | 2.33 ± 0.29 | 2.50 ± 1.33 |
| 20Hz /400mV (2.3 cmH ₂ O) | 1.88 ± 0.19 ; | 1.51 ± 0.69 |

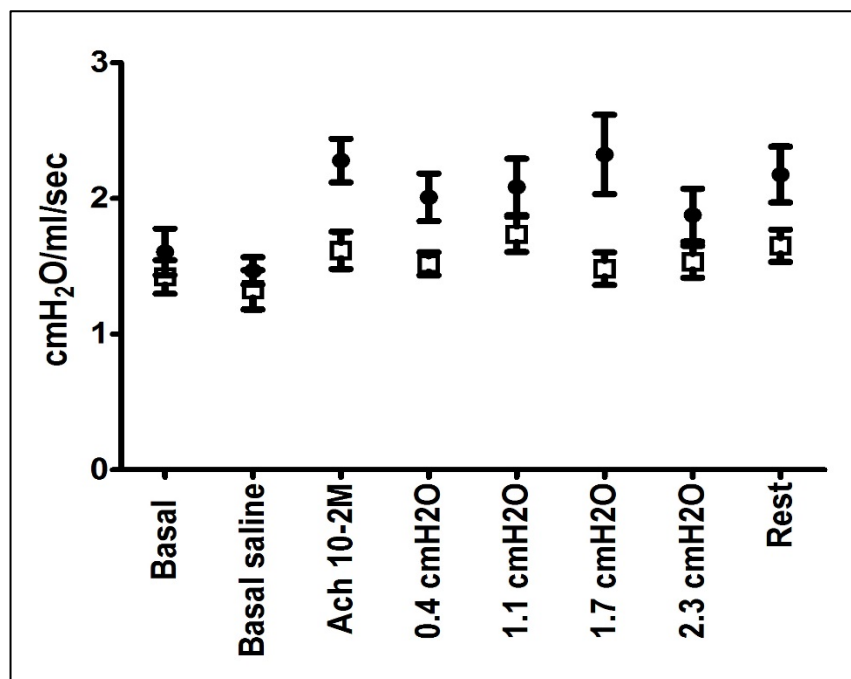


Figure 6.9: Changes of R_L observed as result of the application of SILO with 20Hz frequency and amplitudes in the range of 100 – 400 mV are presented in axis y for each experimental condition presented in axis x (□ = healthy; ● = asthmatic; n=10).

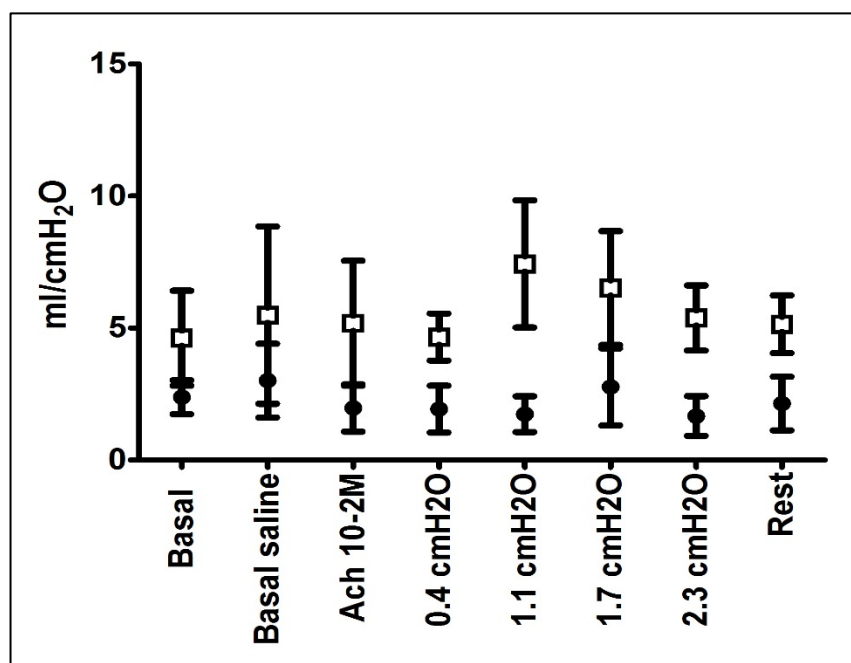


Figure 6.10: Changes of C_{dyn} observed as result of the application of SILO with 20Hz frequency and amplitudes in the range of 100 – 400 mV are presented in axis y for each experimental condition presented in axis x (□ = healthy; ● = asthmatic; n=10).

6.4. Statistical analysis of results

In the statistical analysis, the pressure observed with saline (NaCl 0.9%), which was considered the experimental baseline, was subtracted from all the experimental data, in order to evaluate directly the pressure changes as a result of the application of the different experimental interventions (ACh, oscillations, etc.), rather than the placebo response from the airways as response to Saline. The results obtained for the different superimposed pressure oscillations were compared then with the pressure observed during the bronchospasm (induced with ACh 10^{-4} M) in order to observe how airways during the simulated asthmatic attack respond to these type of Broncho relaxant agents.

6.4.1. Statistical Program

GraphPad Prism 5.0 TM (Fig 6.11) was used for the statistical analysis; this program combines scientific graphing, comprehensive curve fitting (nonlinear regression), understandable statistics, and data organization. This statistical program was originally designed for experimental biologists in medical schools and drug companies, especially those in pharmacology and physiology, which make it ideal for the analysis of the data obtained.

GraphPad Prism 5.0 TM performs basic statistical tests commonly used by laboratory and clinical researchers such as t tests, nonparametric comparisons, one- and two-way ANOVA, analysis of contingency tables, and survival analysis.

For the purpose of this study and the type of data obtained during the experimental protocols (normal distribution) the tests that fit better for its analysis were the t test and one way ANOVA. Other post-test were also used in this research to satisfy our curiosity of the behaviour of the data under different conditions of normality (Wilcoxon).

- **T-test:** for analysis of only two groups unpaired t test was selected. Unpaired t test is capable to analyse and compare the means of two unmatched groups, assuming that the values follow a Gaussian distribution.
- **One way ANOVA:** One-way ANOVA assumes that you have sampled your data from populations that follow a Gaussian distribution. While this assumption is not too important with large samples, it is important with small sample sizes like in this study ($n = 6-12$). One-way ANOVA also is capable of comparing three or more groups defined by one factor. For example, you might compare a control group, with a drug treatment group and a group treated with drug plus antagonist. Or you might compare a control group with five different drug treatments (in our case ISO, oscillations and SILO).

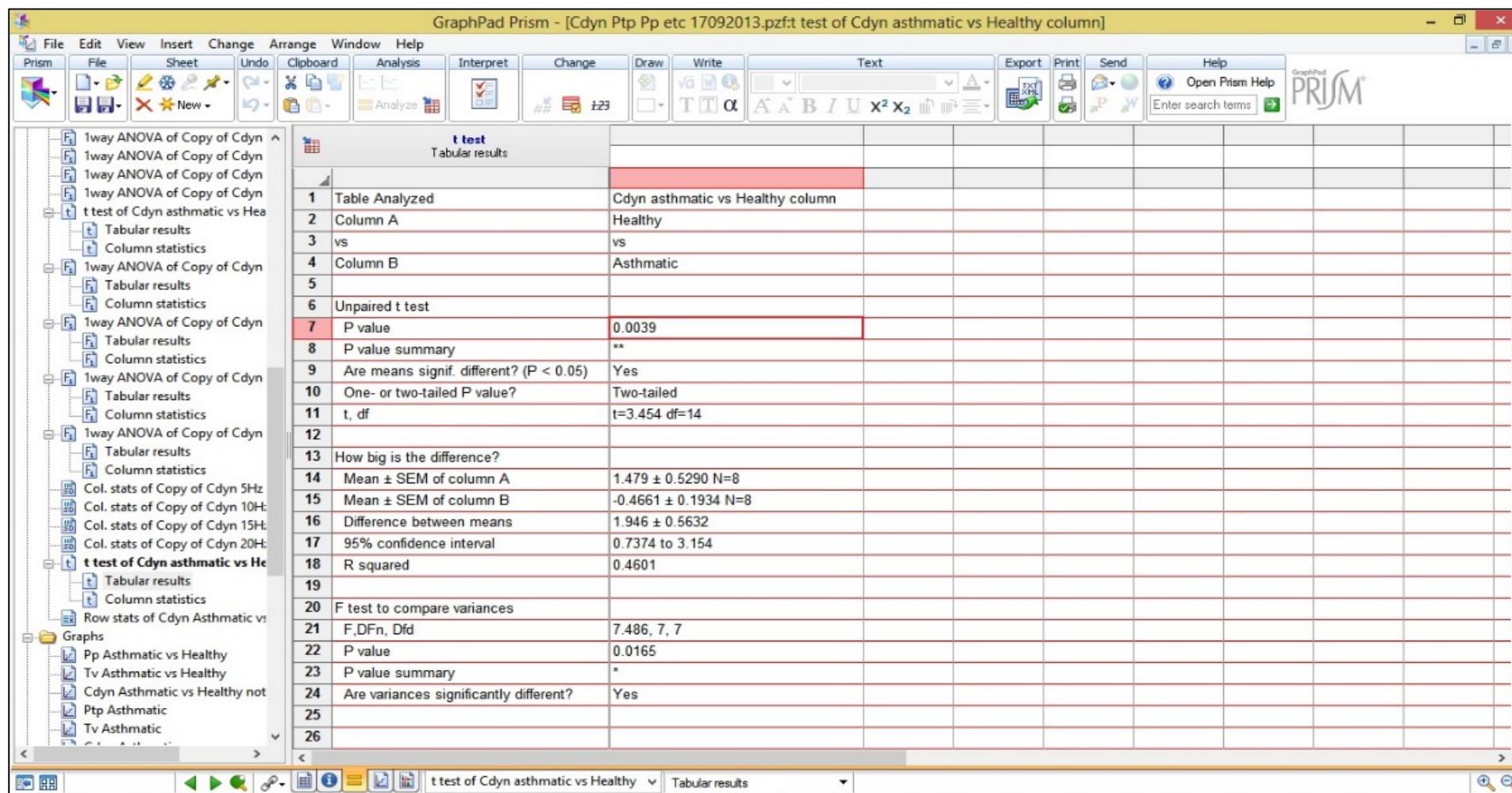


Figure 6.11: GraphPad Prism 5.0™ screenshot.

6.4.2. Data Analysis

The data obtained was analysed using *t test* for pair columns, one way ANOVA for multiple columns and variables, and as post analyses Dunnet was selected. The *t test* is a great tool to compare means between two independent columns and spot differences between them, ANOVA on the other hand can compare several means (3 or more) from different (independent) groups and report if there is significant difference between them, and finally Dunnet test is capable of multiple comparison between the means from each group (considered as treatment) with a single control and spot differences between them.

When the means for R_L obtained for healthy (controls) and the asthmatic mice (sensitized) were compared in figure 6.12, differences on the response to the same concentration of ACh ($10^{-2}M$) was observed with a mean for R_L of 0.38 ± 0.07 and 0.9 ± 0.17 cmH₂O/ml/sec respectively, this difference was analysed using a paired *t test*, showing a significant increase of the response to the bronchoconstrictor in asthmatics with a p value of 0.01. This result confirms the presence of AHR in the airways from the sensitized mice.

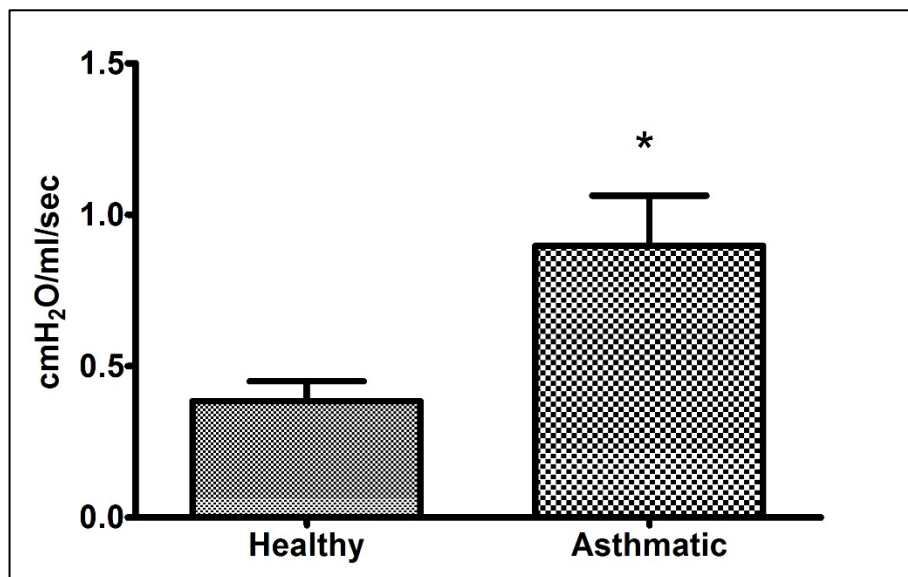


Figure 6.12: Comparison of the R_L response to ACh $10^{-2}M$ observed from healthy (control) and asthmatic (sensitized) subjects, axis y corresponds to R_L obtained for each experimental condition presented in axis (n=10).

When the means for C_{dyn} obtained for healthy (controls) and the asthmatic mice (sensitized) were compared in figure 6.13, also differences on the response to the same concentration of ACh ($10^{-2}M$) were observed with a mean for C_{dyn} of 1.47 ± 0.52 and -

0.47 ± 0.19 ml/cmH₂O respectively, this difference was analysed using also paired *t test*, showing a significant decrease in the C_{dyn} for the sensitized mice compared with the controls with a p value < 0.05 .

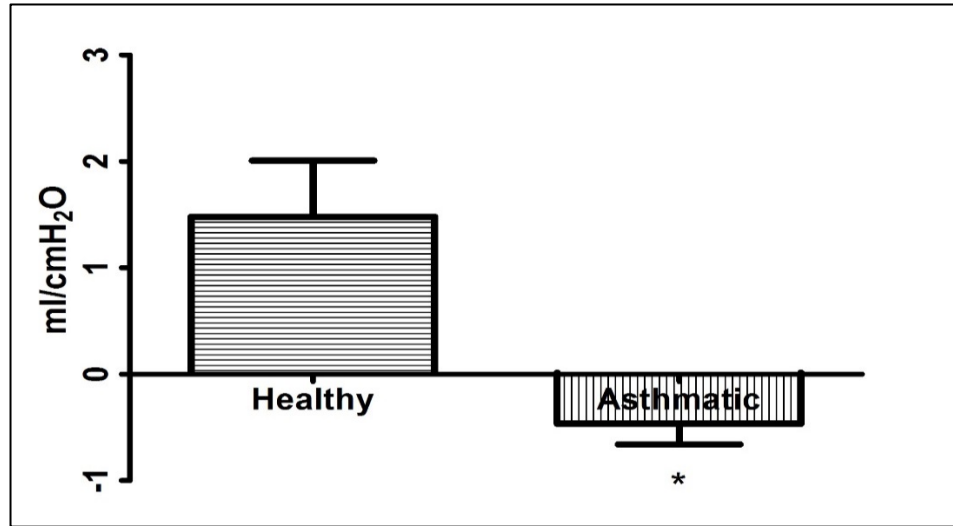


Figure 6.13: Comparison of the C_{dyn} response to ACh $10^{-2}M$ observed from healthy (control) and asthmatic (sensitized) subjects, axis y corresponds to C_{dyn} obtained for each experimental condition presented in axis (n=10).

When the analysis was focus on the response of the pre constricted airways to the different set of oscillations, it was found that each set of frequencies followed similar patterns inducing reduction of R_L obtained when the airways were previously stimulated with ACh $10^{-2}M$ (mimicking an asthmatic attack).

The results were expressed as means for R_L ; $C_{dyn} \pm$ Std. error. Table 6.5 shows the experimental data obtained for Ach and for the set of SILO at 5Hz, with amplitudes of 100, 200, 300 and 400 mV.

Table 6.5: Data for R_L and C_{dyn} for 5Hz

| Experimental condition | $R_L \pm \text{Std. error}$ cmH ₂ O/ml/sec | $C_{dyn} \pm \text{Std. error}$ ml/cmH ₂ O |
|-------------------------------------|--|--|
| Ach (10^{-2} M) | 0.91 ± 0.18 | -0.59 ± 0.17 |
| 5Hz /100mV (0.7 cmH ₂ O) | 0.45 ± 0.07 | -0.82 ± 0.29 |
| 5Hz /200mV (1.6 cmH ₂ O) | 0.37 ± 0.12 | -0.59 ± 0.19 |
| 5Hz /300mV (2.6 cmH ₂ O) | 0.41 ± 0.14 | -0.80 ± 0.24 |
| 5Hz /400mV (3.6 cmH ₂ O) | 0.30 ± 0.09 | -0.82 ± 0.30 |

The data was further analysed with ANOVA and Dunnet (as post analysis) and presented in figures 6.14 and 6.15 for their comparison. ANOVA and Dunnet showed significant reduction of R_L for all the amplitudes analysed with a p value of 0.02 and a p value < 0.05 respectively. When ANOVA and Dunnet were used to analyse C_{dyn} , neither ANOVA nor Dunnet showed significant changes when the means were compared (p value > 0.05). Details for p values obtained are presented in table 6.6.

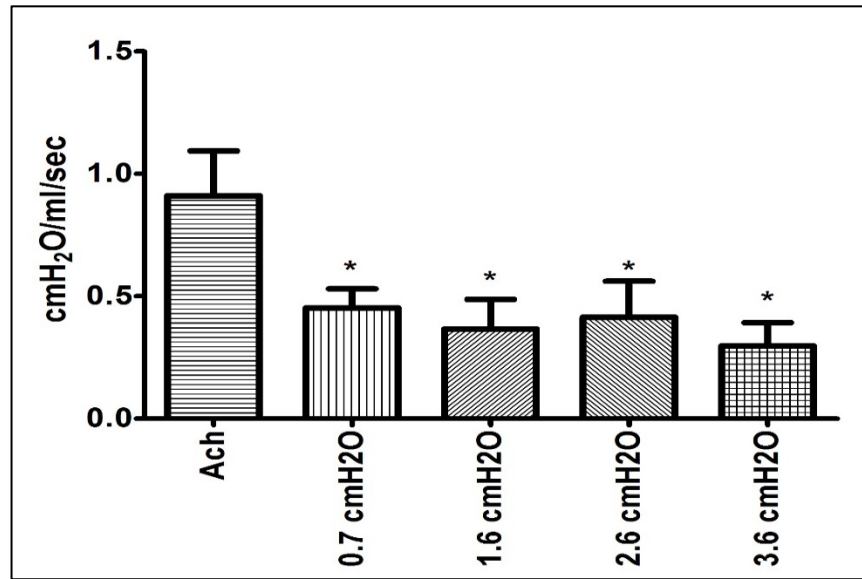


Figure 6.14: Data for changes of R_L obtained as result of the application of SILO with 5Hz frequency and amplitudes in the range of 100 – 400 mV are presented in axis y for each experimental condition presented in axis x (* p value < 0.05 , $n=10$).

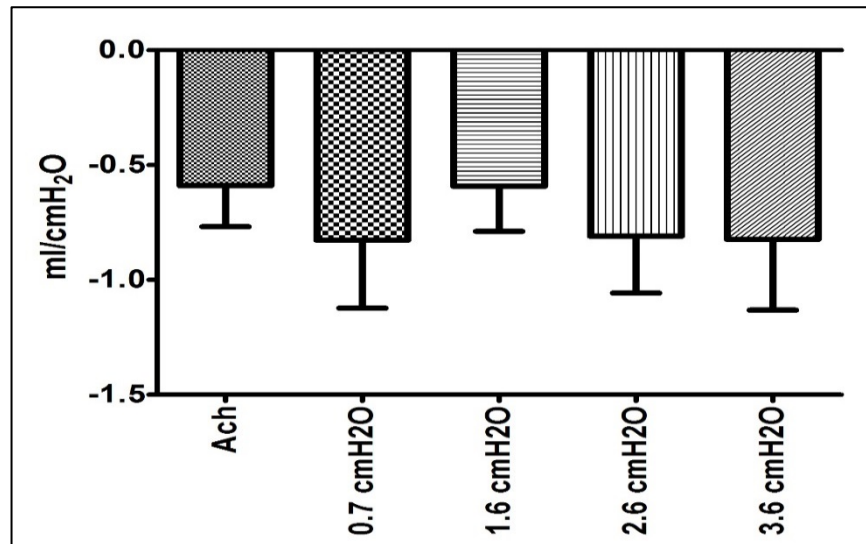


Figure 6.15: Data for changes of C_{dyn} obtained as result of the application of SILO with 5Hz frequency and amplitudes in the range of 100 – 400 mV are presented in axis y for each experimental condition presented in axis x (n=10).

Table 6.6: Statistical significance table for the effect of SILO at 20Hz and all amplitudes. Yellow box indicate statistical significance.

| 5Hz | ANOVA " Are means signif. different? (p value < 0.05)" | |
|--------------------------|---|------|
| Condition | RL | Cdyn |
| Group comparison | 0.01 | 0.33 |
| | Dunnet "Significant? p value < 0.05?" | |
| Multiple comparison test | RL | Cdyn |
| Ach vs 0.7 cmH2O | Yes | No |
| Ach vs 1.6 cmH2O | Yes | No |
| Ach vs 2.6 cmH2O | Yes | No |
| Ach vs 3.6 cmH2O | Yes | No |

Table 6.7 shows the experimental data obtained for Ach and for the set of SILO at 10Hz, with amplitudes of 100, 200, 300 and 400 mV.

Table 6.7: Data for R_L and C_{dyn} for 10Hz

| Experimental condition | $R_L \pm \text{Std. error}$ cmH ₂ O/ml/sec | $C_{dyn} \pm \text{Std. error}$ ml/cmH ₂ O |
|--------------------------------------|--|--|
| Ach (10^{-2} M) | 0.91 ± 0.18 | -0.58 ± 0.17 |
| 10Hz /100mV (0.7 cmH ₂ O) | 0.43 ± 0.07 | -0.79 ± 0.31 |
| 10Hz /200mV (1.5 cmH ₂ O) | 0.39 ± 0.04 | -0.75 ± 0.30 |
| 10Hz /300mV (2.4 cmH ₂ O) | 0.37 ± 0.13 | -0.82 ± 0.20 |
| 10Hz /400mV (3.3 cmH ₂ O) | 0.36 ± 0.12 | -0.75 ± 0.23 |

The data was further analysed with ANOVA and Dunnet (as post analysis) and presented in figures 6.16 and 6.17 for their comparison. ANOVA and Dunnet showed significant reduction of R_L for all the amplitudes analysed with a p value of 0.01 and a p value < 0.05 respectively. When ANOVA and Dunnet were used to analyse C_{dyn} , neither ANOVA nor Dunnet showed significant changes on C_{dyn} (p value > 0.05). Details for p values obtained are presented in table 6.8.

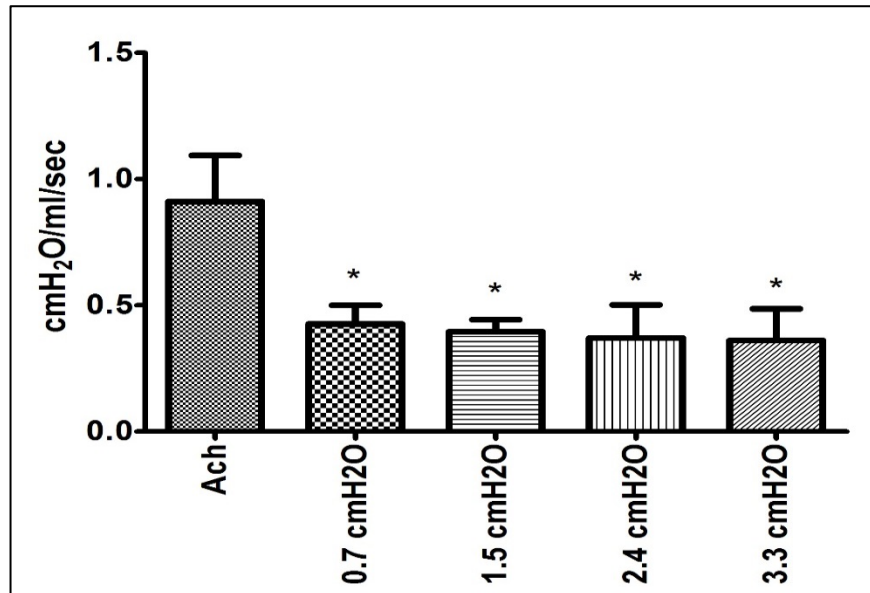


Figure 6.16: Data for changes of R_L obtained as result of the application of SILO with 10Hz frequency and amplitudes in the range of 100 – 400 mV are presented in axis y for each experimental condition presented in axis x (* p value < 0.05 , $n=10$).

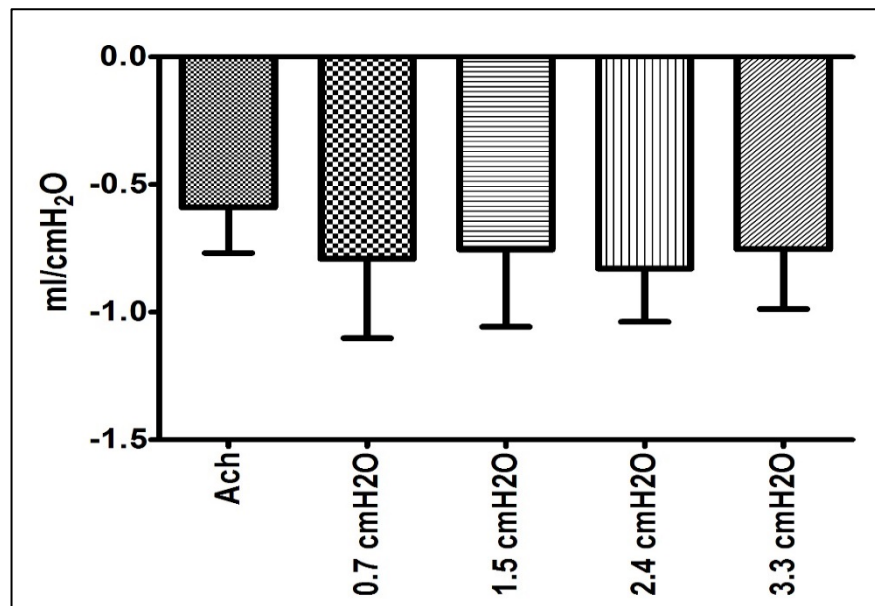


Figure 6.17: Data for Changes of C_{dyn} obtained as result of the application of SILO with 10Hz frequency and amplitudes in the range of 100 – 400 mV are presented in axis y for each experimental condition presented in axis x (n=10).

Table 6.8: Statistical significance table for the effect of SILO at 10Hz and all amplitudes. Yellow box indicate statistical significance.

| 10Hz | ANOVA " Are means signif. different? (p value < 0.05)" | |
|--------------------------|---|------|
| Condition | RL | Cdyn |
| Group comparison | 0.02 | 0.42 |
| | Dunnet "Significant? p value < 0.05?" | |
| Multiple comparison test | RL | Cdyn |
| Ach vs 0.7 cmH2O | Yes | No |
| Ach vs 1.5 cmH2O | Yes | No |
| Ach vs 2.4 cmH2O | Yes | No |
| Ach vs 3.3 cmH2O | Yes | No |

Table 6.9 shows the experimental data obtained for Ach and for the set of SILO at 15Hz, with amplitudes of 100, 200, 300 and 400 mV.

Table 6.9: Data for R_L and C_{dyn} for 15Hz

| Experimental condition | $R_L \pm \text{Std. error}$ cmH ₂ O/ml/sec | $C_{dyn} \pm \text{Std. error}$ ml/cmH ₂ O |
|--------------------------------------|--|--|
| Ach (10^{-2} M) | 0.91 ± 0.18 | -0.40 ± 0.08 |
| 15Hz /100mV (0.4 cmH ₂ O) | 0.29 ± 0.16 | -0.77 ± 0.20 |
| 15Hz /200mV (1.1 cmH ₂ O) | 0.28 ± 0.13 | -0.90 ± 0.27 |
| 15Hz /300mV (1.7 cmH ₂ O) | 0.34 ± 0.16 | -0.72 ± 0.20 |
| 15Hz /400mV (2.4 cmH ₂ O) | 0.45 ± 0.20 | -0.61 ± 0.21 |

The data was further analysed with ANOVA and Dunnet (as post analysis) and presented in figures 6.18 and 6.19 for their comparison. ANOVA showed significant reduction of R_L with a p value of 0.03 and Dunnet showed significant reduction of R_L for the amplitudes 100, 200 and 300 mV analysed with p values < 0.05, but not for 400mV. When ANOVA and Dunnet were used to analyse C_{dyn} , neither ANOVA nor Dunnet spotted significant changes on C_{dyn} (p value > 0.05). Details for p values obtained are presented in table 6.6.

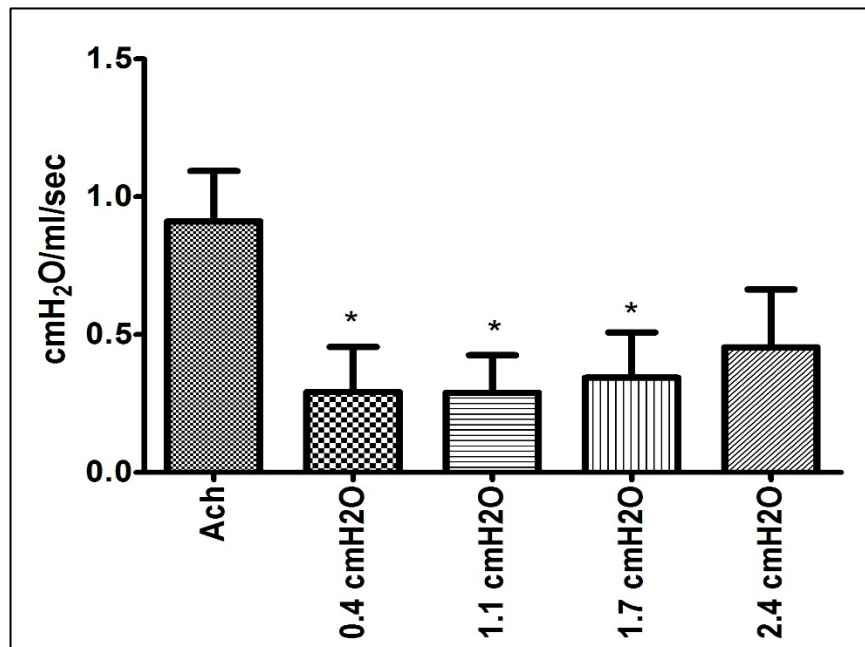


Figure 6.18: Data for changes of R_L obtained as result of the application of SILO with 15Hz frequency and amplitudes in the range of 100 – 400 mV (* p value <0.05, n=10).

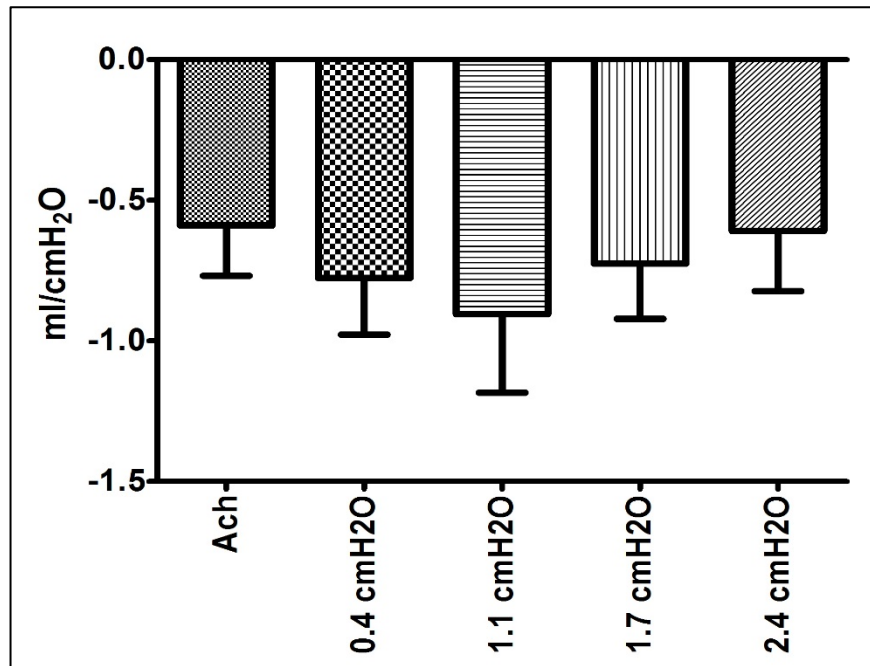


Figure 6.19: Data for changes of C_{dyn} obtained as result of the application of SILO with 15Hz frequency and amplitudes in the range of 100 – 400 mV (n=10).

Table 6.10: Statistical significance table for the effect of SILO at 15Hz and all amplitudes. Yellow box indicate statistical significance.

| 15Hz | ANOVA " Are means signif. different? (p value < 0.05)" | |
|-------------------------------|---|------|
| Condition | RL | Cdyn |
| Group comparison | 0.03 | 0.15 |
| | Dunnet "Significant? p value < 0.05?" | |
| Multiple comparison test | RL | Cdyn |
| Ach vs 0.4 cmH ₂ O | Yes | No |
| Ach vs 1.1 cmH ₂ O | Yes | No |
| Ach vs 1.7 cmH ₂ O | Yes | No |
| Ach vs 2.4 cmH ₂ O | No | No |

Table 6.11 shows the experimental data obtained for Ach and for the set of SILO at 20Hz, with amplitudes of 100, 200, 300 and 400 mV.

Table 6.11: Data for R_L and C_{dyn} for 20Hz

| Experimental condition | $R_L \pm \text{Std. error}$ cmH ₂ O/ml/sec | $C_{dyn} \pm \text{Std. error}$ ml/cmH ₂ O |
|--------------------------------------|--|--|
| Ach (10^{-2} M) | 0.91 ± 0.18 | -0.04 ± 0.08 |
| 20Hz /100mV (0.4 cmH ₂ O) | 0.59 ± 0.12 | -0.62 ± 0.28 |
| 20Hz /200mV (1.1 cmH ₂ O) | 0.55 ± 0.16 | -0.66 ± 0.31 |
| 20Hz /300mV (1.7 cmH ₂ O) | 0.90 ± 0.24 | -0.79 ± 0.24 |
| 20Hz /400mV (2.3 cmH ₂ O) | 0.45 ± 0.12 | -0.85 ± 0.27 |

The data was further analysed with ANOVA and Dunnet (as post analysis) and presented in figures 6.20 and 6.21 for their comparison. Neither ANOVA nor Dunnet showed significant reduction for R_L (p value > 0.05). When ANOVA and Dunnet were used to analyse C_{dyn} , neither ANOVA nor Dunnet spotted significant changes on C_{dyn} (p value > 0.05). Details for p values obtained are presented in table 6.6.

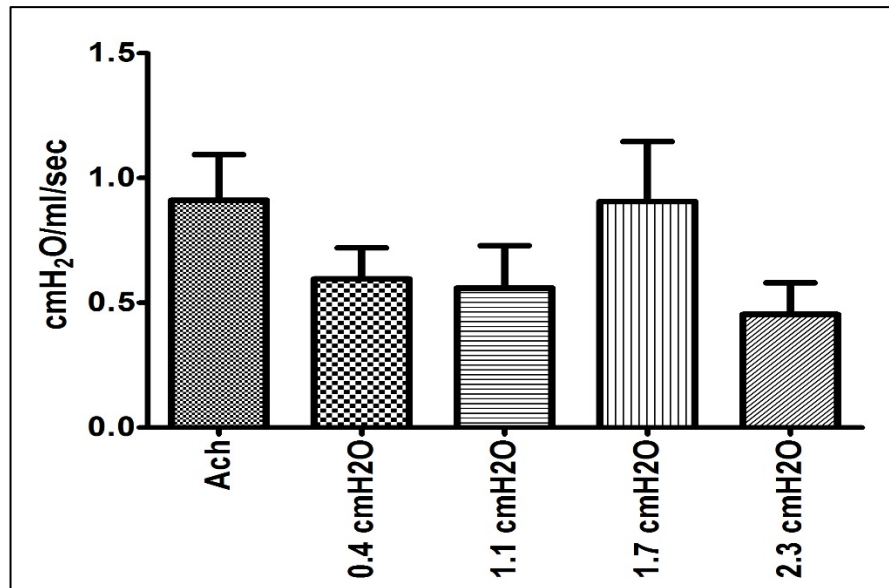


Figure 6.20: Data for changes of R_L obtained as result of the application of SILO with 20Hz frequency and amplitudes in the range of 100 – 400 are presented in axis y for each experimental condition presented in axis x mV (n=10).

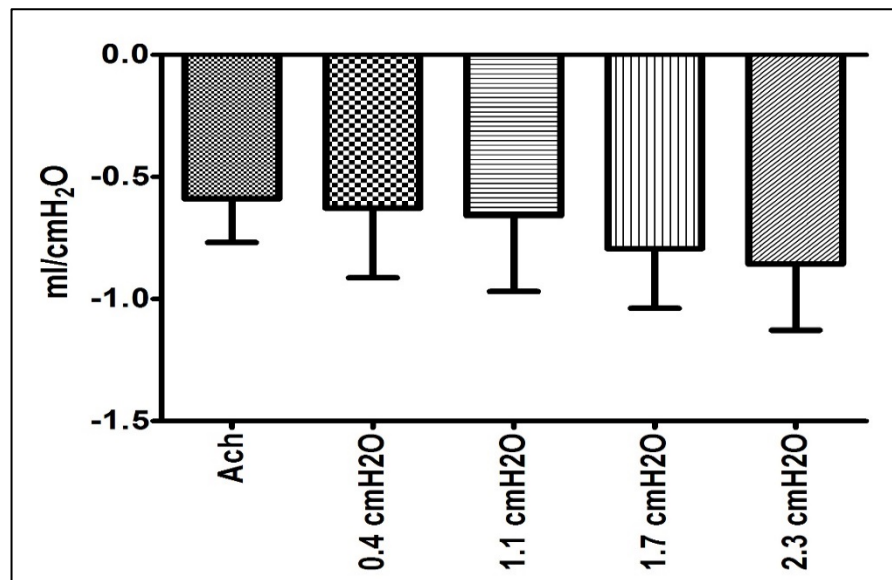


Figure 6.21: Data for changes of C_{dyn} obtained as result of the application of SILO with 20Hz frequency and amplitudes in the range of 100 – 400 mV are presented in axis y for each experimental condition presented in axis x (n=10).

Table 6.12: Statistical significance table for the effect of SILO at 20Hz and all amplitudes. Yellow box indicate statistical significance.

| 20Hz | ANOVA " Are means signif. different? (p value < 0.05)" | |
|--------------------------|---|------|
| Condition | RL | Cdyn |
| Group comparison | 0.12 | 0.49 |
| | Dunnet "Significant? p value < 0.05?" | |
| Multiple comparison test | RL | Cdyn |
| Ach vs 0.4 cmH2O | No | No |
| Ach vs 1.1 cmH2O | No | No |
| Ach vs 1.7 cmH2O | No | No |
| Ach vs 2.4 cmH2O | No | No |

6.5. Closure

The results presented in this chapter show that airways from sensitized subjects are more reactive to bronchoconstrictor drugs than those considered healthy (controls), this

is known as airway hyperresponsiveness or AHR and is one of the main features observed in human asthma [51, 89, 105, 106].

Also it was observed that the use of SILO in different frequencies and amplitudes overlapped to spontaneous breathing has a bronchorelaxant effect in sensitized subjects, where tidal and deep inspiration oscillations have failed. This reinforces the findings presented in Chapter 4 (*in vitro*), showing that the application of SILO onto spontaneous breathing patterns not only can induce relaxation in pre-constricted asthmatic airways *in vitro*, but also *in vivo*.

Most of the frequencies and their amplitude range resulted in reduction of R_L , with the only exception of 20Hz (at all its amplitudes). On the other hand most of the frequencies used for this study did not show significant changes for C_{dyn} .

The results presented in this and previous chapters will be further analysed and discussed in the following chapter.

Chapter 7

Discussion and conclusions

7.1. *Introduction*

In the previous chapters, the results obtained in the *in vitro* and *in vivo* experiments from healthy and sensitized subjects were presented. This chapter discusses the results obtained and compares them between healthy and asthmatic subjects, *in vitro* and *in vivo*. The effect of super imposed mechanical oscillations and Isoproterenol is analysed in detail and is compared with current knowledge in the area (presented in chapter 1 and 2). Finally, suggestions for future work are provided in the thesis conclusion.

7.2. *Length oscillations*

Different groups have studied the effect of length oscillations on airway smooth muscle with findings that length oscillations similar to those occurring during deep inspiration [7, 8, 81, 82, 85, 163] or tidal breathing [7, 10, 81-83, 98, 101, 163] can induce bronchoprotection or bronchodilation [26] on healthy subjects depending on the timing of application (before or after bronchoconstriction). Fredberg et al. [9] proposed the theory of perturbed equilibrium, which suggests that oscillations can disrupt the function crossbridges. Some studies have shown that the arrangement of the contractile components change with length modifications [157] and as a result of this, the contractile behaviour of ASM could be affected. All these studies have been conducted on healthy airways. To the best of our knowledge, there have not been similar studies on asthmatic tissue, with the only exception of that of Chin et al [158] who studied length adaptation, force-velocity relationship and force recovery after length oscillations on isolated tissue, finding that only passive stiffness was increased in ASM from asthmatic subjects when compared with non-asthmatics. This has left a gap, filled only with hypotheses and theories regarding why in asthmatic airways oscillations are either less or not effective at all at inducing relaxation of asthmatic airways [7, 158]. In a recent paper published in the journal of applied physiology, Lutchen K reviewed [94] several studies that have tried to explain the different response of asthmatic airways and its connection with the hyperresponsiveness observed in the disease. Most of the studies

cited by Lutchen have only used oscillations similar to those occurring normally during breathing (TO and DI) under static conditions to postulate their theories. The use of only normal breathing oscillations patterns in these studies has been questioned by the author and an open discussion has been left on the table to join.

This study attempted to fill part of this gap of knowledge, studying the response of sensitized airways to the imposition of oscillations directly using: traditional studied oscillations (such as TO or DI), untraditional oscillations (SILO), *in vitro* test (at Do), and *in vivo* test (dynamic conditions).

7.3. SILO *in vitro*

a) Healthy airways

- The results presented in chapter 4 (Sections 8 and 13) showed that the imposition of breathing oscillations on pre constricted ASM (at Do), have a bronchorelaxant effect in two healthy strains of mice (C57 and Balb/c), which reinforces previous findings in ASM tissues [7, 10, 36, 81-83, 98, 99, 101, 156].
- ISO and breathing oscillations induce similar relaxation patterns on healthy airways and the bronchorelaxant effect of ISO increases when combined with mechanical oscillations similar to breathing (2.7Hz/4%). This agrees with previous findings from Gump et al. [10].
- When superimposed length oscillations (SILO) with a frequency in the range of 10-30Hz with amplitude of 1% were tested on the C57 mice tissue, they were not as effective as normal breathing alone, ISO, or both agents combined to induce relaxation on healthy airways (Section 10).

b) Asthmatic (sensitized airways)

- As observed in chapter 4 (Section 13), the relaxation produced by either ISO or breathing was smaller in asthmatics than healthy airways, and their combination did not show significant increase of relaxation either when compared with ISO or normal breathing alone.
- When SILO were applied to asthmatic airways, similar findings to those obtained in healthy airways were observed with an amplitude of 1% and frequencies between 5-20Hz on sensitized airways from Balb/c, showing no

significant improvement on relaxation. However when the superimposition of length oscillations was tested on breathing oscillations with an amplitude of 1.5% and in the same frequency range, an increase in relaxation on asthmatic airways was observed when SILO were compared with oscillations equivalent to breathing or ISO alone (Section 13).

It has been proposed that structural changes on the composition of ASM (presented in chapter 2) and the rearrangement of structures within the cell, or the adaptation to a new tone during the development of the disease (asthma) could be responsible for the changes in the response of asthmatic airways to breathing oscillations [26, 33, 81, 102, 104, 157, 158].

These *in vitro* findings seem to confirm that physiological oscillations (mechanically reproduced by us) similar to those occurring during breathing can disturb the mechanical components of the contraction (crossbridge cycling of actin and myosin) as suggested by Fredberg on healthy subjects rather than affecting chemical pathways. However, they are not capable of reproducing the same relaxation pattern in asthmatic airways, which could be the result of the adaptation of the ASM to the new conditions of the progressing disease [7, 78]. According to our new findings here, SILO applied onto breathing patterns can still induce relaxation in pre-constricted asthmatic airways where TO have failed, as observed in the results. These could corroborate the theory that the effector (crossbridge) remains the same as its components (myosin and actin) and it could be disrupted. This data, in addition to previous data published by our team in healthy airways [16, 83], seems to indicate that the relaxation of ASM in asthmatic airways is possible and could be related to the crossbridge rate (speed of attachment). The crossbridge rate is due to changes in the arrangement of intracellular structures, cellular basal tone, etc., and this rate could be disrupted by changes in amplitude and frequency independently, as observed with physiological oscillations (DI or TO) on healthy airways. These findings need to be tested and probed *in vivo* (under dynamic conditions) in order to advance in the direction of a possible new therapy to treat asthmatic attacks.

7.4. SILO *in vivo*

The results presented in chapter 6 (section 4) correspond to the data obtained *in vivo* (dynamic conditions), using the plethysmograph (built in-house) and the parameters of R_L and C_{dyn} to evaluate the level of bronchoconstriction.

- Airways from sensitized subjects resulted in being more reactive to bronchoconstrictive drugs than those subjects considered to be healthy (controls).

This is known as airway hyperresponsiveness or AHR [51, 89, 105, 106] and is one of the main features observed in human asthma. The AHR has been suggested to be related to the increased basal tone of the airways as a result of the development of the disease, as mentioned in the previous section [26, 33, 81, 102, 104, 157, 158]. It has been observed that when the tone of the ASM is increased, the total force as a result of stimulation of the airways with ACh is also increased (feature observed in the results).

- It was also observed that the use of SILO (induced using Pressure oscillations) in different frequencies and amplitudes that overlap spontaneous breathing (dynamic conditions) has a bronchorelaxant effect in sensitized subjects, where TO and DI have failed as previously stated.

This reinforces the findings presented in chapter 4 (*in vitro*), showing that the application of SILO onto spontaneous breathing patterns not only can induce relaxation in pre constricted asthmatic airways *in vitro*, but also *in vivo*.

- Most of the frequencies and their amplitude range tested, resulted in reduction of R_L with the only exception of 20Hz (at all its amplitudes) (Chapter 6, section 4).
- On the other hand most of the frequencies used for this study did not show significant changes for C_{dyn} .

The accuracy of the reported data depends on the experimental setup, in particular the transducer used for measuring. We expect that the associated noise signal might be a source of significant error. Future improvement such as adding special types of filters may help to improve accuracy.

The results obtained *in vivo* are novel and promising for non-invasive treatments for asthma.

7.5. *SILO vs ISO*

The interaction of bronchorelaxant drugs and length oscillations has been previously studied by other groups showing improvement in the relaxation of pre constricted healthy airways when these two agents are combined and presenting similar relaxation when compared between them, indicating that both agents acts over different pathways of the broncoconstriction [10]. It has been proposed that ISO is acting over the chemical pathways while length oscillations act over the mechanical and structural components of the contractile machinery of the cell [10].

- When ISO was combined in healthy subjects with length oscillations equivalent to breathing in this study an increase of relaxation was observed (*in vitro*) in the two mice strains studied (Chapter 4 section 8 and 13).
- However, when the effect of ISO was assessed in asthmatic airways, its relaxant effect was not as effective as the imposition of SILO, neither *in vitro* nor *in vivo* tests.
- When ISO was combined with SILO *in vitro* no significant changes were observed (data not shown).

7.6. *Summary*

For many years several groups have studied the effect of traditional oscillations such as tidal breathing and deep inspiration on airways smooth muscle, finding that these types of oscillations have a relaxant effect on healthy pre-constricted airways.

- Most of these groups have focused on isolated tissue [21, 82-84, 87, 98, 99, 101, 157] and a minority of them on intact airways [164].
- Almost every study has been performed using ASM from healthy airways [7, 9, 10, 16, 21, 33, 82, 83, 98, 99, 102, 164], and their findings were extrapolated to asthmatic airways.

- Those more adventurous, have tested some oscillations on asthmatic airways and have not found relaxation of the airways [7, 158], suggesting that some changes on the airways during the development of the disease could be responsible for the lack of response to oscillations in these types of airways [26, 33, 81, 102, 104, 157, 158].
- Also some groups have also suggested that in order to induce similar findings to those observed in healthy airways, non-physiological oscillations need to be used [104].

Non-physiological oscillations are not considered as a therapy, because the breathing patterns change completely.

This study focuses on analysing the response of sensitized airways on super-imposed length oscillations (SILO) therapies. SILO is a good alternative to non-physiological oscillations because the oscillations barely change the main breathing pattern, and in accordance with the results presented in this study, SILO seem to fulfil the objective of length oscillations inducing the disruption of the cross bridge as suggested in previous studies [9, 82, 83, 98] and eliciting relaxation.

In this study SILO was studied on pre-constricted intact airways (*in vivo* and *in vitro*) and they were more effective than TO and ISO when relaxation was expected in sensitized airways, indicating that the relaxation of these airways can be achieved using mechanical oscillations. The whole breathing pattern does not need to be drastically changed. These superimposed oscillations were not as effective on healthy airways. We believe the changes on the arrangement of structures in the cell and the change of tone could be responsible for this difference in response between healthy and sensitized airways as suggested by previous groups [26, 33, 81, 102, 104, 157, 158]. The changes are likely affecting not only the force generated during an asthma attack but also on the attachment and detachment rate of the crossbridge. Previous data published by our group on healthy airways [83] seems to support this idea when using even higher frequencies than the ones used in this study, whilst still obtaining relaxation.

7.7. Conclusions

The objective of the study was to experimentally investigate the effect of SILO in sensitized airways and determine the response of these airways to these types of oscillations. The research objectives were detailed in chapter 2 along with detailed

literature review in the area of ASM and asthma. Chapter 3 presented asthma models, selection and sensitization, followed by chapter 4 detailing the techniques, experiments and results for the *in vitro* testing. Chapter 5 presented all the equipment and protocols to be used for the *in vivo* testing and chapter 6 showed in detail the experiments and results for the *in vivo* testing. Finally chapter 7 presented a discussion for the results obtained in chapters 4 and 6.

The results presented in this study seem to corroborate the theory that length oscillations act over the interaction of actin and myosin during contraction, disrupting the crossbridge [9, 10, 82, 83, 98]. SILO seems to be effective on sensitized airways and the different frequency or amplitude used in the experiments could be responsible for this effect. This hypothesis is supported by a previous study by Ansell et al [93] where they found that the level of bronchodilation was affected differently by the magnitude of the strain and the stress. The fact that these types of oscillations are capable of inducing relaxation on pre-constricted sensitized airways corroborates the hypothesis that the main components of the crossbridge (actin, myosin and the actinomyosin crossbridge) do not change and can be disrupted. However, changes occurring during the development of the disease such as length adaptation, change of the basal tone, or rearrangement of cell structures seems to change the useful range for oscillations for these type of airways, creating ineffective normal breathing patterns. Considering the findings of this study, the application of oscillation in asthmatic airways could be a new element to be considered for the treatment of asthma and should not be discarded only because normal breathing patterns (TO and DI) are ineffective.

7.8. *Future work*

The results obtained in this study are novel, as the work experimentally investigates the effect of length oscillations (SILO) different to those occurring during normal breathing (TO and DI) on sensitized airways, and compares the effect of these oscillations *in vitro* and *in vivo* (dynamic conditions). This research only studied the effect of SILO in acute models of asthma that correspond to an early stage of the disease -- obtaining promising results in the area of length oscillations and asthma. However more studies to investigate the effect of SILO on chronic states are needed to reach the long term goal of developing a new therapy for alleviation of asthma with the intent to possibly reduce the use of medications.

Short-term implementation for future work in this area would involve the study of SILO on chronic asthma models with and without medications, in order to study the effect of these oscillations on chronic states of the disease. The testing of a wider range of frequencies and amplitudes also needs consideration.

Further examination into the use of oscillations to reduce or prevent length adaptation of the airways during the development of the disease can also be useful.

In addition, other animal models closer to human physiology need to be considered in order to reach our long-term goal.

REFERENCES

1. Bateman, E.D., et al., *Global strategy for asthma management and prevention: GINA executive summary*. European Respiratory Journal., 2008. **31**(1): p. 143-178.
2. Masoli, M., et al., *Global burden of asthma*, 2004. p. 122.
3. Holt, S. and R. Beasley, *The burden of asthma in New Zealand* 2002, Wellington. 48.
4. Marieb EN and M. SJ., *Human anatomy and physiology laboratory manual*, 2008, Pearson; Benjamin Cummings.
5. Green RH, et al., *Management of asthma in adults: current therapy and future directions*. Postgrad Med J 2003. **79**: p. 259-267.
6. Rizzo, M.C.V. and D. Sole, *Inhaled corticosteroids in the treatment of respiratory allergy: safety vs. efficacy*. Jornal de Pediatria, 2006. **82**(5): p. 198-205.
7. An, S.S., et al., *Airway smooth muscle dynamics: a common pathway of airway obstruction in asthma*. European Respiratory Journal, 2007. **29**(5): p. 834-860.
8. Fredberg, J.J., *Airway obstruction in asthma: does the response to a deep inspiration matter?* Respiratory Research, 2001. **2**(5): p. 273 - 275.
9. Fredberg, J.J., et al., *Perturbed equilibrium of myosin binding in airway smooth muscle and its implications in bronchospasm*. American journal of respiratory and critical care medicine, 1999. **159**: p. 959-967.
10. Gump, A., L. Haughney, and J. and Fredberg, *Relaxation of activated airway smooth muscle: relative potency of isoproterenol vs. tidal stretch*. Journal of applied physiology, 2001. **90**: p. 2306-2310.
11. Mijailovich, S.M., J.P. Butler, and J.J. and Fredberg, *Perturbed Equilibria of Myosin Binding in Airway Smooth Muscle: Bond-Length Distributions, Mechanics, and ATP Metabolism*. Biophysical Journal, 2000. **79**: p. 2667-2681.
12. Guyton A and a.H. J., *Medical Physiology*, in *Textbook of Medical Physiology*, E. Sanders, Editor 2006, Elsevier Inc.: Philadelphia.
13. Ijpma, G., *Airway smooth muscle dynamics*, in *Engineering School* 2010, Auckland University of Technology: Auckland. p. 206.
14. Wikipedia. *respiratory system*. 2008 [cited 2010; Available from: http://commons.wikimedia.org/wiki/File:Respiratory_system_complete_en.svg.

15. Berne, R.M., et al., *Physiology*. fifth edition ed2004: Mosby Year Book. 1014.
16. Du, Y., A.M. Al-Jumaily, and H. and Shukla, *Smooth muscle stiffness variation due to external longitudinal oscillations*. . Journal of Biomechanics, 2007. **40**(14): p. 3207 - 3214.
17. Huxley, A.F. and R. Niedergerke, *Structural changes in muscle during contraction: Interference microscopy of living muscle fibres* Nature, 1954. **173**: p. 971-973.
18. Huxley, H. and J. Hanson, *Changes in the Cross-Striations of Muscle during Contraction and Stretch and their Structural Interpretation* Nature, 1954. **173**: p. 973-976.
19. Seow, C.Y. and P.D. and Paré, *Ultrastructural basis of airway smooth muscle*. Canadian Journal of Physiology and Pharmacology, 2007. **85**: p. 659 - 665.
20. Zhang, J., et al., *Dense-body aggregates as plastic structures supporting tension in smooth muscle cell*. American journal physiological lung cellular and molecular physiology, 2010. **299**: p. L631 - L638.
21. Gunst, S.J. and D.D. Tang, *The contractile apparatus and mechanical properties of airway smooth muscle*. European Respiratory Journal., 2000. **15**: p. 600 - 616.
22. Ansari, S., et al., *Role of caldesmon in the Ca^{2+} regulation of smooth muscle thin filaments*. Journal of biological chemistry, 2008. **283**(1): p. 47-56.
23. Vibert, P., R. Craig, and W. and Lehman, *Three-dimensional Reconstruction of Caldesmon-containing Smooth Muscle Thin Filaments*. The Journal of Cell Biology, 1993. **123**: p. 313 - 321.
24. Léguillete, R. and A.-M. and Lauzon, *Molecular mechanics of smooth muscle contractile proteins in airway hyperresponsiveness and asthma*. Proceedings of American Thoracic Society., 2008. **5**(44 - 46).
25. Mulvihill, D.P. and J.S. and Hyams, *Shedding a little light on light chains*. Nature Cell Biology, 2001. **3**: p. E1 - E2.
26. Wang, L., P. Chitano, and T.M. and Murphy, *A maturational model for the study of airway smooth muscle adaptation to mechanical oscillation*. Canadian Journal of Physiology and Pharmacology, 2005. **83**: p. 817 - 824.
27. Burridge, K. and M. Chrzanowska-Wodnicka, *Focal adhesions, contractility, and signaling*. Ann Rev Cell Dev Biol, 1996. **12**: p. 463-518.
28. McGregor, A., et al., *Identification of the vinculin-binding site in the cytoskeletal protein α -actinin*. Biochemistry journal, 1994. **301**(225-233).

29. Otey, C.A., et al., *Mapping of the α -Actinin Binding Site within the $\beta 1$ integrin cytoplasmic domain*. The journal of biological chemistry 1993. **268**(5): p. 21193-21197.
30. Draeger, A., et al., *The cytoskeletal and contractile apparatus of smooth muscle: contraction bands and segmentation of the contractile elements*. The Journal of Cell Biology, 1990. **111**: p. 2463 - 2473.
31. Gunst, S.J., D.D. Tang, and A. Opazo Saez, *Cytoskeletal remodeling of airway smooth muscle cell: a mechanism for adaptation to mechanical forces in the lung* Respiratory physiology and Neurobiology, 2003. **137**: p. 151 - 168.
32. Mehta, D. and S.J. Gunst, *Actin polymerization stimulated by contractile activation regulates force development in canine tracheal muscle*. Journal of physiology, 1999. **519**(3): p. 829 - 840.
33. Bosse, Y., et al., *Length Adaptation of Airway Smooth Muscle*. Proceeding of the american thoracic society, 2008. **5**: p. 62-67.
34. Silveira, P.S.P. and J.J. and Fredberg, *Smooth muscle length adaptation and actin filament length: a network model of the cytoskeletal dysregulation*. Canadian Journal of Physiology and Pharmacology, 2005. **83**: p. 923-931.
35. Fabry, B. and J.J. Fredberg, *Remodeling of the airway smooth muscle cell: are we built of glass?* Respiratory Physiology & Neurobiology, 2003. **137**(2-3): p. 109 - 124.
36. Wang, L. and P.D. Paré, *Deep inspiration and airway smooth muscle adaptation to length change*. Respiratory Physiology & Neurobiology, 2003. **137**(2-3): p. 169-178.
37. Herrera, A.M., E.C. Martinez, and C.Y. Seow, *Electron microscopic study of actin polymerization in airway smooth muscle*. American journal of physiology, 2004. **286**: p. L1161–L1168.
38. Kuo, K.H., A.M. Herrera, and C.Y. Seow, *Ultrastructure of airway smooth muscle*. Respiratory Physiology and Neurobiology, 2003. **137**(2-3): p. 197-208.
39. Smolensky, A.V., et al., *Length-dependent filament formation assessed from birefringence increases during activation of porcine tracheal muscle*. Journal of Physiology, 2005. **563**: p. 517-527.
40. Veigel, C., et al., *Load-dependent kinetics of force production by smooth muscle myosin measured with optical tweezers*. Nature Cell Biology, 2003. **5**(11): p. 980 - 986.

41. Hai, C.M. and R.A. Murphy, *Cross-bridge phosphorylation and regulation of latch state in smooth muscle*. American journal of physiology: Cell Physiology, 1988. **254**(1): p. C99-106.
42. Hai, C.M. and R.A. Murphy, *Regulation of shortening velocity by cross-bridge phosphorylation in smooth muscle*. American journal of physiology: Cell physiology, 1988. **255**(1): p. C86-94.
43. Mitchell, R.W., et al., *Relationship between myosin phosphorylation and contractile capability of canine airway smooth muscle*. Journal of applied physiology, 2001. **90**: p. 2460-2465.
44. Aubier, M., et al., *[COPD and inflammation: statement from a French expert group: inflammation and remodelling mechanisms]*. Rev Mal Respir, 2010. **10**: p. 1254-1266.
45. Lee, J.-Y., et al., *Vascular Smooth Muscle Dysfunction and Remodeling Induced by Ginsenoside Rg3, a Bioactive Component of Ginseng*. Toxicological sciences, 2010. **17**(2): p. 505-514.
46. Leonardi, R. and M. Alemanni, *The management of erectile dysfunction: innovations and future perspectives*. Arch Ital Urol Androl, 2011. **83**(1): p. 60-62.
47. Whorwell, P.J., et al., *Bladder smooth muscle dysfunction in patients with irritable bowel syndrome*. Gut 1986. **27**(9): p. 1014-1017.
48. Eder, W., M.J. Ege, and E. & von Mutius, *CURRENT CONCEPTS: The Asthma Epidemic*. The New England Journal of Medicine, 2006. **355**(21): p. 2226-2235,2269.
49. (GINA), G.I.f.A. *Pocket Guide for Asthma Management and Prevention*. 2009; Available from: <http://www.ginasthma.com/Guidelineitem.asp??i1=2&i2=1&intId=1562>.
50. WHO. *Fact sheet N°307*. 2008 [cited 2010 May 21]; Available from: <http://www.who.int/topics/asthma/en/>.
51. O'Byrne, P.M. and M.D. and Inman, *Airway Hyperresponsiveness*. Chest, 2003 **123**(3): p. 411S-416S.
52. Bentley, J.K. and M.B. and Hershenson, *Airway Smooth Muscle Growth in Asthma Proliferation, Hypertrophy, and Migration*. Proceedings of american thoracic society. , 2008. **5**: p. 89 - 96.

53. National Heart, L.a.B.I.N. *Expert Panel Report 3 (EPR3): Guidelines for the Diagnosis and Management of Asthma* 2007; Available from: <http://www.nhlbi.nih.gov/guidelines/asthma/asthgdln.htm>.
54. Neal, M.J., *Medical pharmacology at a glance* B. Science, Editor 1997, Blackwell Science ltd. p. 103.
55. Giembycz, M.A. and R. and Newton, *Beyond the dogma: novel b2-adrenoceptor signalling in the airways*. European Respiratory Journal, 2006. **27**: p. 1286-1306.
56. Angus, R., R. Reagon, and A. and Cheesbrough, *Short-acting β 2-agonist and oral corticosteroid use in asthma patients prescribed either concurrent beclomethasone and long-acting β 2-agonist or salmeterol/fluticasone propionate combination*. International journal of clinical practice, 2005. **59**: p. 156-162.
57. Rang, H.P., et al., *Pharmacology*. Fifth ed2003: Elsevier
58. Prenner, B.M., *Role of long-acting b2-adrenergic agonists in asthma management based on updated asthma guidelines*. Current Opinion in Pulmonary Medicine, 2008. **14**: p. 57 - 63.
59. McHugh, P., et al., *Buteyko Breathing Technique for asthma: an effective intervention*. Journal of the New Zealand Medical Association, 2003. **116**(1187).
60. Bowler, S.D., A. Green, and C.A. Mitchell, *Buteyko breathing techniques in asthma: a blinded randomised controlled trial*. The medical journal of Australia, 1998. **169**(11-12): p. 575 - 578.
61. Alkhalil, M., E.S. Schulman, and J. and Getsy, *Obstructive sleep apnea syndrome and asthma: the role of continuous positive airway pressure treatment*. Annals of allergy, asthma & immunology., 2008. **101**(4): p. 350-357.
62. Bonekat, H.W. and K.A. Hardin, *Severe upper airway obstruction during sleep*. Clinical reviews in allergy & immunology, 2003. **25**(2): p. 191 - 210.
63. Lafond, C., F. Sériès, and C. and Lemièrre, *Impact of CPAP on asthmatic patients with obstructive sleep apnoea*. European respiratory journal, 2007. **29**: p. 307-311.
64. Castro, M., et al., *Bronchial thermoplasty: a novel technique in the treatment of severe asthma*. Therapeutic advances in respiratory disease, 2010. **4**(2): p. 101 - 116.

65. Herrag, M., S. AitBatahar, and A.A. Yazidi, *Bronchial thermoplasty in developing countries: is it really worth it?* American journal of respiratory and critical care medicine., 2010. **182**(5): p. 719.
66. Rubin, A.S. and P.F. Cardoso, *Bronchial thermoplasty in asthma*. Journal brasileiro de pneumologia, 2010. **36**(4): p. 506 - 512.
67. Constantino, G.d.T. and J.J.F. Mello, *Remodeling of the lower and upper airways*. Brazilian journal of otorhinolaryngology, 2009. **75**(1): p. 151 -156.
68. Homer, R.J. and J.A. Elias, *Airway remodeling in asthma: therapeutic implications of mechanisms*. Physiology (Bethesda, Md.), 2005. **20**: p. 28 - 35.
69. Gupta, S., et al., *Quantitative analysis of high-resolution computed tomography scans in severe asthma subphenotypes*. Thorax, 2010. **65**(9): p. 775 - 781.
70. Benayoun, L., et al., *Airway structural alterations selectively associated with severe asthma*. American journal of respiratory and critical care medicine, 2003. **167**(10): p. 1360 - 1368.
71. Jeffery, P.K., *Remodeling in asthma and chronic obstructive lung disease*. American journal of respiratory and critical care medicine, 2001. **164**: p. S28 - S38.
72. Elias, J.A., et al., *New insights into the pathogenesis of asthma*. Journal of clinical investigation, 2003. **111**(3): p. 291 - 297.
73. Kumar, S.D., et al., *Airway mucosal blood flow in bronchial asthma*. American journal of respiratory and critical care medicine, 1998. **158**: p. 153 - 156.
74. Salvato, G., *Quantitative and morphological analysis of the vascular bed in bronchial biopsy specimens from asthmatic and non-asthmatic subjects*. Thorax, 2001. **56**: p. 902- 906.
75. Broide, D., *Immunomodulation and reversal of airway remodeling in asthma*. Current opinion in allergy and clinical immunology, 2004. **4**(6): p. 529 - 532.
76. Akers, I.A., et al., *Mast cell tryptase stimulates human lung fibroblast proliferation via protease-activated receptor-2*. American journal of physiology., 2000. **278**: p. L193 - L201.
77. Choe, M.M., P.H.S. Sporn, and M.A. Swartz, *Extracellular matrix remodelling by dynamic strain in a three-dimensional tissue-engineered human airway wall model*. American journal of respiratory Cell and Molecular Biology, 2006. **35**: p. 306-313.

78. Martin, J.G., A. Duguet, and D.H. and Eidelman, *The contribution of airway smooth muscle to airway narrowing and airway hyperresponsiveness in disease*. European Respiratory Journal, 2000. **6**(16): p. 349±354.
79. James, A.L., et al., *Airway smooth muscle thickness in asthma is related to severity but not duration of asthma*. European Respiratory Journal, 2009(34): p. 1040–1045.
80. Hughes, J.M., J.F.G. Hoppin, and J. and Mead, *Effect of lung inflation on bronchial length and diameter in excised lungs* Journal of applied physiology, 1972. **32**(1): p. 25-35.
81. Raqeeb, A., et al., *Length oscillation mimicking periodic individual deep inspirations during tidal breathing attenuates force recovery and adaptation in airway smooth muscle*. Journal of applied physiology (1985). , 2010. **109**(5): p. 1476 - 1482.
82. Fredberg, J.J., et al., *Airway smooth muscle, tidal stretches, and dynamically determined contractile states*. American journal of respiratory and critical care medicine, 1997. **156**: p. 1752-1759.
83. Al-Jumaily, A.M., P. Mbikou, and P.R. & Redey, *Effect of length oscillations on airway smooth muscle reactivity and cross-bridge cycling*. American journal of physiology. Lung cellular and molecular physiology, 2012(303(4)): p. L286-L294.
84. Ansell, T.K., et al., *Potent bronchodilation and reduced stiffness by relaxant stimuli under dynamic conditions*. The european respiratory Journal 2009. **33**: p. 844 - 851.
85. Noble, P.B., P.K. McFawn, and H.W. and Mitchell, *Responsiveness of the isolated airway during simulated deep inspirations: effect of airway smooth muscle stiffness and strain*. Journal of Applied Physiology, 2007. **103**: p. 787 - 795.
86. Wang, L. and P.D. Pare, *Deep inspiration and airway smooth muscle adaptation to length change*. Respiratory Physiology and Neurobiology, 2003. **137**(2-3): p. 169-178.
87. Gunst, S.J. and M.F. Wu, *Plasticity in Skeletal, Cardiac, and Smooth Muscle Selected Contribution: Plasticity of airway smooth muscle stiffness and extensibility: role of length-adaptive mechanisms*. Journal of Applied Physiology, 2000. **90**: p. 741-749.

88. Fredberg, J.J., *Airway obstruction in asthma: does the response to a deep inspiration matter?* Respiratory Research, 2001. **2**(5).
89. Skloot, G., S. Permutt, and A. Togias, *Airway Hyperresponsiveness in Asthma: A Problem of Limited Smooth Muscle Relaxation with Inspiration*. Journal of Clinical investigation, 1995. **96**: p. 2393-2403.
90. Burns, G.P. and G.J. Gibson, *Airway Hyperresponsiveness in Asthma: Not Just a Problem of Smooth Muscle Relaxation with Inspiration*. American Journal of Respiratory and Critical Care Medicine, 1998. **158**: p. 203-206.
91. Shen, X., S.J. Gunst, and R. Tepper, *Effect of tidal volume and frequency on airway responsiveness in mechanically ventilated rabbits*. Journal of Applied Physiology, 1997. **83**(4): p. 1202-1208.
92. P.B., N., *Disruption of the bronchodilatory response to deep inspiration in asthma – Extrinsic or intrinsic to the airway smooth muscle?* Respiratory Physiology & Neurobiology 2013(189): p. 655- 657.
93. Ansell K.T., et al., *Bronchodilatory response to deep inspiration in bronchial segments: the effects of stress vs. strain*. Journal of Applied Physiology, 2013(115): p. 505-513.
94. K.R., L., *Airway smooth muscle stretch and airway hyperresponsiveness in asthma: Have we chased the wrong horse?* Journal of Applied Physiology, 2013.
95. Hessel, E.M., et al., *Repeated measurement of respiratory function and bronchoconstriction in unanesthetized mice*. Journal of applied physiology, 1995. **79**(5): p. 1711-1716.
96. Gunst SJ, *Contractile force of canine airway smooth muscle during cyclical length changes*. J Appl Physiol. , 1983. **55**(3): p. 759-769.
97. Ijpma, G., A.M. Al-Jumaily, and S.P. Cairns, *Biomedical Applications of Vibration and Acoustics in Therapy, Bioeffect and Modeling* 2008: ASME press.
98. Du, Y. and A.M. and Al-Jumaily, *Respiratory smooth muscle relaxation using vibrations*. The Journal of the Acoustical Society of America, 2004. **116**(4): p. 2559.
99. Gunst, S.J., *Contractile force of canine airway smooth muscle during cyclical length changes*. Journal of applied physiology, 1983. **55**(3): p. 759 - 769.
100. Galluccio, S.T., S. Rai, and P. Sharley, *An unexpected ending: brain death following acute severe asthma*. Critical care and resuscitation. , 2008. **3**(10): p. 235 - 238.

101. Wang, L., P.D. Pare, and C.Y. Seow, *Effect of length oscillation on the subsequent force development in swine tracheal smooth muscle*. Journal of applied physiology, 2000. **88**: p. 2246-2250.
102. Bossé, Y., et al., *Adaptation of airway smooth muscle to basal tone: relevance to airway hyperresponsiveness*. American journal of respiratory cell and molecular biology., 2009. **40**(1): p. 13 - 18.
103. Leigh, R., et al., *Dysfunction and Remodeling of the Mouse Airway Persist after Resolution of Acute Allergen-Induced Airway Inflammation*. Am. J. Respir. Cell Mol. Biol. , 2002. **27**: p. 526-535.
104. Pascoe, C., et al., *Force oscillations simulating breathing maneuvers do not prevent force adaptation*. American journal of respiratory cell and molecular biology. , 2012. **47**(1): p. 44 - 49.
105. Bates, J.H.T., M. Rincon, and C.G. Irvin, *Animal models of asthma*. American journal of physiology. Lung cellular and molecular physiology, 2009. **297**: p. L401–L410.
106. Bice, D.E. and J.C. Seagrave, *ANIMAL MODELS OF ASTHMA: Potential Usefulness for Studying Health Effects of Inhaled Particles*. Inhalation Toxicology, 2000. **12**: p. 829 - 862.
107. Blyth, D.I., et al., *Airway subepithelial fibrosis in a murine model of atopic asthma: suppression by dexamethasone or anti-interleukin-5 antibody*. American journal of respiratory cell and molecular biology, 2000. **23**(2): p. 241 - 246.
108. Fernandez-Rodriguez, S., et al., *Establishing the phenotype in novel acute and chronic murine models of allergic asthma*. International Immunopharmacology. , 2008. **8**(5):: p. 756-763.
109. Goplen, N., et al., *Combined sensitization of mice to extracts of dust mite, ragweed, and Aspergillus species breaks through tolerance and establishes chronic features of asthma*. J Allergy Clin Immunol., 2009. **123**(4): p. 925-932.
110. Karol, M.H., *Animal models of occupational asthma*. European respiratory journal., 1994. **7**(3): p. 555-568.
111. Keir, S. and C. Page, *The rabbit as a model to study asthma and other lung diseases*. Pulmonary Pharmacology & Therapeutics, 2008. **21** p. 721-730.
112. Kumar, R.K. and P.S. Foster, *Murine model of chronic human asthma*. Immunology and Cell Biology., 2001. **79**: p. 141-144.

113. Kumar, R.K. and P.S. Foster, *Modeling Allergic Asthma in Mice Pitfalls and Opportunities*. Am. J. Respir. Cell Mol. Biol. , 2002. **27**: p. 267-272.
114. Moir, L.M., et al., *Repeated allergen inhalation induces phenotypic modulation of smooth muscle in bronchioles of sensitized rats*. American Journal Physiological lung cellular and molecular physiology, 2003. **284**: p. L148-L159.
115. Nials, A.T. and S. Uddin, *Mouse models of allergic asthma: acute and chronic allergen challenge*. Disease Models & Mechanisms 2008. **1**: p. 213 - 220.
116. Singh, P., et al., *Phenotypic comparison of allergic airway responses to house dust mite in three rat strains*. American journal of physiology. Lung cellular and molecular physiology., 2003. **284**: p. L588 - L598.
117. Ulrich, K., et al., *Anti-inflammatory modulation of chronic airway inflammation in the murine house dust mite model*. Pulmonary pharmacology & therapeutics, 2008. **21**(4): p. 637 - 647.
118. Zosky, G.R., and P.D. Sly, *Animal models of asthma. Clinical and Experimental Allergy*, 2007. **37**: p. 973 - 988.
119. Epstein MM., *Are mouse models of allergic asthma useful for testing novel therapeutics?* Experimental and Toxicologic Pathology 2006. **57**(S2): p. 41-44.
120. Plopper CG and H. DM., *The non-human primate as a model for studying COPD and asthma*. Pulmonary Pharmacology & Therapeutics 2008. **21**: p. 755-766.
121. Ricciardolo, w.F.L.M., et al., *Proliferation and inflammation in bronchial epithelium after allergen in atopic asthmatics*. Clinical and experimental allergy, 2003. **33**: p. 905 - 911.
122. Kumar, R.K., C. Herbert, and P.S. Foster, *The "Classical" Ovalbumin Challenge Model of Asthma in Mice*. Current Drug Targets, 2008. **9**: p. 485-494.
123. Blyth DI, et al., *Airway subepithelial fibrosis in a murine model of atopic asthma: suppression by dexamethasone or anti-interleukin-5 antibody*. Am J Respir Cell Mol Biol. , 2000. **23**(2): p. 241-246.
124. Choi IS, et al., *Strain-dependent suppressive effects of BCG vaccination on asthmatic reactions in BALB/c mice*. Ann Allergy Asthma Immunol. , 2005. **95**(6) p. 571-578.
125. Choi IW, et al., *TNF-alpha induces the late-phase airway hyperresponsiveness and airway inflammation through cytosolic phospholipase A(2) activation*. J Allergy Clin Immunol. , 2005. **116**(3): p. 537-543.

126. Janssen EM, et al., *The efficacy of immunotherapy in an experimental murine model of allergic asthma is related to the strength and site of T cell activation during immunotherapy.* J Immunol., 2000. **15;165(12)**: p. 7207-7214.
127. Johnson JR, W.R., Fattouh R, Swirski FK, Gajewska BU, Coyle AJ, Gutierrez-Ramos JC, Ellis R, Inman MD, Jordana M., *Continuous exposure to house dust mite elicits chronic airway inflammation and structural remodeling.* Am J Respir Crit Care Med. , 2004. **169(3)**: p. 378-385.
128. Kenehiro, D., et al., *Inhibition of Phosphodiesterase 4 Attenuates Airway Hyperresponsiveness and Airway Inflammation in a Model of Secondary Allergen Challenge.* American journal of respiratory and critical care medicine. , 2001. **163**: p. 173-184.
129. McMillan SJ, Xanthou G, and L. CM., *Manipulation of allergen-induced airway remodeling by treatment with anti-TGF-beta antibody: effect on the Smad signaling pathway.* J Immunol. , 2005. **174(9)**: p. 5774-5780.
130. Tomkinson A, et al., *A murine IL-4 receptor antagonist that inhibits IL-4- and IL-13-induced responses prevents antigen-induced airway eosinophilia and airway hyperresponsiveness.* J Immunol., 2001. **166(9)**: p. 5792-5800.
131. Henderson WR Jr, et al., *A role for cysteinyl leukotrienes in airway remodeling in a mouse asthma model.* Am J Respir Crit Care Med., 2002. **165(1)**: p. 108-116.
132. Temelkovski, J., et al., *An improved murine model of asthma: selective airway inflammation, epithelial lesions and increased methacholine responsiveness following chronic exposure to aerosolised allergen.* Thorax., 1998. **53(10)**: p. 849 - 856.
133. Lloyd, C.M. and D.S. Robinson, *Allergen-induced airway remodelling.* European respiratory journal. , 2007. **29**: p. 1020-1032.
134. Pathology, C.f.G. *Respiratory system.* 2013; Available from: <http://ctrngenpath.net/static/atlas/mousehistology/Windows/respiratory/diagrams.html>.
135. Glabb, T., et al., *Review: Invasive and noninvasive methods for studying pulmonary function in mice.* Respiratory Research, 2007. **8**.
136. Glaab, T., et al., *Repetitive measurements of pulmonary mechanics to inhaled cholinergic challenge in spontaneously breathing mice.* Journal of Applied Physiology, 2004. **97**: p. 1104 - 1111.

137. Kanehiro, A., et al., *Timing of administration of anti-VLA-4 differentiates airway hyperresponsiveness in the central and peripheral airways in mice*. American journal of respiratory critical care medicine. , 2000. **3**(162): p. 1132 - 1139.
138. Dvorkin, M.A., D.P. Cardinali, and L. R., *Best & Taylor. Bases Fisiológicas de la Práctica Médica*. 14ª ed 2010: Editorial medica panamericana. 1164
139. Wang, W., et al., *Peroxisome proliferator-activated receptor- γ agonist induces regulatory T cells in a murine model of allergic rhinitis*. Otolaryngology head and neck surgery 2011 **144**(4): p. 506 - 513.
140. Balsley, M.A., et al., *A cell-impermeable cyclosporine A derivative reduces pathology in a mouse model of allergic lung inflammation*. Journal of Immunology. , 2010 **185**(12): p. 7663 - 7670.
141. Carr, V.M., A.M. Robinson, and R.C. Kern, *Tissue-specific effects of allergic rhinitis in mouse nasal epithelia*. Chemical Senses. , 2012. **37**(7): p. 655 - 668.
142. Vanoirbeek, J.A., et al., *Immunological determinants in a mouse model of chemical-induced asthma after multiple exposures*. Scandinavian journal of immunology. , 2009. **70**(1): p. 25 - 33.
143. Siddiqui, S., et al., *Pulmonary eosinophilia correlates with allergen deposition to the lower respiratory tract in a mouse model of asthma*. Clinical and experimental allergy., 2008. **38**(8): p. 1381 - 1390.
144. Choi, I.S., et al., *Strain-dependent suppressive effects of BCG vaccination on asthmatic reactions in BALB/c mice*. Annals of allergy, asthma & immunology, 2005. **95** (6): p. 571 - 578.
145. Brewer, J.P., A.B. Kisselgof, and T.R. Martin, *Genetic variability in pulmonary physiological, cellular, and antibody responses to antigen in mice*. American journal of respiratory and critical care medicine. , 1999. **160**(4): p. 1150 - 1156.
146. Kelada, S.N., et al., *Strain-dependent genomic factors affect allergen-induced airway hyperresponsiveness in mice*. American Journal of respiratory cell and molecular biology. Oct., 2011. **45**(4): p. 817 - 824.
147. Hoymaan, H., *New developments in lung function measurements in rodents*. Experimental and Toxicologic Pathology, 2006. **57**(S2): p. 5 - 11.
148. Welker, L., et al., *Predictive value of BAL cell differentials in the diagnosis of interstitial lung diseases*. European respiratory journal., 2004. **24**: p. 1000 - 1006.

149. Bai, Y. and M.J. and Sanderson, *Airway smooth muscle relaxation results from a reduction in the frequency of Ca^{2+} oscillations induced by a cAMP-mediated inhibition of the IP3 receptor*. Respiratory Research, 2006. **7**: p. 34.
150. Shen, X., S.J. Gunst, and R.S. Tepper, *Effect of tidal volume and frequency on airway responsiveness in mechanically ventilated rabbits*. Journal of applied physiology, 1997. **83(4)**: p. 1202-1208.
151. Bai, T.R., et al., *On the terminology for describing the length-force relationship and its changes in airway smooth muscle*. Journal of Applied Physiology, 2004. **97**: p. 2029-2034.
152. Dowell, M.L., et al., *Latrunculin B increases force fluctuation-induced relengthening of ACh-contracted, isotonically shortened canine tracheal smooth muscle*. Journal of Applied Physiology, 2005. **98**: p. 489-497.
153. Fredberg, J.J., *Airway narrowing in asthma: dose speed kill?* American Journal of Physiology -- Lung Cellular and Molecular Physiology, 2002. **283**: p. L1179-L1180.
154. Turner, D.J., et al., *Decreased airway narrowing and smooth muscle contraction in hyperresponsive pigs*. Journal of Applied Physiology, 2002. **93(4)**: p. 1296-1300.
155. Faffe, D.S., et al., *Comparison of rat and mouse pulmonary tissue mechanical properties and histology*. Journal of applied physiology (1985), 2002. **1(92)**: p. 230-234.
156. Mitchell, R.W., et al., *Force Fluctuation–induced Relengthening of Acetylcholine-contracted Airway Smooth Muscle*. Proceedings of American Thoracic Society, 2008. **5**: p. 68 - 72.
157. Ali, F., et al., *Mechanism of partial adaptation in airway smooth muscle after a step change in length*. Journal of applied physiology (1985). , 2007. **2(103)**: p. 569 - 577.
158. Chin, L.Y., et al., *Mechanical properties of asthmatic airway smooth muscle*. European respiratory journal. , 2012. **40(1)**: p. 45-54.
159. Pascoe, C.D., et al., *Decrease of airway smooth muscle contractility induced by simulated breathing maneuvers is not simply proportional to strain*. Journal of applied physiology (1985). 2013. **114(3)**: p. 335 - 343.
160. Epstein, M.M., *Are mouse models of allergic asthma useful for testing novel therapeutics?* Experimental and Toxicologic Pathology 2006. **57(S2)**: p. 41-44.

161. Henderson, W.R.J., et al., *A role for cysteinyl leukotrienes in airway remodeling in a mouse asthma model*. American journal of respiratory and critical care of medicine., 2002. **165**(1): p. 108-116.
162. Rao, S. and A.S. Verkman, *Analysis of organ physiology in transgenic mice*. american journal of physiology cell physiology, 2000. **279**: p. C1 - C18.
163. LaPrad, A.S., et al., *Maintenance of airway caliber in isolated airways by deep inspiration and tidal strains*. Journal of applied physiology, 2008. **105**: p. 479-485.
164. LaPrad, A.S., et al., *Tidal stretches do not modulate responsiveness of intact airways in vitro*. Journal of applied physiology (1985). 2010. **109**(2): p. 295 - 304.
165. Oostveen, E., et al., *Respiratory transfer impedance and derived mechanical properties of conscious rats*. Journal of applied physiology. , 1992. **73**(4): p. 1598 - 1607
166. MGI. *Mouse Genome Informatics*. 2013 10/02/2013 [cited 2013; Available from: <ftp://nasbio2.vet.ucm.es/Nacho/Laboratorio/cursos/cat%20c/Curso%20cat%20egor%C3%ADa%20C/13-MODELOS%20ANIMALES/MOUSE%20GENOME%20INFORMATICS.htm>].

APPENDIX

Appendix A: Ethical approval

This appendix presents all the paperwork regarding the ethical regulations obtained and approved AEC from the University of Auckland for the project “Investigation of the combined effect of mechanical oscillations and bronchodilators on smooth muscle of normal and sensitized mice airways (AEC No 894).

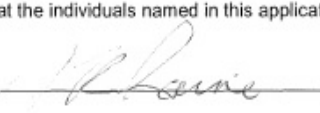


Application to use animals in RESEARCH, TESTING AND TEACHING under the University of Auckland Code of Ethical Conduct (in accordance with the Animal Welfare Act 1999).

AUT Researchers : Please submit this coversheet and the completed application to the Ethics Coordinator* in the Auckland University of Technology Ethics Committee (AUTC) Secretariat who will forward it to the University of Auckland Animal Ethics Committee.

*WAS05D, 55 Wellesley Street East, Auckland 1010, AUT internal mail code D-89.

| | | | |
|--|---|----------------------------------|----|
| Project/ Course Title: | Investigation of the combined effects of mechanical oscillations and bronchodilators on the smooth muscle of normal and sensitised mice airways | | |
| Responsible Investigator /Course co-ordinator: | Prof. Ahmed Al-Jumaily | | |
| Department/ Organisation: | Institute of Biomedical Technologies (IBTec), AUT | | |
| Please indicate ratio (%): | | | |
| Teaching: No | Public good or academic research: No | Commercially funded contract: No | No |

CLEARANCES: This section must be completed by the appropriate people before the submission will be considered by the Committee.

| | |
|--|---|
| Human Ethics approval required? If yes, please provide details: | No |
| DOC Approval required? If yes, please provide details: | No |
| Is any substance covered by the ACVM (Agricultural Compounds & Veterinary Medicines Act) going to be used by a non-veterinarian as a part of this project? | Yes |
| If yes are the compounds being prescribed by a veterinarian? | Yes |
| If not, the use of prescription medicines on AEC-approved protocols requires the completion of an Institutional Drug Administration Orders (IDAO) by your institutional veterinarian | |
| Delegated authority: I am satisfied that the individuals named in this application will follow the procedures as defined in this application. | |
| HOD Signature:  | Name: J.K. Raine |
| Dean Signature:  | Name: Desna Jury |
| FOR AEC USE ONLY | |
| Date received: 11 APR 2011 | IDAO Not Required/Required AEC Number: 4R0894 |
| Approved by Signature:  | Name: M. van der Meer |
| Approval date: 20 JUL 2011 | |
| Expiration date: 20 JUL 2014 | |

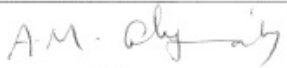

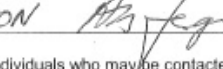
Version: 30 January 2008

Every person involved in this application shall complete and sign the following declaration:

I have read the University Of Auckland Code Of Ethical Conduct. Copies of the Code can be obtained from the AEC Secretary on request

I have read this application and approved the approach to the study, with particular reference to the ethics of experimentation and the welfare of the animals being used,

I agree to follow the procedures, defined in this application, and not deviate from them.

| | NAME | SIGNATURE | EMAIL | Phone number |
|----|--------------------|---|----------------------------|------------------------|
| 1. | Ahmed AL-Jumaily |  | ahmed.al-jumaily@aut.ac.nz | 9 921 9999 ext 9777 |
| 2. | Prisca Mbikou |  | pmbikou@aut.ac.nz | 9 921 9999 ext 7994 |
| 3. | Miguel Jo Avila |  | mjoavila@aut.ac.nz | 021456087 |
| 4. | | | | |
| 5. | ALEXANDER FERGUSON |  | Sandy@tergvet.co.nz | (621) 765 503 |

Please nominate two of these named individuals who may be contacted 24 hours 7 days if any animal health or welfare issues arise outside the normal working hours of the facility in which you will carry out the manipulations in this protocol.

Name: Ahmed Al-Jumaily Contact numbers: Work: 9 921 999 ext 9777 Home: Mobile: 021524468

Name: Prisca Mbikou Contact numbers: Work: 9 921 999 ext 7994/8617 Mobile: 0211 863207

Appendix B: Labview programs used for in vitro test

The Labview programs used during the course of the experimental investigation are discussed in this appendix. Initially, simple programs were used to acquire data from the setup. New programs created at a later stage consisted of more advanced features to suit the protocols designed. All the programs were created in Labview 8.5[®].

a) Converter.vi

This program was used for converting .scl files into .txt files for easy readability into MATLAB. It prompted a user to select the .scl file and saved a copy in .txt format. This program was created in Labview 6.1. Figure A.1 shows the back panel of the program.

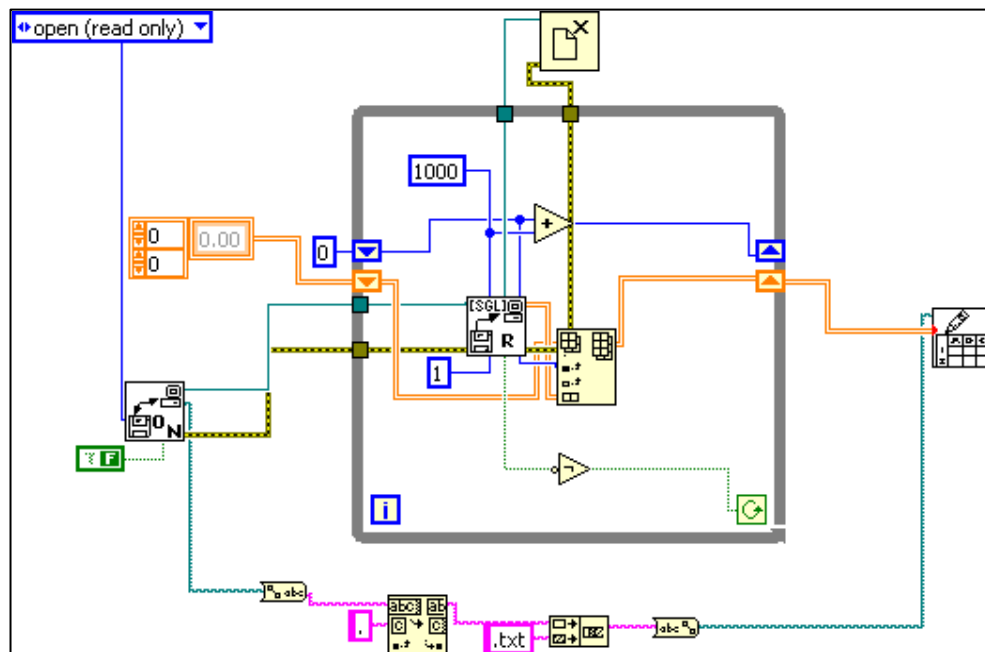


Figure A.1: back panel Converter.vi

b) ASM_Length.vi

This program acquires force and length data from the setup. It also allows for imposing simple sinusoidal, superimposed sinusoidal and superimposed square oscillations. It also includes the ability to impose sinusoidal oscillations with gradual frequency change. The user can choose the starting and the ending frequency for the amount of duration to be run. It saves the data in two versions – high resolution data acquired at 3000 samples per second and low resolution data acquired at 100 samples per second. Figure A.2 and A.3 show the front and the back panel of the program respectively.

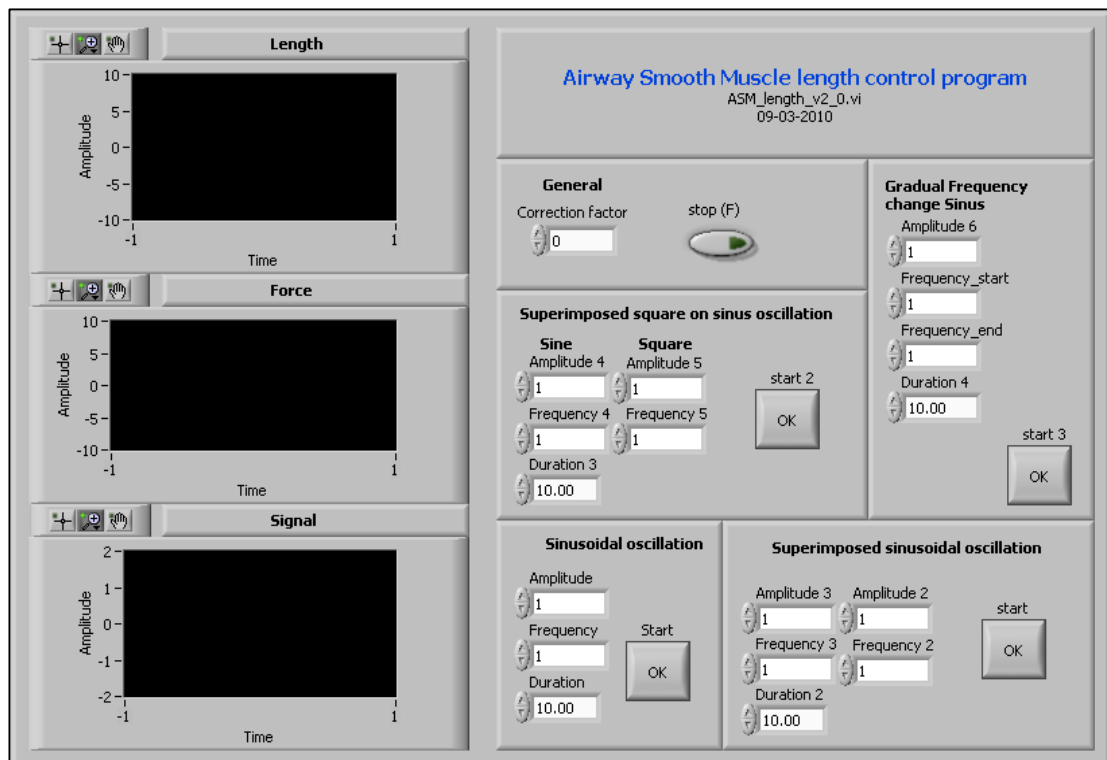


Figure A.2: Front panel ASM_Length.vi front panel

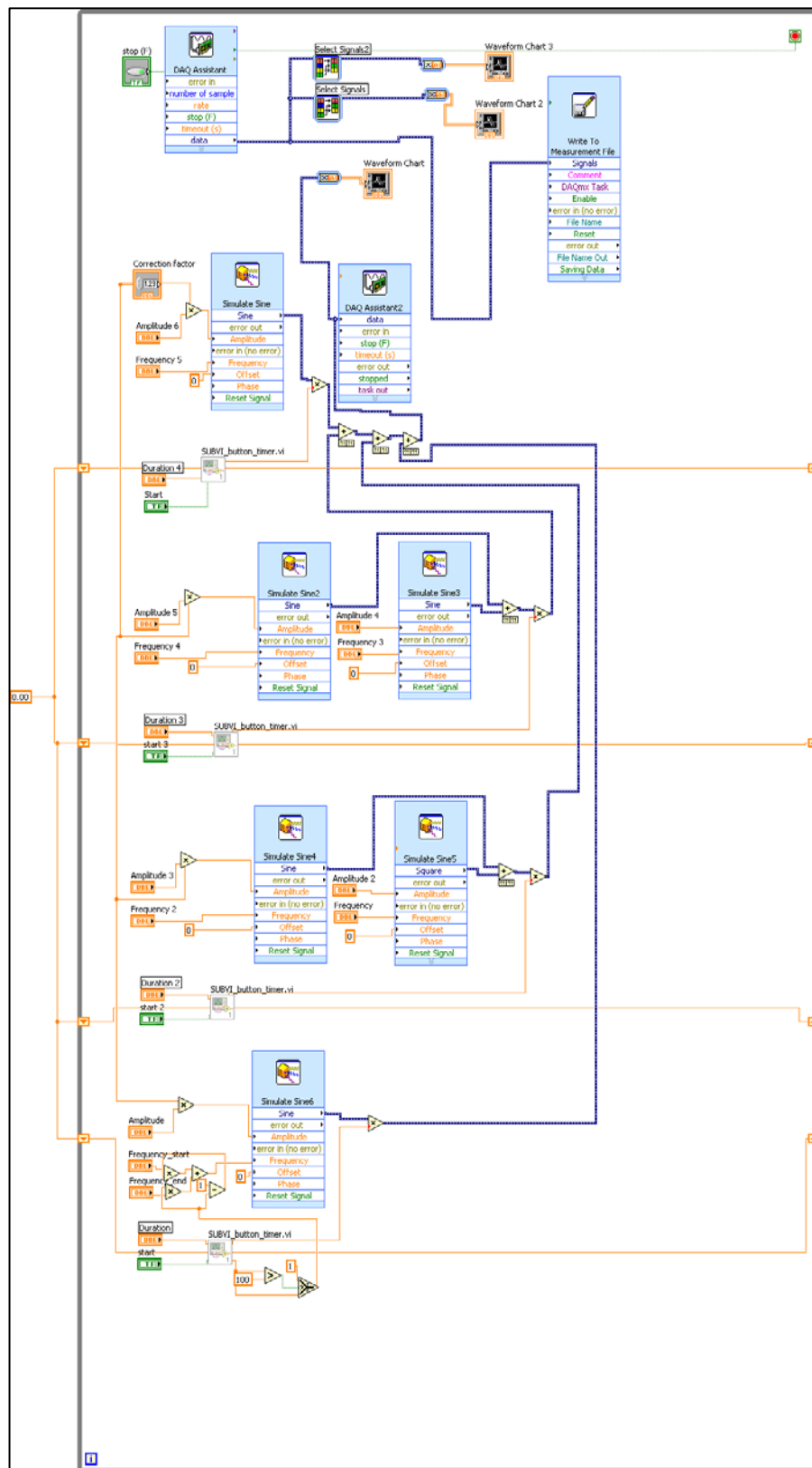


Figure A.3: Back panel ASM_Length.vi back panel

c) Low_res_signal.vi

This program acquires force and length data from the setup. It also allows for imposing simple sinusoidal, superimposed sinusoidal and superimposed square oscillations. It also includes the ability to impose sinusoidal oscillations with gradual frequency change. The user can choose the starting and the ending frequency for the amount of duration to be run. It saves the data in two versions – high resolution data acquired at 3000 samples per second and low resolution data acquired at 100 samples per second. In addition, it gives user the idea of time left of the oscillations applied. Figure A.4 and A.5 show the front and the back panel of the program respectively.

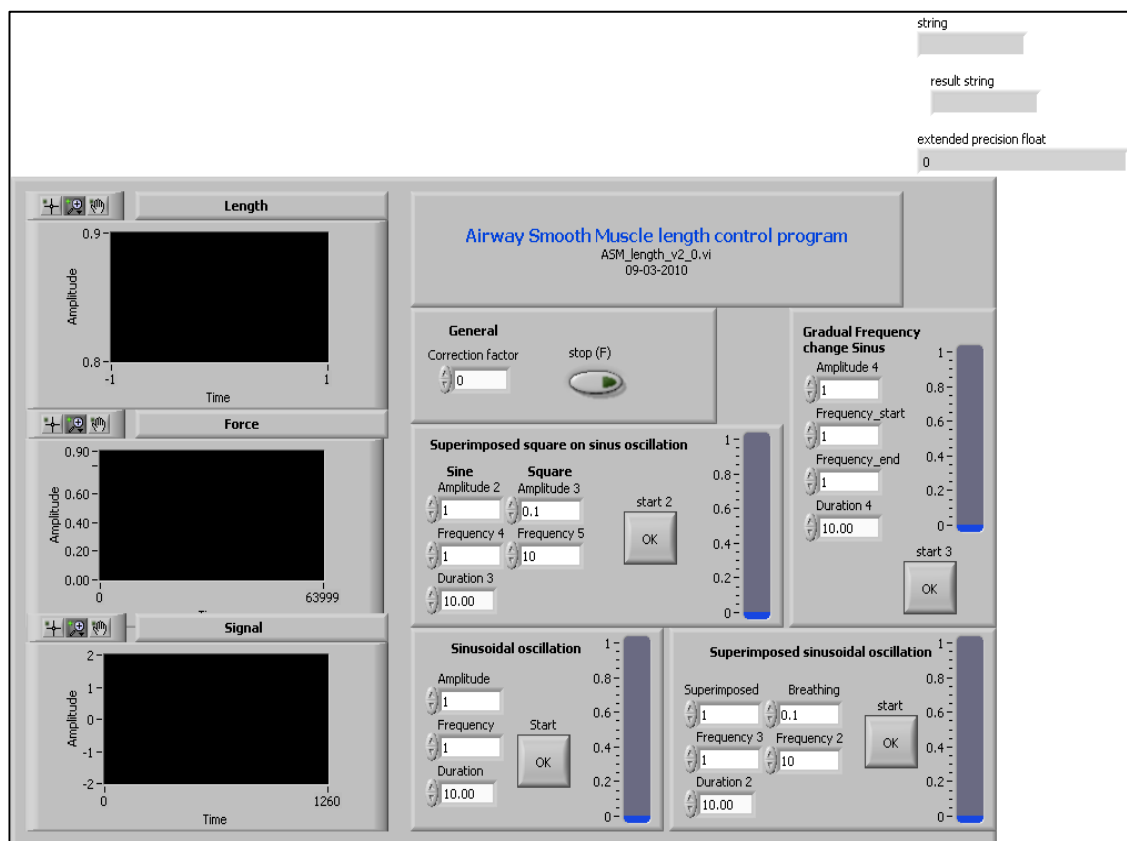


Figure A.4: Front panel Low_res_signal.vi front panel

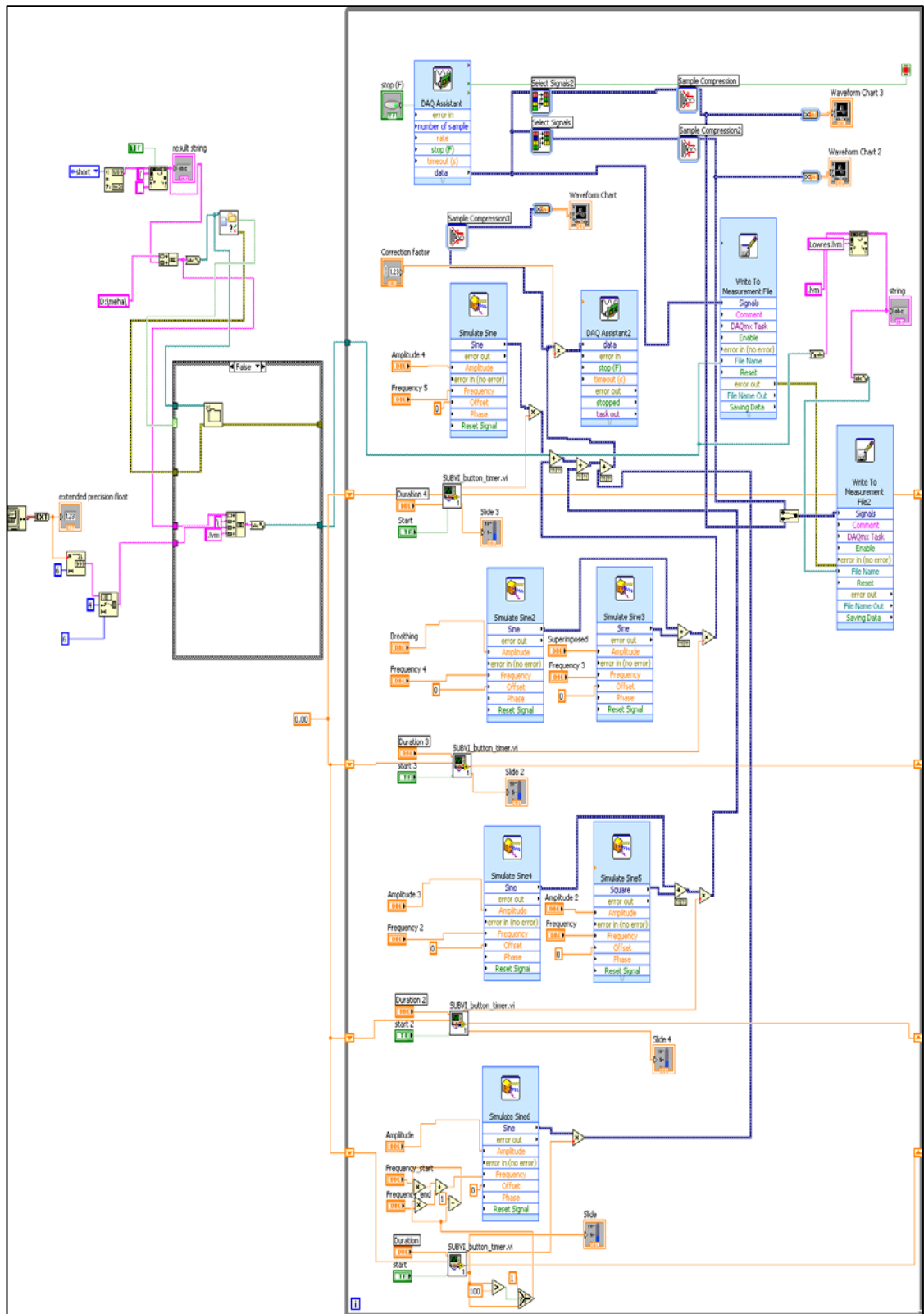


Figure A.5: Back panel Low_res_signal.vi back panel

a) SUBVI_button_timer.vi

This subvi controls the timing of the loop. It feedbacks to the program the time before the next loop should start. Figure A.6 shows the back panel of the program

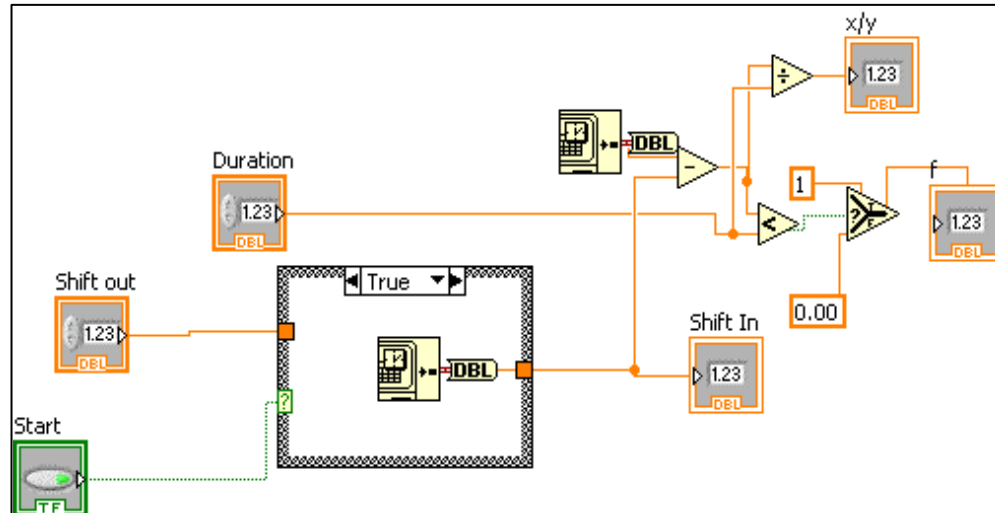


Figure A.6: *SubVI_button_timer.vi* back panel

Appendix C: Matlab analysis code

a) Preliminary experiments

```
clear all
close all
%set file pathname and load the files
l(2).path='D:\Meha\Experiments\2010\April\010410 - 13apr\set2\';
for d = 1:36;
s = ['load data_' int2str(d) '.lvm'];
eval(s);
end;
% define time, force and length variables
for d = 1:36;
s = ['Time' int2str(d) '=data_' int2str(d) '(:,1)'];
eval (s);
end;
for d = 1:36;
s = ['Force' int2str(d) '=data_' int2str(d) '(:,2)'];
eval (s);
end;
for d = 1:36;
s = ['Length' int2str(d) '=data_' int2str(d) '(:,4)'];
eval (s);
end;
% select the required samples of data
Force = [Force18; Force19; Force20; Force21; Force22; Force23; Force24; Force25;
Force26; Force27; Force28; Force29; Force30; Force31; Force32; Force33; Force34;
Force35; Force36];
Length = [Length18; Length19; Length20; Length21; Length22; Length23; Length24;
Length25; Length26; Length27; Length28; Length29; Length30; Length31; Length32;
Length33; Length34; Length35; Length36];
% plot and save
figure(1);
plot(Force);
hold on
a = plot(Length, 'r');
figure(2);
b = plot(Length, Force);
saveas(a,['D:\Meha\Experiments\2010\April\010410 - 13apr\set2\' 'data.png'])
saveas(a,['D:\Meha\Experiments\2010\April\010410 - 13apr\set2\' 'data.fig'])
saveas(b,['D:\Meha\Experiments\2010\April\010410 - 13apr\' 'Loop19-21.png'])
saveas(b,['D:\Meha\Experiments\2010\April\010410 - 13apr\' 'Loop19-21.fig'])
```

b) Protocols - Read and Plot

```
close all  
clear all
```

```
% Define the time variable
```

```
ts = filename(:,1);  
tm = ts/60;
```

```
% Define the force variable
```

```
F = filename(:,2);  
plot(F);  
% Normalize the force with Fmax (differs for each contraction)  
Fmax = 0.6;  
Fnorm = F/Fmax;
```

```
% Define the length variable
```

```
L = filename(:,4) - 0.8550;
```

```
% Plot the normalized force and length data as subplots
```

```
subplot(2,1,1), plot(tm, Fnorm), xlabel('Time (minutes)'), ylabel('Force (normalized)');  
subplot(2,1,2), plot(tm, L, 'r'), xlabel('Time (minutes)'), ylabel('Length');
```


Appendix D: *in vivo* no processed data

a) Flow

The data obtained for flow (L/s) is presented in figure A.7.

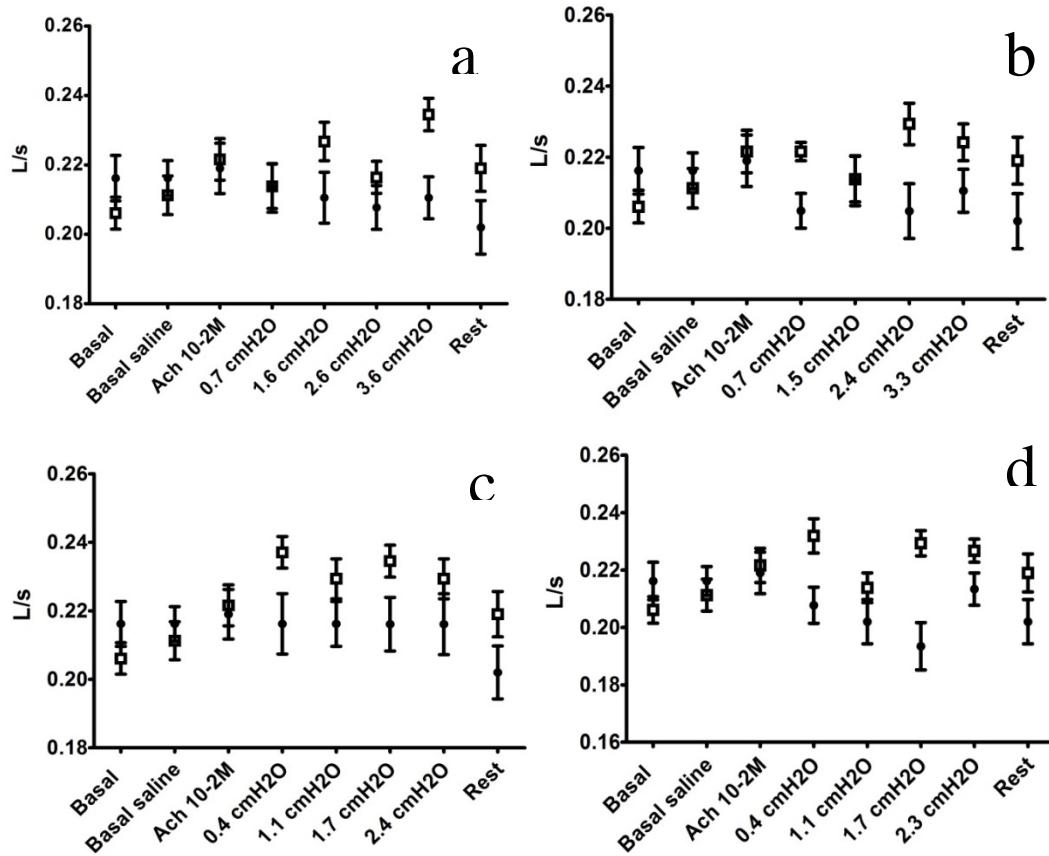


Figure A.7: Changes of flow observed as result of the application of SILO: a) 5Hz; b) 10Hz; c) 15Hz; and d) 20Hz frequency and amplitudes in the range of 100 – 400 mV are presented in axis y for each experimental condition presented in axis x (□ = healthy; ● = asthmatic; n=10).

b) Tp (tracheal pressure)

The data obtained for Tp (mmH₂O) is presented in figure A.8.

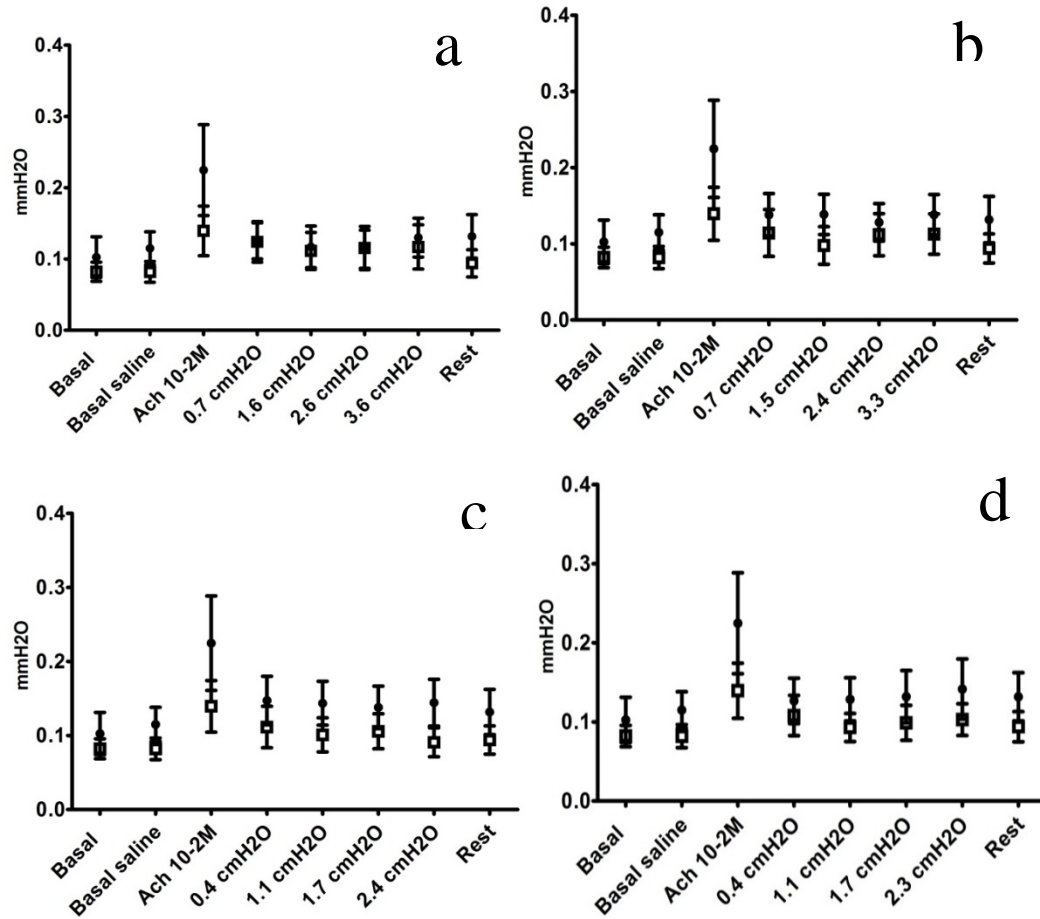


Figure A.8: Changes of Tp observed as result of the application of SILO: a) 5Hz; b) 10Hz; c) 15Hz; and d) 20Hz frequency and amplitudes in the range of 100 – 400 mV are presented in axis y for each experimental condition presented in axis x (□ = healthy; ● = asthmatic; n=10).

c) Ptp (Transpulmonar pressure)

The data obtained for Ptp (mmH₂O) is presented in figure A.9.

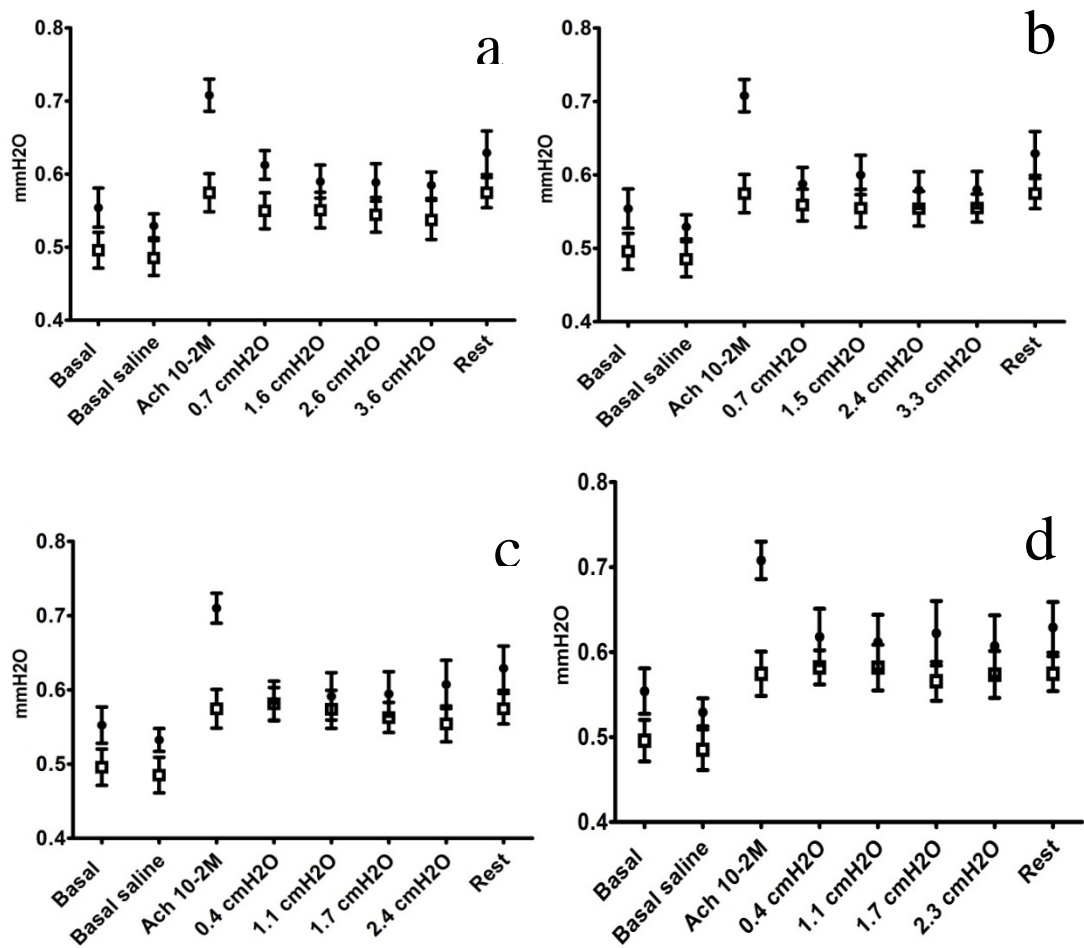


Figure A. 9: Changes of Ptp observed as result of the application of SILO: a) 5Hz; b) 10Hz; c) 15Hz; and d) 20Hz frequency and amplitudes in the range of 100 – 400 mV are presented in axis y for each experimental condition presented in axis x (□ = healthy; ● = asthmatic; n=10).

d) Tv (Tidal volume)

The data obtained for Tv (mL) is presented in figure A.10.

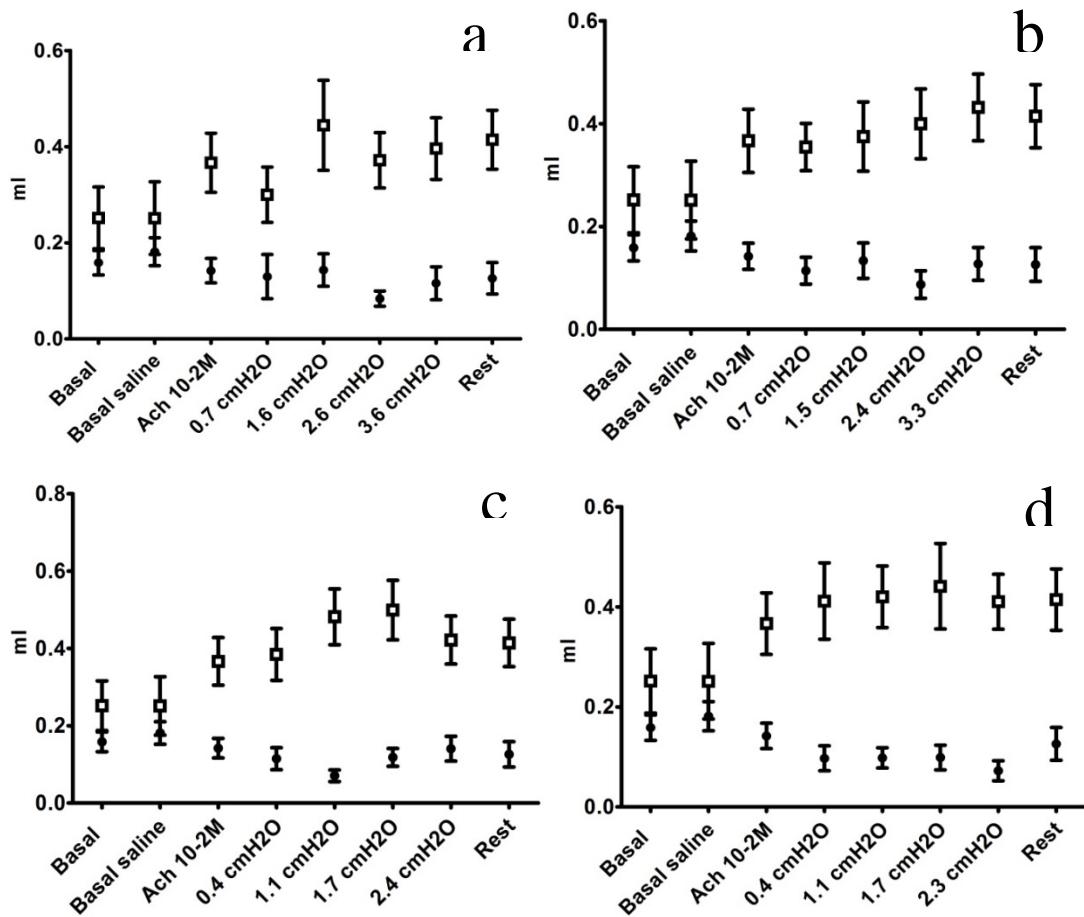


Figure A. 10: Changes of Tv observed as result of the application of SILO: a) 5Hz; b) 10Hz; c) 15Hz; and d) 20Hz frequency and amplitudes in the range of 100 – 400 mV are presented in axis y for each experimental condition presented in axis x (□ = healthy; ● = asthmatic; n=10).

e) Summary tables per frequency

Data presented in figures A.7, A.8, A.9, and A.10 was grouped and summarized in the following tables according to data set for each frequency: 5, 10, 15 and 20Hz.

Table A.1: Summary table for flow, T_p , P_{tp} and T_v for 5Hz and all amplitudes tested.

| 5Hz | | | | | | | | |
|------------------------|------------------|----------------------------|-------------------------------|------------|--------------------|----------------------------|-------------------------------|------------|
| | Healthy (n = 10) | | | | Asthmatic (n = 10) | | | |
| | Flow (L/s) | T_p (mmH ₂ O) | P_{tp} (mmH ₂ O) | T_v (mL) | Flow (L/s) | T_p (mmH ₂ O) | P_{tp} (mmH ₂ O) | T_v (mL) |
| Basal | 0.206 | 0.496 | 0.082 | 0.252 | 0.216 | 0.554 | 0.103 | 0.159 |
| Basal saline | 0.211 | 0.485 | 0.082 | 0.251 | 0.216 | 0.529 | 0.115 | 0.181 |
| Ach 10-2M | 0.222 | 0.575 | 0.139 | 0.367 | 0.219 | 0.708 | 0.225 | 0.142 |
| 0.7 cmH ₂ O | 0.214 | 0.550 | 0.124 | 0.300 | 0.213 | 0.612 | 0.125 | 0.130 |
| 1.6 cmH ₂ O | 0.227 | 0.551 | 0.111 | 0.444 | 0.211 | 0.590 | 0.117 | 0.143 |
| 2.6 cmH ₂ O | 0.216 | 0.544 | 0.115 | 0.372 | 0.208 | 0.589 | 0.114 | 0.084 |
| 3.6 cmH ₂ O | 0.235 | 0.537 | 0.117 | 0.396 | 0.211 | 0.585 | 0.130 | 0.116 |
| Rest | 0.219 | 0.575 | 0.094 | 0.414 | 0.202 | 0.629 | 0.132 | 0.126 |

Table A.2: Summary table for flow, T_p , P_{tp} and T_v for 10Hz and all amplitudes tested.

| 10Hz | | | | | | | | |
|------------------------|------------------|----------------------------|-------------------------------|------------|--------------------|----------------------------|-------------------------------|------------|
| | Healthy (n = 10) | | | | Asthmatic (n = 10) | | | |
| | Flow (L/s) | T_p (mmH ₂ O) | P_{tp} (mmH ₂ O) | T_v (mL) | Flow (L/s) | T_p (mmH ₂ O) | P_{tp} (mmH ₂ O) | T_v (mL) |
| Basal | 0.206 | 0.496 | 0.082 | 0.252 | 0.216 | 0.554 | 0.103 | 0.159 |
| Basal saline | 0.211 | 0.485 | 0.082 | 0.251 | 0.216 | 0.529 | 0.115 | 0.181 |
| Ach 10-2M | 0.222 | 0.575 | 0.139 | 0.367 | 0.219 | 0.708 | 0.225 | 0.142 |
| 0.7 cmH ₂ O | 0.222 | 0.559 | 0.114 | 0.355 | 0.205 | 0.588 | 0.138 | 0.114 |
| 1.5 cmH ₂ O | 0.214 | 0.555 | 0.098 | 0.375 | 0.213 | 0.600 | 0.139 | 0.134 |
| 2.4 cmH ₂ O | 0.229 | 0.554 | 0.112 | 0.400 | 0.205 | 0.579 | 0.128 | 0.087 |
| 3.3 cmH ₂ O | 0.224 | 0.555 | 0.113 | 0.432 | 0.211 | 0.580 | 0.138 | 0.127 |
| Rest | 0.219 | 0.575 | 0.094 | 0.414 | 0.202 | 0.629 | 0.132 | 0.126 |

Table A.3: Summary table for flow, T_p , P_{tp} and T_v for 15Hz and all amplitudes tested.

| 15Hz | | | | | | | | |
|-----------------------------|-------------------------|--|---|----------------------------------|---------------------------|--|---|----------------------------------|
| | Healthy (n = 10) | | | | Asthmatic (n = 10) | | | |
| | Flow (L/s) | T_p (mmH₂O) | P_{tp} (mmH₂O) | T_v (mL) | Flow (L/s) | T_p (mmH₂O) | P_{tp} (mmH₂O) | T_v (mL) |
| Basal | 0.206 | 0.496 | 0.082 | 0.252 | 0.216 | 0.552 | 0.103 | 0.159 |
| Basal saline | 0.211 | 0.485 | 0.082 | 0.251 | 0.216 | 0.533 | 0.115 | 0.181 |
| Ach 10-2M | 0.222 | 0.575 | 0.139 | 0.367 | 0.219 | 0.710 | 0.225 | 0.142 |
| 0.4 cmH₂O | 0.237 | 0.581 | 0.112 | 0.385 | 0.216 | 0.585 | 0.147 | 0.115 |
| 1.1 cmH₂O | 0.229 | 0.574 | 0.101 | 0.482 | 0.216 | 0.591 | 0.144 | 0.071 |
| 1.7 cmH₂O | 0.235 | 0.563 | 0.106 | 0.499 | 0.216 | 0.595 | 0.138 | 0.118 |
| 2.4 cmH₂O | 0.229 | 0.554 | 0.091 | 0.422 | 0.216 | 0.607 | 0.144 | 0.141 |
| Rest | 0.219 | 0.575 | 0.094 | 0.414 | 0.202 | 0.629 | 0.132 | 0.126 |

Table A.4: Summary table for flow, T_p , P_{tp} and T_v for 20Hz and all amplitudes tested.

| 20Hz | | | | | | | | |
|-----------------------------|-------------------------|--|---|----------------------------------|---------------------------|--|---|----------------------------------|
| | Healthy (n = 10) | | | | Asthmatic (n = 10) | | | |
| | Flow (L/s) | T_p (mmH₂O) | P_{tp} (mmH₂O) | T_v (mL) | Flow (L/s) | T_p (mmH₂O) | P_{tp} (mmH₂O) | T_v (mL) |
| Basal | 0.206 | 0.496 | 0.082 | 0.252 | 0.216 | 0.554 | 0.103 | 0.159 |
| Basal saline | 0.211 | 0.485 | 0.082 | 0.251 | 0.216 | 0.529 | 0.115 | 0.181 |
| Ach 10-2M | 0.222 | 0.575 | 0.139 | 0.367 | 0.219 | 0.708 | 0.225 | 0.142 |
| 0.4 cmH₂O | 0.232 | 0.582 | 0.108 | 0.412 | 0.208 | 0.618 | 0.127 | 0.097 |
| 1.1 cmH₂O | 0.214 | 0.582 | 0.093 | 0.420 | 0.202 | 0.612 | 0.129 | 0.098 |
| 1.7 cmH₂O | 0.229 | 0.566 | 0.099 | 0.441 | 0.193 | 0.622 | 0.132 | 0.099 |
| 2.3 cmH₂O | 0.227 | 0.574 | 0.103 | 0.410 | 0.213 | 0.607 | 0.142 | 0.072 |
| Rest | 0.219 | 0.575 | 0.094 | 0.414 | 0.202 | 0.629 | 0.132 | 0.126 |